Pilot System Utilizing Electrical Properties to Monitor

Rubber Vulcanization

Narong Chueangchayaphan

A Thesis Submitted in Partial Fulfillment of the Requirements for the

Degree of Doctor of Philosophy in Polymer Technology

Prince of Songkla University

2022

Thesis Title   Pilot System Utilizing Electrical Properties to Monitor Rubber
                     Vulcanization

Author   Mr. Narong Chueangchayaphan

Major Program   Polymer Technology

Academic Year   2021

Major Advisor   **Examining Committee**

…………………………………….   ...……………………………….Chairperson

(Dr. Nattapong Nithi-Uthai)   (Asst. Prof. Dr.Atitaya Tohsan)

                                           …….……………………..Committee

Co-Advisor   (Dr. Nattapong Nithi-Uthai)

……………………………………….   …………………………..Committee

(Prof. Dr. Hathaikarn Manuspiya)   (Prof. Dr. Hathaikarn Manuspiya)

……….……………………………….   ……………………………. Committee

(Asst. Prof. Dr. Kittiphan Techakittiroj) (Asst. Prof. Dr. Adisai Rungvichaniwat)

                                           ……………………………..…..Committee

                                           (Asst. Prof. Dr. Subhan Salaeh)

        The Graduate School, Prince of Songkla University, has approved this thesis as partial fulfillment of the requirements for the Doctor of Philosophy Degree in Polymer Technology.

                              …………………………………...
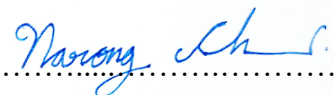
                              (Prof. Dr. Damrongsak Faroongsarng)

                              Dean of Graduate School

This is to certify that the work here submitted is the result of the candidate's own investigation. Due acknowledgment has been made of any assistance received.

…………...……….……………Signature

(Dr. Nattapong Nithi-Uthai)

Major Advisor

…………...……….……………Signature

(Mr. Narong Chueangchayaphan)

Candidate

I hereby certify that this work has not been accepted in substance for any degree, and is not being currently submitted in candidature for any degree.

……………………………………………………Signature

(Mr. Narong Chueangchayaphan)

Candidate

ชื่อวิทยานิพนธ์	ระบบต้นแบบการใช้สมบัติเชิงไฟฟ้าเพื่อติดตามการวัลคาไนเซชั่นยาง
ผู้เขียน	นายณรงค์ เชื่องชยะพันธุ์
สาขาวิชา	เทคโนโลยีพอลิเมอร์
ปีการศึกษา	2564

บดคัดย่อ

ระบบติดตามการคงรูปยาง (Rubber cure monitoring system, RCMS) ได้รับการ
พัฒนาขึ้นสำหรับการติดการวัลคาไนซ์ยางผ่านกระบวนการวัดสมบัติทางไฟฟ้า โดยทำการติดตั้ง
เซนเซอร์ฝังในเบ้าที่ใช้ในการขึ้นรูปซึ่งเชื่อมต่อกับเครื่อง แอลซีอาร์ (LCR meter) เพื่อวัดการ
เปลี่ยนแปลงของความจุไฟฟ้าและการนำไฟฟ้าในกระบวนการคงรูปยาง ปัจจัยที่ทำการศึกษา
ประกอบด้วยอิทธิพลของความถี่สนามไฟฟ้าที่ใช้ทดสอบ อุณหภูมิที่ใช้ในการวัลคาไนซ์ ระบบวัล
คาไนซ์ และปริมาณเขม่าดำของยางคอมปาวด์ เปรียบเทียบระยะเวลาสกอร์ช ระยะเวลาคงรูป ระดับ
การคงรูป และอัตราการคงรูปที่ได้จากการทดสอบโดยใช้เครื่องรีโอมิเตอร์แบบดายเคลื่อนที่
(Moving Die Rheometer, MDR) และ RCMS พบว่าค่าความจุไฟฟ้ามีความสัมพันธ์กับค่าแรงบิด
จาก MDR ในขณะคงรูปยาง ความถี่ของสนามไฟฟ้าที่ 5 kHz มีความเหมาะสมในการติดตามการวัล
คาไนซ์ของยางธรรมชาติ นอกจากนั้นเมื่อเพิ่มอุณหภูมิที่ใช้ในการคงรูปพบว่าแรงบิดต่ำสุด แรงบิด
สูงสุด ผลต่างของแรงบิด ระยะเวลาสกอร์ซและระยะเวลาการคงรูปมีค่าลดลง โดยมีความสัมพันธ์
กับค่าความจุไฟฟ้าจาก RCMS ทุกอุณหภูมิที่ใช้ในการคงรูป ระยะเวลาการคงรูป (t_{c90}) ที่ได้จาก
MDR และ RCMS ณ อุณหภูมิต่างๆ มีความสัมพันธ์กันแบบเชิงเส้น นอกจากนั้นพบว่าระบบวัลคา
ไนซ์และชนิดของสารวัลคาไนซ์ของยางคอมปาวด์มีผลต่อการเปลี่ยนแปลงของค่าแรงบิดและความ
จุไฟฟ้าของยางในกระบวนการวัลคาไนซ์ โดย RCMS สามารถใช้ติดตามการคงรูปของยาง
ธรรมชาติ บ่งบอกระยะเวลาสกอร์ซและระยะเวลาการคงรูปได้ทั้งระบบวัลคาไนซ์แบบกำมะถัน
และเปอร์ออกไซด์ ส่วนในกรณีที่ใช้เขม่าดำเป็นสารตัวเติมพบว่าสามารถติดตามการคงรูปของยาง
คอมปาวด์ที่ใส่เขม่าดำไม่เกิน 30 phr ดังนั้น RCMS ที่พัฒนาขึ้นจึงมีศักยภาพในการติดตาม
กระบวนการวัลคาไนซ์ของยาง เพื่อหาระยะเวลาการคงรูปที่เหมาะสมในสภาวะการขึ้นรูปจริงโดย
ใช้เทคนิคการอัดเบ้าได้ ซึ่งตอบสนองต่อความท้าทายในการพัฒนากระบวนการขึ้นรูปผลิตภัณฑ์
ยางในอุตสาหกรรม

คำหลัก: การวัลคาไนซ์, ลักษณะการคงรูปยาง, ระบบติดตามการคงรูปยาง

Thesis Title   Pilot system utilizing electrical properties to monitor rubber vulcanization

Author   Mr. Narong Chueangchayaphan

Major Program   Polymer Technology

Academic Year   2021

ABSTRACT

An *in situ* rubber cure monitoring system (RCMS) has been developed based on the measurement of electrical properties to monitor the vulcanization progress. The sensors are connected to an LCR meter and measured the changes in the capacitance and conductance of rubber during vulcanization in the compression mold. The parameters are investigated in this study including, the effect of frequency, vulcanization temperatures, vulcanization systems and carbon black contents. The scorch time, optimum cure time, degree of cure, and the cure rate from a moving die rheometer (MDR) and RCMS methods were compared. The results show that capacitance during curing correlated with the time profile of torque from MDR, which the frequency at 5 kHz is suitable for monitoring the progress of natural rubber vulcanization. Moreover, the decrease in the minimum torque, maximum torque, delta torque, scorch time, and optimum cure time was observed with increasing vulcanization temperature. Torque and capacitance showed a close correlation at all cure temperatures. A linear correlation of optimum cure time obtained from RCMS and MDR with different vulcanization temperatures was achieved. The vulcanization system and type of curing agent have affected the changes of the torque and the capacitance during the vulcanization process.The RCMS can be used to indicates the scorch time and optimum cure time for both sulfur and peroxide vulcanization systems. In the case of using carbon black no more than 30 phr, RCMS can monitor the rubber vulcanization. Which supports the potential of RCMS for real-time determination of the optimum cure time during the vulcanization of natural rubber by compression molding, which is a challenge in the rubber industry.

Keywords: Vulcanization, Cure characterization, Rubber cure monitoring system

ACKNOWLEDGEMENTS

CONTENTS

CONTENTS (CONTINUED)
<div align="right">Page</div>

LIST OF TABLES

LIST OF FIGURES

LIST OF FIGURES (CONTINUED)

LIST OF FIGURES (CONTINUED)

LIST OF ABBREVIATIONS AND SIMBOLS

AC	Alternating electric fields
ASTM	American Society for Testing and Materials
DC	Direct current
DCP	Dicumyl peroxide
DEA	Dielectric analysis
DMA	Dynamic mechanical analysis
DSC	Differential scanning calorimetry
Hz	Hertz
MDR	Moving die rheometer
NR	Natural rubber
ODR	Oscillating disc rheometer
phr	Part per hundred rubber
PTFE	Polytetrafluoroethylene
RCMS	Rubber cure monitoring system
RPA	Rubber processing analyzer
STR	Standard Thai Rubber
TBBS	N-tert-Butyl-2-benzothiazole sulfonamide
ZnO	Zinc oxide
C	Capacitance
C_0	Capacitance of vacuum
D_0	Electric flux density of vacuum
E	Electric field
G	Conductance
$Ires$	Response current
L	Inductance
M_H	Maximum torque
M_L	Minimum torque
M_H-M_L	Delta torque
pF/m	Picofarad per meter

LIST OF ABBREVIATIONS AND SIMBOLS (CONTINUED)

Q	Charge on the plate
R	Resistance
S/m	Siemens per meter
V	Voltage
$Vexc$	Excitation voltage
X	Reactance
Y	Admittance
Z	Impedance
ε_0	Dielectric permittivity of vacuum
ε	Permittivity of sample
ε_r	Dielectric constant or relative dielectric permittivity
ε^*	Complex permittivity
ε'	Relative permittivity or Dielectric constant
ε''	Dielectric loss
σ'	Relative conductivity

CHAPTER 1

INTRODUCTION

1.1 Background and Rationale

Natural rubber (NR) is an essential agricultural product obtained from Hevea Basiliensis trees in which the cis-1,4-polyisoprene molecule consisted of only carbon and a hydrogen atom is obtained from the biosynthetic process. NR plays a key role in the socio-economic structure of many countries, especially in Thailand. It is comprehensively used in a wide range of products, such as mechanical goods and tires. Unvulcanized NR has low mechanical properties; hence the vulcanization process of compound NR is necessarily required to convert into high mechanical properties. Among vulcanization systems, sulfur vulcanization is the most popular process which has usually used to crosslink the rubber (Khang and Ariff, 2012). In the literature, several techniques have been used to characterize curing of an elastomer, such as differential scanning calorimetry (DSC), oscillating disc rheometer (ODR), dynamic mechanical analysis (DMA), rubber processing analyzer (RPA), and moving die rheometer (MDR) (Wang *et al*., 2003; Arrillaga *et al*., 2007; Zhang *et al*., 2013; Khimi *et al*., 2014; Hosseini *et al*., 2014). The analysis of rheometer curves is an indirect method to evaluate the vulcanization level in rubbers by monitoring of an increase in the torque value. The crosslink density of the rubber network is related to the delta torque value in the curing curves (Rosca *et al*., 2003; Maiti *et al*., 2006; Chueangchayaphan *et al*., 2018). However, the limitations of rheometry tests are the different mold geometry, sample thickness, and the different processing conditions leading to waste of materials, defective products, and longer cycle time (Magill and Demin, 1999; Jaunich *et al*., 2009). Therefore, a direct or real-time cure monitor is very important to solve the drawback of rheometry tests. The dielectric analysis (DEA) is one of the methods which are generally used to monitor the cure of thermoset materials such as resins and adhesives (Rath *et al*., 2000; Kim and Lee, 2002; Kortaberria *et al*., 2006; Chen and Hojjati, 2007; Skordos and Partridge, 2007; Zhou *et al.*, 2012; Hardis *et al.*, 2013; Steinhausa *et al*., 2014; Müller *et al*., 2016). An applying DEA to monitor the real-time NR vulcanization is an essential advantage to good vulcanizate properties.

Because cis-1,4-polyisoprene is a main component of NR which has a non-zero dipole moment and the changes in dipole moment are occurred due to added the sulfur and form the rubber-sulfur dipoles (Tuckett 1942; Desanges 1958; Ortiz-Serna *et al*., 2010), DEA observe the changes in viscosity and dipole moment of the NR vulcanization. However, a few of the research reported the use of DEA to measure elastomer vulcanization (Desanges, 1958; Bakule and Havranek, 1975; Persson, 1986; Magill and Demin, 1999; Magill and Demin, 2000). Nevertheless, the basics of association between chemistry and rheology of NR vulcanization are necessary to clarify. So, natural rubber compound vulcanization by compression molding was investigated to test dielectric cure monitoring for its suitability to real-time monitoring. This research aimed to improve and extend the use of dielectric cure monitoring in the rubber industry, displaying application to practical production methods, to support improving product quality and productivity.

In addition, the vulcanization process condition, for example, vulcanization temperature and vulcanization time have an extreme impact on the structure, physio-mechanical properties, and quality of the final products (Mansilla *et al*., 2015; Erfanian *et al*., 2016). Hence, during the vulcanization process, the vulcanization temperature becomes of great interest because it has a major influence on the three-dimensional crosslinked network structure, chemical crosslink density, type of crosslinks, and mechanical properties of vulcanized rubber (Wang *et al*., 2013; Mansilla *et al*., 2015; Zhang *et al*., 2016; Lee *et al.*, 2017).

To enable DEA to online monitor the NR vulcanization in the rubber product molding process, the rubber cure monitoring system (RCMS) was set up. The effects of signal frequency on capacitance (C) and conductance (G) are discussed. Moreover, the effect of three different vulcanization temperatures, vulcanization systems and carbon black content on cure characteristics of natural rubber compounds are reported and compared with both MDR and RCMS methods.

1.2 Objectives

In this research, the main objective is the development of the online pilot system for utilizing electrical properties to control rubber vulcanization, aligned and calibrated. Toward this objective, the following lists of sub-objectives are;

1.2.1 To find out the dielectric properties such as capacitance and conductivity that related to changing of the viscosity (Torque) in rubber during vulcanization.

1.2.2 To study the parameters including frequency range of electric field, vulcanization temperature, vulcanization systems and carbon black content which affect on dielectric properties of rubber compounds in the curing process.

1.3 Expected Advantages

1.3.1 To track the real-time electrical data during vulcanization of natural rubber compounds.

1.3.2 To understand the effect of frequency, vulcanization temperature, vulcanization systems and carbon black contents on dielectric properties of rubber during vulcanization.

1.3.3 To improved techniques for online monitoring the curing of natural rubber compounds.

1.3.4 To lead to commercial production of the dielectric monitoring system to optimize the curing process of rubber manufacture.

CHAPTER 2

LITERATURE REVIEW

This chapter is presented in three major topics: theory of dielectric in an electric field, dielectric analysis, and dielectric cure monitoring. The phenomena of dielectric in the static and alternating electric field are introduced with the focus on elastomers in 2.1. In 2.2, the dielectric measurement systems, techniques, and methods are described briefly. Additionally, previous works that relate to the dielectric properties of resin, rubber, and the development of dielectric monitoring systems are shortly reviewed in 2.3. Understanding the nature of dielectric material, dielectric analysis, and cure monitoring techniques are crucial for observing the change of dielectric properties in rubber vulcanization.

2.1 Theory of dielectric in an electric field

One of the main characteristics of materials is their ability to conduct electrical currents. According to their conductivity, they are divided into conductors, semiconductors, and insulators (dielectrics) as seen in figure 2.1. A dielectric material is any material that supports charge without conducting it to a significant degree. Dielectrics can conduct electricity because of the contaminations and flaws within the materials. However, their conductivity is ranging from 10^{-18} to 10^{-8} S/cm (Alemour *et al.*, 2019; Shakun, 2014). In principle all insulators are dielectrics. The response of materials to an applied direct current (DC) electric field can be simply described in the case of a parallel plate capacitor in figure 2.2.
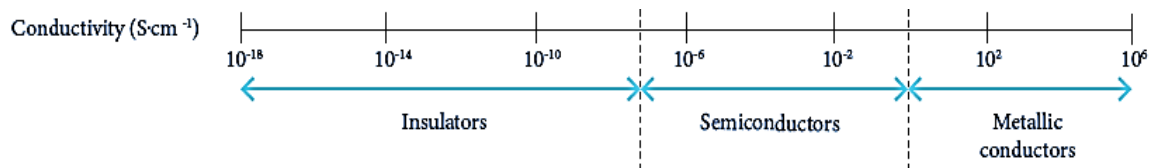
Figure 2.1 Conductivity ranges of materials (Alemour *et al.*, 2019)
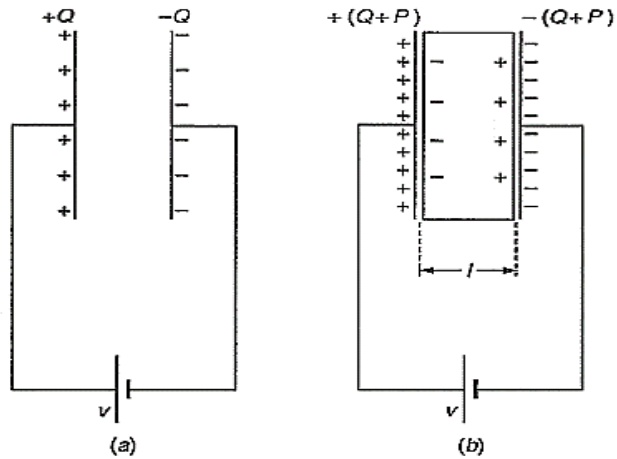
Figure 2.2 Charge on a parallel plate capacitor with (a) a vacuum between the plates and (b) a dielectric between the plates (Blythe and Bloor, 2005)

In a static electrical field, a fixed voltage (*V*) is connected across such a capacitor where the plates are separated by a distance (*d*) in a vacuum, as shown in figure 2.2(a). The electric field (*E*) is produced between the parallel plates and is calculated as equation 2.1.

$$E = \frac{V}{d} \tag{2.1}$$

The magnitude of the field is directly proportional to the charges +Q and –Q per unit area stored on the plates. The electric flux density of vacuum (D_0) arising from the charge density is directly proportional to the electric field can be express as equation 2.2

$$D_0 = \varepsilon_0 E \tag{2.2}$$

where ε_0 is the dielectric permittivity of vacuum and has a value of 8.854 pF/m. Area *A* is the area of parallel plate electrodes. The capacitance of vacuum (C_0) is defined as a ratio of the charge on the plate (*AQ*) to the voltage (*V*) as shown in equation 2.3.

$$C_0 = \frac{AQ}{V} = \frac{\varepsilon_0 A}{d} \tag{2.3}$$

The dielectric responds to the applied electric field when a dielectric material is placed between the electrodes. The positive charge is attracted to the negative electrode and vice versa. This effect is called polarization of the material. Thus, when a dielectric material is placed between the electrodes as seen in figure 2.2b, the charge Q then includes bound charge densities P due to the effect of polarization. Therefore, total charge density becomes ($Q+P$). The increase in charge densities will lead to an increase in flux density (D) as seen in equation 2.4

$$D = \varepsilon_0 E + P \tag{2.4}$$

Capacitance (C) is the ability of a material to hold a charge when the electric field is applied across it. The capacitance of dielectric depends on the permittivity of the dielectric (ε), area of parallel plate electrode, and distance between two plates. Therefore, the capacitance of dielectric in the electric field may be express as Equation 2.5.

$$C = \frac{\varepsilon A}{d} \tag{2.5}$$

Dielectric permittivity of a material is the material's ability to polarize in presence of an electric field (Shakun, 2014). Thus, relative dielectric permittivity (ε') is defined as the ratio of the permittivity of the dielectric material to the permittivity of the free space. Besides, it is the ratio of the capacitance (C) formed by two plates with material between them to the capacitance of the same plates with air as the dielectric (C_0).

$$\varepsilon' = \frac{\varepsilon}{\varepsilon_0} = \frac{C}{C_0} \tag{2.6}$$

Thus, the capacitance of the sample in the electric field can be expressed as Equation 2.7.

$$C = \frac{\varepsilon_0 \varepsilon' A}{d} \tag{2.7}$$

When a dielectric material is placed between the electrodes the dielectric will respond to the applied electric field. However, the polarization of a dielectric material always fails to respond instantaneously to variations of an applied field and heating the material (Blythe and Bloor, 2005; Li, 2011). Therefore, the response of dielectric to external fields depends on the frequency of the field. If an alternating current (AC) is applied, the polarization of the dielectric material differs from that of the static case. An alternating electric field may be express as Equation 2.8.

$$E = E_0 e^{i\omega t} \tag{2.8}$$

where E_0 represents a constant, ω is the angular frequency and t denote the time, then

$$D = \varepsilon E_0 e^{i\omega t} \tag{2.9}$$

For most dielectric material, there is a small phase difference (δ) between D and E. Therefore, the flux density of dielectric in an alternating electric field can be express as equation 2.10 (Codrington, 1948).

$$D = \varepsilon_0 E_0 e^{i(\omega t - \delta)} = (\varepsilon_0 cos\delta - i\varepsilon_0 sin\delta)E_0 e^{i\omega t} \tag{2.10}$$

Within the framework of the Maxwell theories, complex permittivity (ε^*) is time or frequency-dependent. This leads to different time dependences of electric field and flux density. Therefore, the relative permittivity or dielectric constant (ε') can be described by a complex number in Equation 2.11.

$$\varepsilon^* = \varepsilon' - i\varepsilon'' \tag{2.11}$$

The real part ε' is a dielectric constant and related to the ability of the material to store the energy in the electrical field. The imaginary part is the dielectric loss (ε'') that represents the amount of electrical energy which is lost by the material in the electrical field. The ratio between the loss with the permittivity is quantified as "dissipation factor" or tanδ as shown in equation 2.12 (Blythe and Bloor, 2005).

$$tan\,\delta = \frac{\varepsilon''}{\varepsilon'} \tag{2.12}$$

The lack of polarizing ability of molecules to follow the changing of the alternating electric field causes dielectric loss. The relaxation time (τ) is the time it takes for the dipoles to return to their original random orientation. In the case of relaxation time being slower than the oscillating rate of an electric field, the loss is minimum. However, when the alternating electric field frequency faster than the relaxation time, the energy absorption and dissipation as heat are increased due to the molecules cannot follow the oscillating frequency (Ahmad, 2012). Moreover, the dielectric loss is the combined effect of energy losses due to the relaxation mechanisms and the conduction of the material as shown in equation 2.13.

$$\varepsilon'' = \varepsilon''_d + \frac{\sigma}{\omega\varepsilon_0} \tag{2.13}$$

where ε''_d is the dielectric loss associated with relaxation, $\dfrac{\sigma}{\omega\varepsilon_0}$ is conduction loss. σ is the conductivity of the medium and ω is the angular frequency of the oscillating electric field.

2.1.1 Dielectric polarization mechanisms

When an electric field is applied to a dielectric material that is homogeneous, the electron cloud from the nucleus moves in the opposite direction of the applied field, causing positive and negative charges to separate and the molecules to behave like an electric dipole. Modes of polarizations are divided into three modes, as shown in Figure 2.2 (Blythe and Bloor, 2005; Li, 2011; Shakun, 2014).

1. Electronic polarization – In the electric field, the electron cloud is moved to the opposite direction of the electric field. This type of polarization is quite small. However, the effect is more pronounced for heavy atoms.

2. Atomic or ionic polarization –The atomic position in a molecule can distort the electric field. This mechanism is responsible for the displacement of canters of positively charged ions relative to negatively charged ions leading to high polarizability. The movement of heavy nuclei is slowly than electrons. Thus ionic polarization cannot occur at high frequency as electronic polarization. For this reason, it is not detected above infrared frequency.

3. Dipolar or orientation polarization – This polarization arises in the presence of molecular groups containing atoms with different electronegativity, polar molecules. If these molecules are independent, they easily align in the applied electric field. In the case of some polymers, such as poly(vinyl chloride), polarization may also arise from a rotation of side polar groups and can be detected.

A dielectric constant as ε_{static} in static electric field is the permanently polarized of dipoles. When an alternating electric field is applied, the dipoles will be oscillate with the electric field direction. The frequency of the alternating electric field is affect to all three modes of polarization and dielectric constant (relative permittivity). Clearly, electronic polarization can follow the oscillating of the electric field better than atomic polarization and orientation polarization, respectively (Ahmad, 2012).
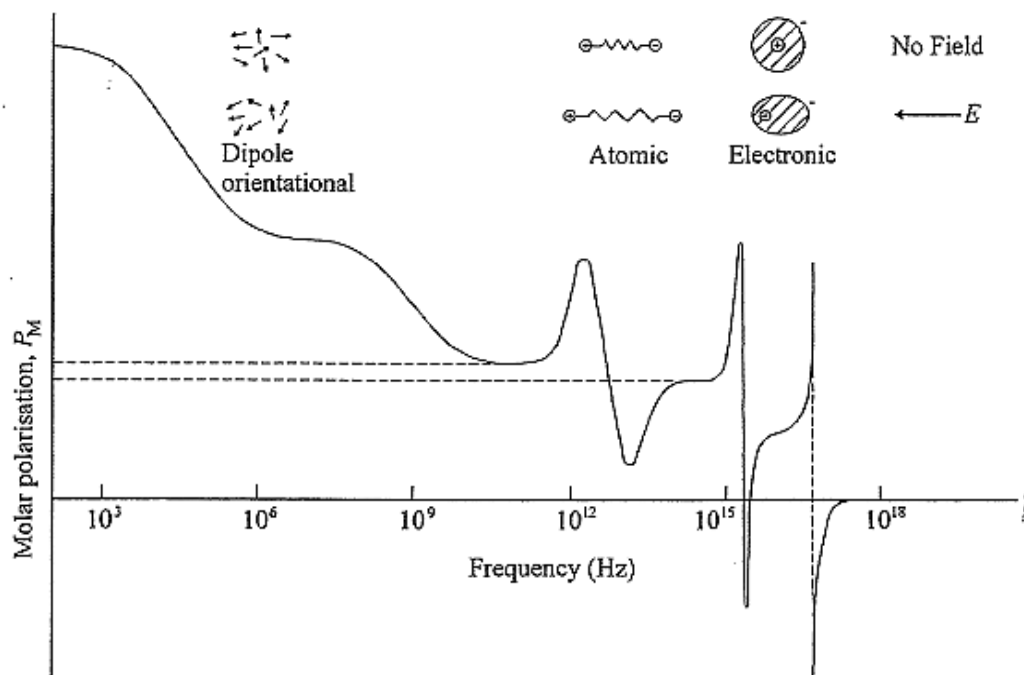
Figure 2.3 Dispersion of molar polarization in a dielectric (Blythe and Bloor, 2005).

The main types of dielectric polarizability as a function of frequency are presented in Figure 2.3. The total polarization shows itself completely at low frequencies. However, the orientation of the polar groups is relatively slow. Thus, when the frequency reaches a value of about 10^{12} Hz. The dipoles cannot follow the oscillations of the field (P_{dip} disappears). Therefore, at a frequency above 10^{12} Hz, the total polarization of the atomic (P_{at}) and the electronic polarization (P_{el}) remain. At a higher frequency, the stretching and bending of the bonds turn too sluggish, no atomic polarization takes place. Because the atomic polarization's resonance frequency is on the order of 10^{13} Hz, an infrared absorption band can be seen. Only P_{el} remains above a frequency of 10^{14} Hz after that. Finally, in the ultraviolet spectrum (frequencies greater than 10^{15} Hz), the distortion of electron clouds near nuclei slows down. (van Krevelen, 2009).

In practice, a material is non-uniform and impurities may be present as a second phase. Effect on dielectric properties to material discontinuities is typically called the

"Maxwell-Wagner effect". When a discontinuity appears in a dielectric material, such as crack or voids, the relative permittivity will reduce which depending on the amount and distribution of the enclosed space or air (Blythe and Bloor, 2005).

In the case of rubber compounds, interfacial polarization or space charge polarization occurs in a rubber containing mobile charge carriers (such as impurities, additives, and filler) (Hernández *et al.*, 2012). In an applied electric field, charges are hindered in their motion because they become trapped at surfaces or grain boundaries of charge carriers. This phenomenon is resulting in the charges gathering and can move through the material in an electric field, showing the increase in interfacial polarization of heterogeneous material. Thus, four polarization mechanisms contribute to the permittivity (Li, 2011; Shakun, 2014).

(1) Interfacial polarization or space charge polarization (P_{sp})

(2) Dipolar polarization (P_{dip})

(3) Atomic polarization (P_{at})

(4) Ionic polarization or electronic polarization (P_{el})

The net polarizability, P, of the dielectric material consists of the four terms in Equation 2.14.

$$P = P_{sp} + P_{dip} + P_{at} + P_{el} \qquad (2.14)$$

Each polarization mechanism leads to the dielectric properties of a material. Four modes of polarization mechanisms are demonstrated in Figure 2.4.

$$\underrightarrow{E}$$
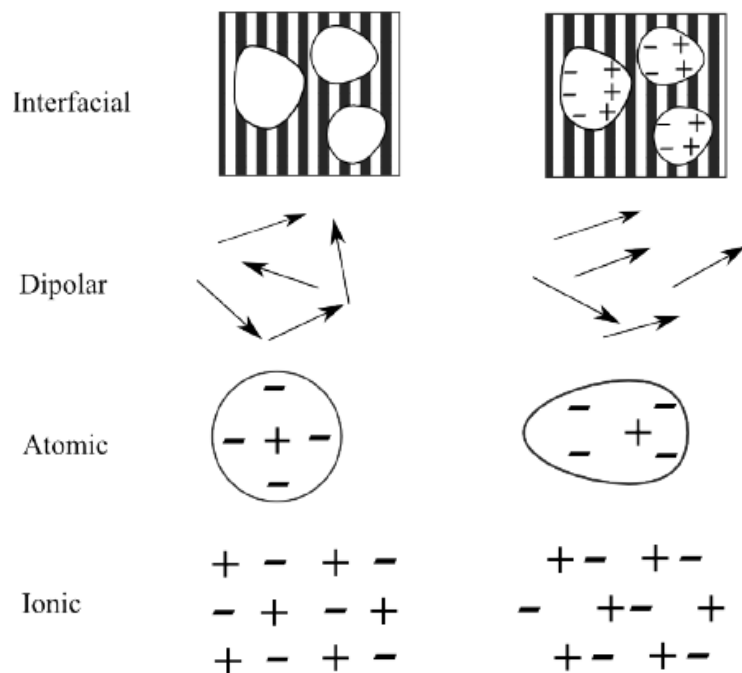
Figure 2.4 Four modes of polarization (Li, 2011)

Figure 2.5 shows the variation in relative permittivity (ε') with the loss (ε''). In the case of static electric fields (Direct Current, DC) and alternating electric fields (Alternating Current, AC) with low frequency, the polarizability of material is the sum of the involved polarizations in Equation 2.14. Molecular mechanisms depend on the movement of charges bound to atoms or molecules. However, charges are hindered or trapped at grain boundaries of impurities resulting in the gathered charges and can move through the material in an electric field showing the rise in conductivity (Shakun, 2014). In AC dielectric response of the material depends on the frequency, a sudden drop in dipole polarization region ($<10^{12}$ Hz) happens for ε' and the maximum dielectric loss. This maximum is the complete failure for the dipole to follow the oscillating electric field.
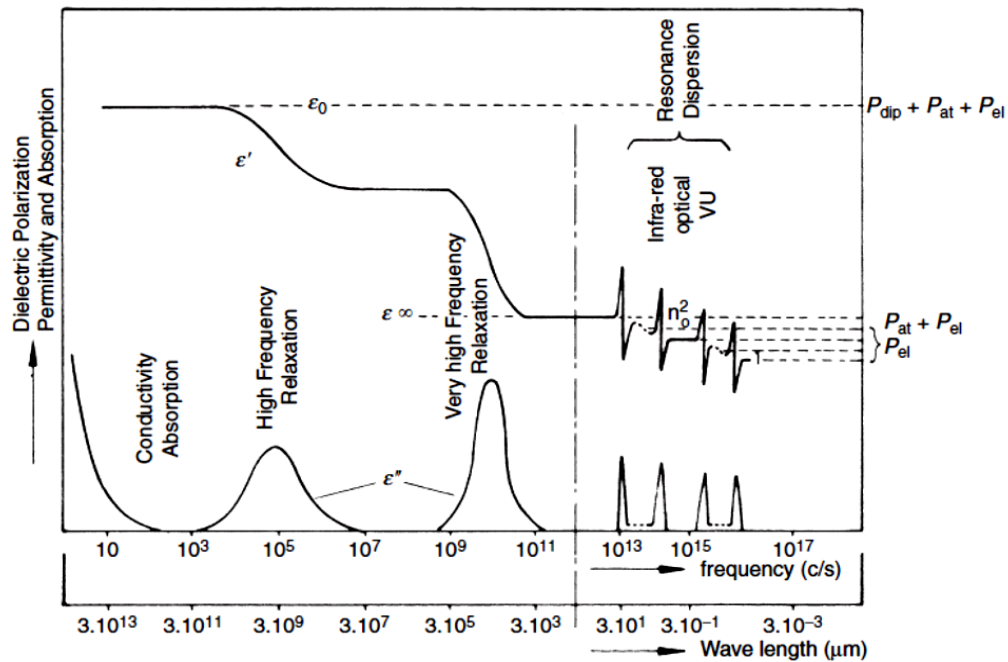
Figure 2.5 Dispersion curves of the dielectric constant (ε') and dielectric absorption or loss (ε'') in the regions of electrical, infrared, and optical frequencies (Van Krevelen, 2009).

At higher frequencies ($>10^{12}$ Hz), there are electronic and atomic polarization mechanisms. The dielectric polarization reaches a peak around a certain frequency before dropping. The optimum polarization in phase with the alternating frequency is expressed by these maximum values. The frequency of the applied electric field resonates with the material's natural frequency. Therefore, there is a maximum absorption (Ahmad, 2012). As mentioned, a dielectric in an electric field displays more than one polarization mechanism. Hence, the average induced dipole moment per molecule will be the sum of all polarization contributions, depending on which to determine the dielectric permittivity of the material. The range of relative permittivity or dielectric constant of natural rubber at 10^3 Hz is 2.40-2.70 (Al-Hartomy *et al.*, 2012). The following Table 2.1 shows the dielectric constant and loss of commercial polymers.

Table 2.1 The dielectric constant and loss tangent of commercial polymers (Ahmad, 2012; Nam *et al*., 2007).

Materials	Dielectric constant(ε')	Loss tangent (tanδ)	Frequency (Hz)
Natural rubber (NR)	2.68	0.002-0.04	10^3 Hz
Chloroprene Rubber (CR)	6.5-8.1	0.03-0.86	10^3 Hz
Acrylonitrile-Butadiene rubber (NBR, 30% acrylonitrile constant)	5.5	35	10^6 Hz
Styrene-Butadiene rubber (SBR, 25% styrene constant)	2.66	0.0009	10^3 Hz
Butyl rubber (IIR)	2.1-2.4	0.003	10^3 Hz
Ethylene-Propylene diene rubber (EPDM)	3.0-3.5	0.0004 at 60 Hz	10^3 Hz
Silicone	3.0-3.5	0.001-0.010	10^3 Hz
Teflon (PTFE)	2.0-2.2	0.0005	100 Hz

Many various mechanisms involving microscopic or macroscopic charge movement can cause polarization of a dielectric applied to an external electric field. In the case of polymer material, the total dipole moment per unit volume corresponds to the vector summation of overall molecular dipole types in the repeating unit, the polymer chain, and overall chains in the system.

In addition, aromatic rings, bromine, and sulfur are highly polarizable. The existence of these groups curse an increment in the dielectric constant. The bond in the aromatic rings is easily polarized because it is lightly attached compared to the sigma bond. Because the electron cloud is huge and far away from the effects of electrostatic attraction of the positive nucleus, large atoms, such as bromine, have a high polarizability. On the contrary, fluorine has a concentrated negative charge and a small atomic radius which can hold the electron cloud closely resulting in low polarizability. For example, Polytetrafluoroethylene (PTFE) has low relative permittivity (2.0-2.2), low

dielectric loss (<0.0002-0.0005), wide-range frequency stability up to 10 GHz, high breakdown strength (19.2 kV/mm), and stability over temperatures up to 260 °C (Li, 2011; Ahmad, 2012).

2.2 Dielectric Analysis

If we consider a dielectric parallel-plate capacitor, dielectric electric analysis (DEA) is done by placing the material between two conducting electrodes then applying a time-varying voltage between the electrodes. The resulting time-varying current (an "admittance, Y" measurement) which is the conductance (G) and capacitance of material between a pair of electrodes were measured. The conductance and capacitance arise from ionic current or dipole rotation in the bulk material between the electrodes, respectively. For polymers, mobile ions are often due to impurities and additives. In contrast, dipoles result from the permanent dipole in the material. When analyzing dielectric properties, it is possible and convenient to separate the influence of ions from dipoles, as shown in figure 2.6. (Senturia and Sheppard, 1986; Lee, 2017)
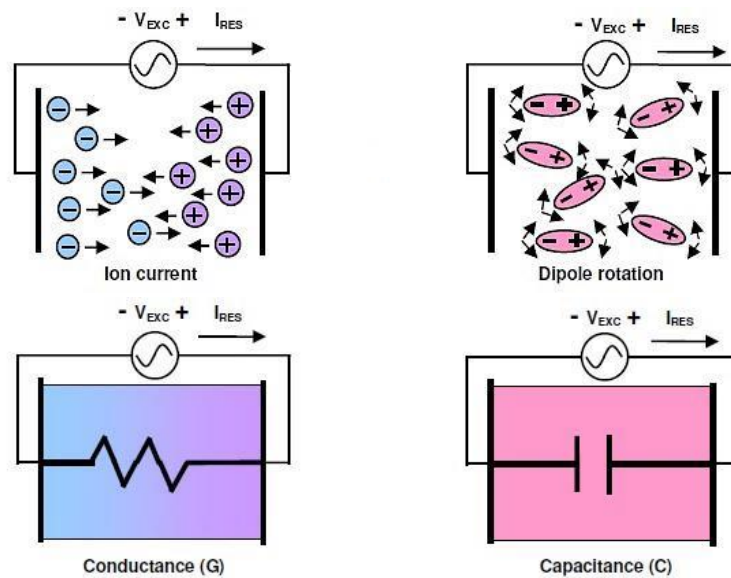
Figure 2.6 Electrical model of dielectric material under alternating field.

(Lee, 2017)

The interfacial polarization mechanism increase charge flow within the material meaning that the angle between current and voltage phase will be (90°- δ). Figure 2.7 describes the calculation of conductance and capacitance from measurement data, response current (I_{res}), and excitation voltage (V_{exc}).
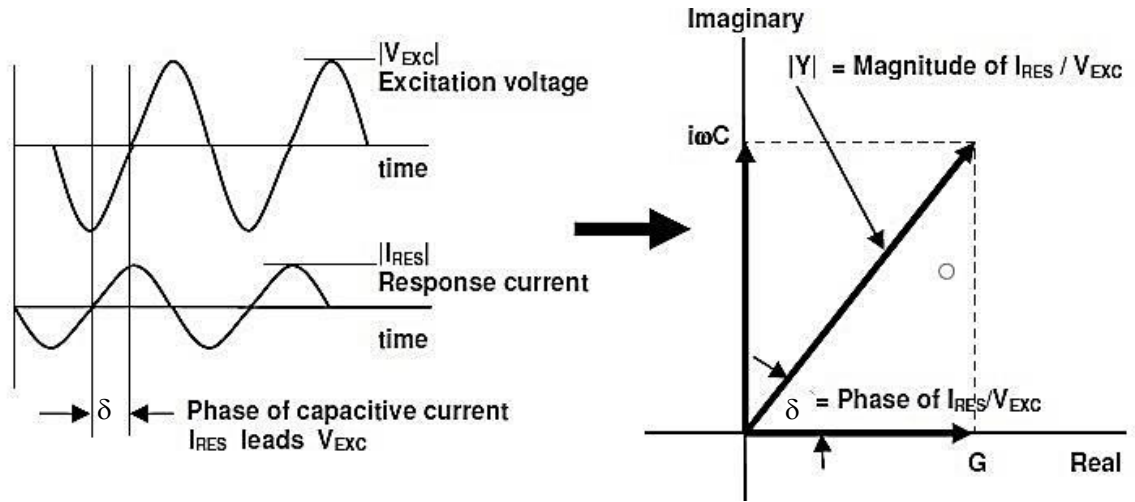
Figure 2.7 Calculation of conductance and capacitance from response current and excitation voltage (Lee, 2017).

An AC excitation voltage is applied between a pair of parallel plate electrodes and the response current is measured expressed as a function of time as shown in equation 2.15 and 2.16, respectively (Lvovich, 2012).

$$V_{exc}(t) = V_0 \sin(\omega t) \tag{2.15}$$

$$I_{res}(t) = I_0 \sin(\omega t + \delta) \tag{2.16}$$

The amplitude and phase difference of V_{exc} and I_{res} provide information to calculate the admittance (Y), as shown in Figure 2.7. Additionally, the conductance and capacitance of the dielectric material are calculated by Equation 2.17.

$$Y = \frac{I_{res}}{V_{exc}} = G + iB = G + i\omega C \qquad (2.17)$$

where ω is $2\pi f$; f is excitation frequency and B is susceptance

If we know the electrode area per thickness of dielectric (A/D ratio, the material properties of relative conductivity (σ') and relative permittivity (ε') can be calculated from Equations 2.18 and 2.19, as shown in Figure 2.8.

$$\sigma' = \frac{G}{(\varepsilon_0 A/D)} \qquad (2.18)$$

$$\varepsilon' = \frac{C}{(\varepsilon_0 A/D)} \qquad (2.19)$$
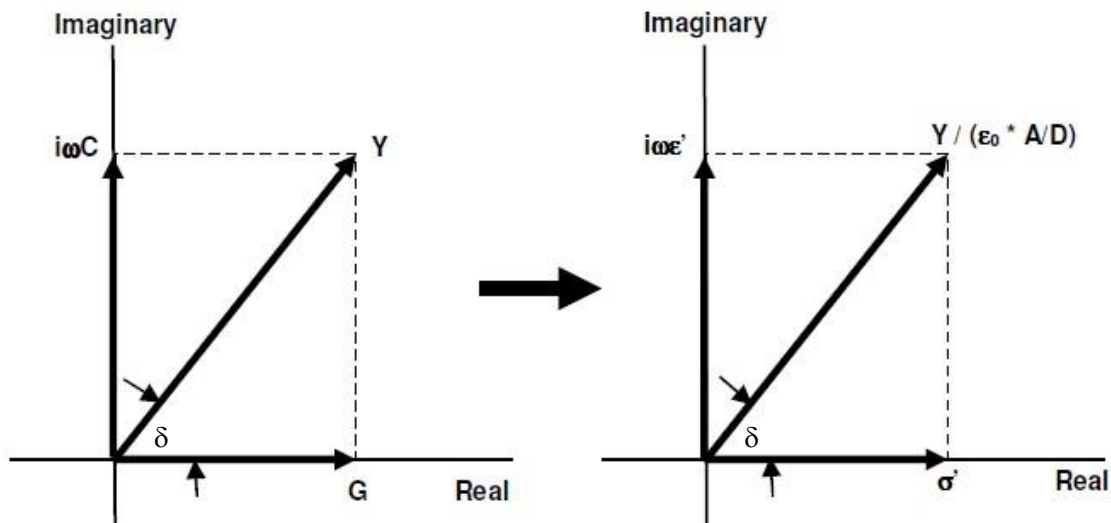
Figure 2.8 Relative conductivity and relative permittivity from the relationship between capacitance and conductance. (Lee, 2017)

The dissipation factor is another quantity also used in admittance measurements because it depends only on the phase of the admittance, not on its magnitude. The dissipation factor or loss tangent of a parallel circuit is defined as Equation 2.20.

$$tan\ \delta = \sigma'' / \omega\varepsilon' \qquad\qquad (2.20)$$

where δ is the angle between admittance and the imaginary axis in the counter-clockwise direction. The loss factor ε'' defined as Equation 2.21.

$$\varepsilon'' = \sigma' / \omega \qquad\qquad (2.21)$$

The studying of dielectric properties often uses parallel plate electrodes. However, in some cases, the distance between plates cannot be accurately controlled because its may change upon the applied pressure or the material between them expands or compress. In those situations, $tan\delta$ is used to characterize dielectric properties of material because $\varepsilon''/\varepsilon'$ does not vary with plate spacing (Lee, 2017).

2.2.1 Measurement systems

In electrical engineering, impedance (Z) is a measurement of a current to flow in the material at a given frequency of an alternating current. It is a parameter used to measure the characteristic of electronic component that is defined as the invert of admittance (Y). The impedance vector includes a real part (resistance (R)) and an imaginary part (reactance (X)) as shown in equation 2.22.

$$Z = 1/Y = R + iX \qquad\qquad (2.22)$$

The modern impedance measuring instruments can operate in a wide frequency range covering 10 Hz up to 10 GHz. A variety of methods for impedance measurement be present, for example, auto-balancing bridge and network analyzer (Dumbrava and Svilainis, 2007).

2.2.1.1 Auto-balancing bridge

An LCR meter, also known as an impedance analyzer, is an electrical testing equipment that measures a specimen's inductance (L), capacitance (C), and resistance (R). The amount of voltage generated proportional to the rate of change of current is determined by inductance. Capacitance is a measure of electrical energy stored for a given electric field and is determined by a material's ability to hold an electrical charge. In contrast, resistance is the moving obstruction of an electric current. Generally, these quantities determined from a measurement of admittance or impedance (*Z*) (KanakaRaju, 2016).

The Impedance analyzers and LCR meters are impedance measurements by using the auto-balancing bridge method which suitable for users to measure the electrical properties of a material at lower frequencies. The material is activated with an AC signal and the actual voltage across the material is observed. Material test parameters are derived by measuring its admittance and the angle between the current and voltage phase. LCR meters using the auto-balancing bridge technique provide highly accurate capacitance, dissipation factor, and conductance between 5 Hz to 40 MHz (Agilent company, 2006).

2.2.1.2 Network analyzer

A measurement of the reflection and transmission of material with knowledge of sample dimensions offers the information to characterize the permittivity and permeability of the material. Network analyzer performs accurate measurement of the ratios of the transmitted signal to the incident signal and the reflected signal to the incident signal. It can be used to characterize both radio frequency (RF) devices and optical transmission systems at high-frequency measurements from 300 kHz to 110 GHz.

A vector network analyzer consists of a signal source, a receiver, and a display as shown in Figure 2.9. The source sends a signal at a single frequency to the material under test (MUT). The fixed frequency receiver detects the reflected and transmitted signals from the material which are the magnitude and phase shift at that

frequency. Then, the source is stepped to the next frequency. The measurement is repeated to display the reflection and transmission measurement response as a function of frequency (Agilent company, 2006). The difference between auto-balancing bridge and network analysis measurements as well as the frequency ranges covered are shown in table 2.2.
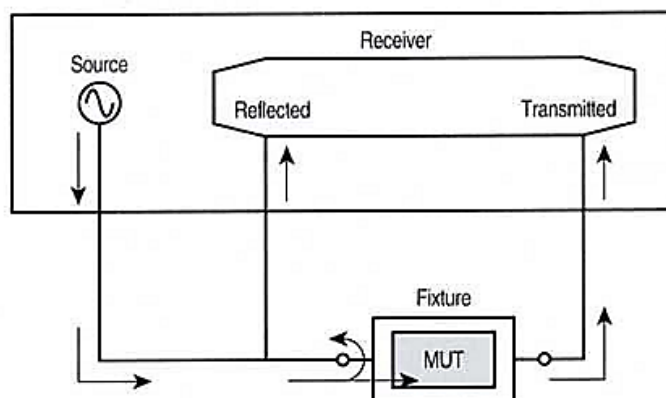
Figure 2.9 Network analyzer (Agilent company, 2006).

Table 2.2 The difference between auto-balancing bridge and network analysis impedance measurements (KanakaRaju, 2016).

Systems	Advantage	Disadvantage	Frequency range	Application
Auto balancing bridge	Most accurate, Wide impedance measurement range Wide frequency coverage	Limited frequency coverage	5 Hz – 40 MHz	All impedance measurement applications in low frequency
Network analyzer	Very broad frequency coverage (LF through microwave)	The range of impedance measurements is limited by the analyzer's characteristic impedance.	≥ 10 kHz	Components and materials measurement

2.2.2 Measurement method

There are many methods developed for measuring dielectric properties of the material, for instance, resistivity cell, coaxial probe, transmission line, resonant cavity, free space, and parallel plate techniques (Hewlett-Packard company, 1992). Many factors, for example, accuracy, convenience, material shape, and form are important in selecting the most appropriate measurement technique. Table 2.3 compares between the measurement methods and the suitable condition of each method for Dielectric Analysis (DEA) measurements.

Table 2.3 Comparison of the suitable conditions of each method for DEA measurement (Hewlett-Packard company, 1992).

Method	Frequency range	Comments
Resistivity cell	DC	Requires flat, disk-shaped sample. Ideal for sheets and film. Inexpensive, simple analysis
Parallel plate	<30 MHz	Requires flat, disk-shaped sample. Ideal for sheets and film. Inexpensive, simple analysis
Coaxial probe	200 MHz-20GHz	Ideal for liquids, semi-solids. Solids must have a flat surface. Easy to use, limited low loss resolution.
Transmission line	500 MHz-110 GHz	Requires brick or toroid-shaped sample. Liquids and gas must be contained. Limited low loss resolution.
Cavity	500 MHz-110 GHz	Requires precisely known sample shape. Very accurate. Sensitive to low loss tangent.
Free space	2 GHz-110 GHz	Requires flat, parallel face sample. A large sample is required.

When using a parallel plate, the basic measurement involves determining the admittance between the electrodes under an alternating electric field. Parallel plates are often used as electrodes in cure studies. Figure 2.10 shows parallel conductors of the area separated by spacing. The sample medium is placed between the plates. Normally, one designs the plate spacing to be much less than the plate size, which minimizes the effects of fringing fields and leads to a very simple calibration. An LCR meter or impedance analyzer is usually used to measure the electrical properties of the sample. The dielectric constant is computed from the capacitance measurement while dielectric loss is computed from the dissipation factor. The advantages of parallel plate electrodes are simple and measured data can be interpreted. The disadvantages are the plate spacing must be control and the admittance measurements at low frequencies (<100 Hz) are difficult to interpret. Additional problems are introduced by the overall admittance level and by cabling and shielding issues (Senturia and Sheppard, 1986).
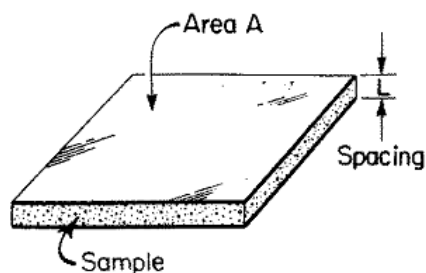
Figure 2.10 Parallel plate electrodes (Senturia and Sheppard, 1986)

In Figure 2.11, the parallel-plate sample is connected to a meter by a coaxial cable (~100 pF/m). A 2-meter cable introduces a capacitance of 200 pF in parallel with the sample, which must be subtracted from the measured capacitance to determine the sample capacitance. When the cable capacitance is comparable to the sample capacitance, sensitivity and accuracy are reduced (Senturia and Sheppard, 1986).
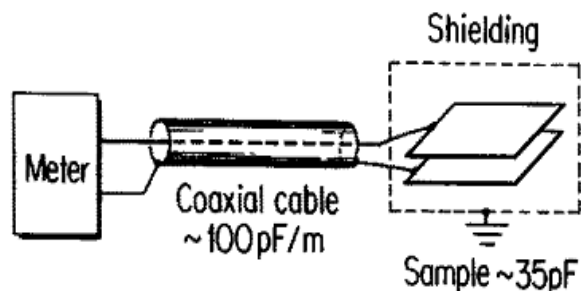
Figure 2.11 Schematic diagram of admittance measurement.

(Senturia and Sheppard, 1986)

The following additional advantages of the parallel plate are exposed. It has the potential for high accuracy measurement. Parallel plate data shows a good correlation with data from thermal analysis techniques such as differential scanning calorimetry (DSC) and dynamic mechanical analysis (DMA). Moreover, the parallel plate configuration measures the average or bulk electrical properties of the sample which is more representative of overall cure than surface-only measurements (McIihagger *et al*., 2000).

In the case of this research, it is aiming to study the capacitance and conductance of natural rubber during the crosslinking process which sample is flat and requires accurate results at low-frequency measurement. From a comparison between the measurement systems and methods that have been shown in Tables 2.2 and 2.3, the suitable method is the parallel plate technique with LCR meter (auto-balancing bridge) measurement.

2.3. Dielectric cure monitoring

The ions and dipoles present in the material cause conductive and capacitive features in dielectric cure monitoring. The ions and dipole in a sample initially have a random orientation before an electric field is introduced. The ions go towards an electrode of opposite polarity when an electric field is applied to the sample, while the dipoles strive to align with the electric field. During the procedure, the resultant signal is

produced by measuring the amplitude and phase shift concerning the ions' mobility and dipole alignment (Hardis *et al*., 2013).

2.3.1 Dielectric cure monitoring of resin

A dielectric analysis is the most promising technique to monitor the cure of thermosetting resin material because it can continuously monitor the resin cure chemistry throughout the process going from liquid to crosslinked solid (Choi *et al*., 2003). The use of dielectric analysis for thermoset cure monitoring is based on the influence of structural change on the material's dielectric and electrical characteristics.

The changes in dielectric properties during cure involve (1) an increase in viscosity that obstructs ion translational diffusion in the medium, resulting in a decrease in ionic conductivity; (2) The relaxation characteristics of field-induced orientation and oscillation of permanent dipoles are changed during structural evolution; and (3) Variations in the dipole moment per unit volume occur while curing as a result of increased branching, greater crosslink density, and changes in the dipole population's nature. (Vassilikou-Dova and Kalogeras, 2009). Previous research has shown that dielectric analysis may be used to track the polymer curing process in real time.

Kim and Char (1999) used differential scanning calorimetry (DSC), rheometrics mechanical spectrometry (RMS), and dielectric analysis to investigate the curing characteristics of diglycidyl ether of bisphenol A (DGEBA) with diaminodiphenylmethane (DDM) as a curing agent (DEA). The inverse correlation between RMS-measured complex viscosity and DEA-measured ionic conductivity was confirmed. The chain segment motion was revealed by the complex viscosity obtained from RMS and the mobility of ionic species was represented by the ionic conductivity in DEA measurement were equivalent. From isothermal curing measurements at different temperatures in the early stages of cure, the ionic conductivity contribution was shown to be dominant in the dielectric loss factor. As the curing progressed, the dipole relaxation's contribution to the dielectric loss factor increased. As the isothermal curing temperature

rises, the critical degrees of cure, or the point at which the dipolar contribution to the dielectric loss factor begins to appear, increases.

Skordos and Partridge (2004) developed a new methodology for the quantitative determination of the progress of the curing reaction of a resin by using the impedance spectroscopy technique. The results show that the imaginary impedance maximum is related to the reaction progress. Moreover, the close correlation between the reaction rate as measured by conventional differential scanning calorimetry and the rate of change of the imaginary impedance spectrum maximum value was observed. Therefore, this technique can be used as a real-time online control tool for thermoset composite manufacturing.

2.3.2 Dielectric cure monitoring of rubber

The prior works of literature have established the relationship between the dielectric properties of polymeric resins which exhibit rheometric and chemical behavior such as melt, gelation, and crosslinking that can be recognized by dielectric properties. Moreover, dielectric spectroscopy can be utilized to study the vulcanization of rubbers. The common method of vulcanization is compounding the rubber with sulfur and additives then curing, resulting in the formation of sulfide crosslinks that affect the changes in dielectric and rheology properties of rubber. The previous works related to rubber's dielectric properties and the development of dielectric monitoring systems are shown below.

Persson (1986) investigated the dielectric properties of rubber materials (natural rubber, butyl rubber, butadiene rubber, and acrylonitrile butadiene rubber) which were cured by sulfur and peroxide vulcanization. It has been found that the width of the dispersion curve correlates well with the crosslink density. In addition, during thermo-oxidative aging of sulfur-cured natural rubber, a large widening of the dispersion curve (*tan δ*) is found at frequencies lower than 1 MHz and the f_{max} value decreases with increasing crosslink density.

Capps and Coughiin (1992) studied the viscoelastic and dielectric behaviors of cure systems and plasticizer loading in chemically crosslinked butyl and chlorobutyl rubbers. Dielectric permittivity and loss were measured as functions of frequency and temperature. It is founded that the viscoelastic and dielectric behaviors were significantly influenced by the type of crosslinking system and by plasticizer loading.

A new technique was proposed by Gondoh *et al*., 1997; Gondoh *et al*., 1998 to monitor the progress of vulcanization of acrylonitrile-butadiene rubber based on the measurement of electrical properties. The loss tangent (tanδ) was measured by a tanδ meter, applying 40 or 120 V of alternating current at 60 Hz. The electrical current was measured by an ammeter. The vulcanization was carried out in the press mold at 140-170°C, equipped with two electrodes insulated from its surroundings by polytetrafluoroethylene as shown in Figure 2.12. The results showed that the curves of electric current and tanδ against cure time showed a rapid increase with the progress of vulcanization reaction followed by saturation after completion of the reaction. The curves obtained in the electrical measurements were found to be similar to conventional torque-cure time curves, suggesting that the tanδ and electrical current curves are very useful as a cure curve.
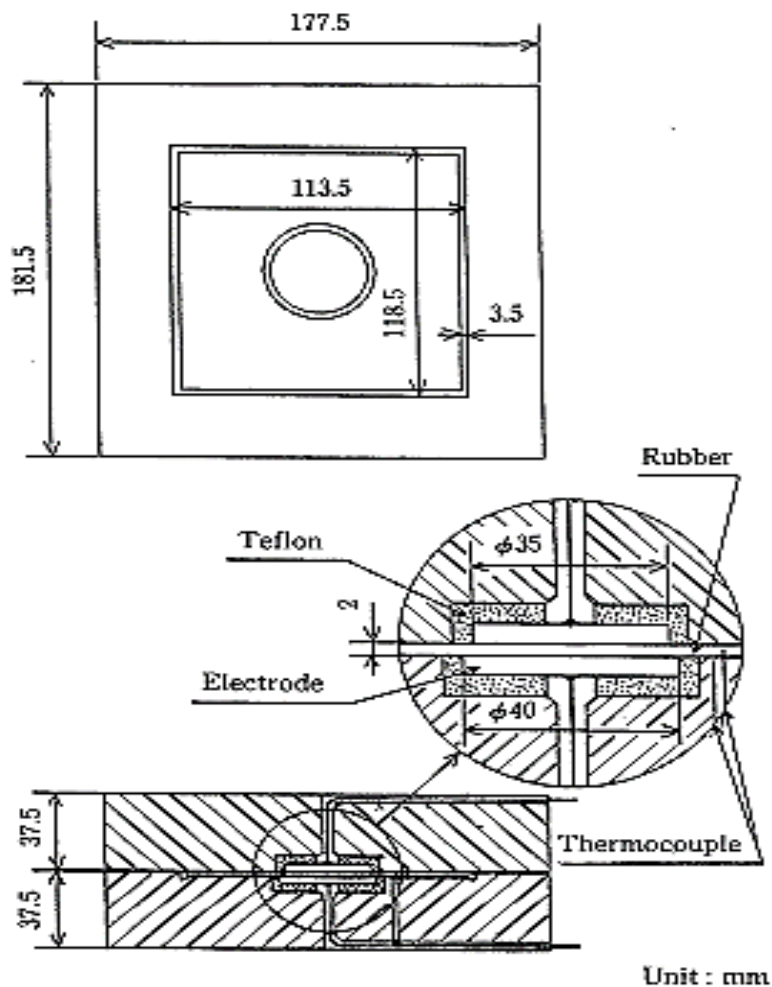
Figure 2.12 Mold design (Gondoh *et al*., 1998).

Hummel and Rodriguez (2000) described a method for measuring the electrical conductivity of rubber during vulcanization, continuous low-level current (CLLC) measurements. Direct-current voltage was applied to the compound with two platinum electrodes, then, the current was recorded during vulcanization. These measurements give direct prove of ions in the rubber during vulcanization. The results showed that the current curves were related to the vulcanization kinetics. Two maxima currents were found in the system NR/S/TMTM/ZnO. They take place at an earlier scorching period corresponding to the formation of temporary ionic species at these stages which is supported by the result from Hummel and Rodriguez (2001). At elevated temperatures,

the conductivity of the rubber compound was increased according to the presence of transitory ionic species. The comparison with the rheometer measurements exhibits a relationship between the formation of ionic intermediates and crosslinking. In addition, Rodriguez *et al*. (2000) suggest the CLLC for detecting ionic species in the course of vulcanization reactions were applied to investigate the vulcanization of a mixture of natural rubber, sulfur, and zinc bis(dimethyl dithiocarbamate). A temperature-dependent current maximum was found because ionic species occur during the vulcanization reactions. The current maxima corresponded to vulcanization times, where a rubber network crosslinking was increased, as measured using vulcametry.

Microwave dielectric measurement for following and monitoring the progress of vulcanization reaction was reported by Bovtun *et al*., 2001; Bovtun *et al.,* 2002. The change of microwave dielectric permittivity may be caused by the change of concentration of the polar molecules and groups during vulcanization. The difference in dielectric behavior between unvulcanized and vulcanized compounds was clearly seen. The main advantage of the method was the ability to measure the fundamental dielectric response of basic polymer molecules and to reflect the polymer network dynamics and their change during crosslinking. The microwave method was effective even in the case when low-frequency dielectric methods fail because of conductivity in carbon black-filled elastomers.

Abd-El-Messieh and Abd-El-Nour (2003) investigated the dielectric properties of styrene-butadiene rubber cured by an increase in either the sulfur content or curing time in a wide range of electric field frequencies from 100 Hz up to 10 MHz at room temperature (25°C). The results showed that the permittivity increased with increasing the sulfur content, but it decreased with increasing applied frequency. The maximum loss seems to be shifted to the lower frequency range with increases in the sulfur content. The values of permittivity slightly increased with increasing curing time. The maximum values of loss decreased with increasing curing time. The relaxation times increased with an increase in either sulfur content or curing time due to the formation of crosslinking.

Van Doren *et al*. (2004) developed the measuring system for natural and synthetic rubber curing processes by using dielectric properties to produce a curing curve (impedance property data versus time) followed by analyzing the curve with software algorithm. The results show that impedance correlated with the rheological properties of the rubber compound and the mechanical properties of the rubber. Moreover, applying the correlation relationship in real-time to end the curing process can produce a uniform quality of rubber parts and reduce process cycle time.

Miratsu *et al*. (2013) measured the electric impedance of acrylonitrile-butadiene rubber compounds during the vulcanization reactions. In the vulcanization region, the crosslink densities and torques increased, while the impedance decreased. This tendency might reflect that the electrons, which form an electric current, flow more by increasing crosslink networks of the rubber sample.

Fillers, such as carbon black is added to rubber formulations to meet material property targets, such as tensile strength, tear strength, abrasion resistance, and to decrease the cost. The filler incorporation in rubber leads to the creation of an interface between two faces of different conductivity and permittivity. Interfacial polarization can be found at the interface between rubber and fillers that affect to electrical properties of materials. The electrical properties of rubber/ filler compounds have been studied by several research groups.

Chung *et al.* (1982) studied the electrical conductivity and permittivity of carbon black-polyvinylchloride composites over a wide frequency spectrum (1.3 GHz). The conductivity of the bulk composites increased with a higher volume fraction of carbon black. The permittivity increased until the composite percolation was reached and then decreased confirmed after fully connected conductive paths. Such highly loaded composites showed a metal-like electrical behavior. The different electrical percolation threshold of the composites was found for different types of carbon black. Carbon blacks with the lowest packing efficiency reach the percolation threshold with the least volume fraction of carbon black loading.

Li *et al*. (2009) studied the effect of carbon blacks (semi-reinforcement furnace black (SRF), fast extruding furnace black (FEF), high abrasion furnace black (HAF), conductive carbon black (CCB), and spraying carbon black (SCB)) on the electrical properties of filled ethylene propylene diene rubber (EPDM). The results from electrical tests showed that EPDM filled with CCB, large surface area carbon black, displays the lowest dielectric constant and highest dissipation factor.

Renukappa et al. (2009) investigated the electrical properties of composites, such as dielectric constant and dissipation factor. Different weight ratios of conductive carbon black were used to produce a series of styrene-butadiene rubber (SBR) composites. The effects of CCB content on electrical characteristics were investigated. The dielectric constant and dissipation factor of SBR composites improved as the CCB content was increased. Until the volume fraction (V_f) of the CCB reaches a critical value, known as the threshold percolation concentration, the conductivity does not change. A significant growth in conductivity was detected beyond the percolation threshold concentration. The development of infinitely long chains of conducting particles causes the dielectric constant to increase at a critical value of V_f. As a result, adding varied amounts of CCB to SBR resulted in compounds with different dielectric properties.

Nanda *et al*. (2010) studied the dielectric relaxation of conductive carbon black reinforced chlorosulfonate polyethylene rubber (CSM) vulcanized in the frequency range of 10^2–10^6 Hz over a wide range of temperature 30–120°C. The results showed that with increasing filler loadings, an increase in dielectric permittivity was observed which could be explained based on interfacial polarization of the fillers in the polymer matrix. The percolation threshold occurred at 30 phr loadings. In addition, the effect of temperature on the loss tangent, dielectric permittivity, and ac conductivity had been studied. When the temperature was raised, the maximum loss tangent peak had been shifted towards higher frequency, increase in dielectric permittivity and increase in ac conductivity due to thermal activation.

Shokr (2011) compared the dielectric properties of EPDM composite crosslinked by gamma irradiation, laser beam irradiation, and chemical vulcanization. The frequency

response of dielectric behavior has been studied for all prepared samples using an LCR meter in the frequency range 10^2- 10^5 Hz. The experimental results indicated that permittivity and conductance increased with the addition of HAF black in the EPDM matrix. A sharp increase in permittivity was detected for EPDM loaded with HAF black more than 30 phr. The percolation threshold was affected by the vulcanizing methods, where the samples vulcanized by 5 and 10 laser shots show the minimum value for the percolation threshold.

As mentioned before, we can summarize that one application that has been studied using dielectric spectroscopy is the vulcanization of rubbers. Natural rubber is non-polar but the process of vulcanization introduces dipoles originating in the carbon-sulfur linkages. The cross-linking process in rubbers may also be initiated by peroxides or radiation. In comparison to vulcanization using sulfur, no polar groups are built into the chains when peroxides are used, hence one may expect a smaller permittivity for the corresponding cross-linked material. Similarly, cross-linking by irradiation does not produce polar groups when the reaction takes place in a vacuum but will result in oxidation if irradiation takes place in the presence of oxygen (Craig, 2005). Moreover, the effects of filler on the electrical properties are reported, when filler loading was increased the dielectric permittivity was raised due to the effect from interfacial polarization of the fillers in the polymer matrix. In the case of conductive filler, the dielectric permittivity increases until the percolation threshold was reached and then decreases after fully connected conductive paths.

CHAPTER 3

EXPERIMENTAL AND METHODOLOGY

3.1 Material

3.1.1 Natural rubber (STR 5L) was obtained from Yala latex industry Co., LTD, Yala Thailand. The molecular formula of repeating unit and its specific gravity are C_5H_8 and 0.92, respectively.

3.1.2 Zinc oxide (ZnO) (White seal grade) was used as an activator in sulfur vulcanization system. It was manufactured by Global Chemical Co. Ltd., Samutprakarn, Thailand. The specific gravity and melting point are 5.57 and 130°C, respectively.

3.1.3 Stearic acid (commercial grade) was used as a co-activator with zinc oxide in sulfur system. It was manufactured by Imperial Chemical Co. Ltd., Pathum Thani, Thailand. The molecular formula is $C_{17}H_{35}COOH$. The molecular weight is 248.48 g / mol. The specific gravity is 0.85. The melting point is 69.6 °C.

3.1.4 N-tert-Butyl-2-benzothiazole sulfonamide (TBBS) was used as an accelerator in vulcanized natural rubber. It has a cream to light brown pigment. The molecular weight is 238 g/mol. The specific gravity is 1.28. The melting point is in the range 107-112 °C. It was produced by Flexsys America L.P., U.S.A.

3.1.5 Sulfur used as curing agent in vulcanized natural rubber in peroxide system. It was manufactured by Ajax Finechem Pty Ltd., Taren Point, Australia. The molecular formula is S_8. The specific gravity is 1.92. The melting point is 115 °C.

3.1.6 Dicumyl peroxide (DCP) is aromatic peroxide used as curing agent. It has a milky white granule, a melting point of 39-41°C, and decomposed at 168 °C. its molecular weight and specific gravity are 270.37 g/mol and 1.02, respectively. It was produced by Wuzhou International Co., Ltd., China.

3.1.7 Carbon black (N330 grade) is a black powder and has a specific gravity of 1.85. It acts as a filler to increase efficiency in rubber. It was manufactured by Thai Carbon Black Public Co., Ltd., Thailand.

3.2 Equipment

3.2.1 Internal mixer, Brabender 50®EHT with 70 cm³ chamber volumes and tangential rotors was manufactured by Brabender GmbH & Co. KG, Duisburg, Germany. It was used to prepare natural rubber compound.

3.2.2 Two-roll mill was used to mix accelerator and sulfur into rubber compounds, and sheet rubber masterbatch. The roll size of two roll mill is 150 mm x 350 mm of diameter x length. It was manufactured by Chaichareon Karnchang Ltd. (Bangkok, Thailand).

3.2.3 Compression machine was manufactured by Chaichareon Karnchang Ltd., Bangkok, Thailand. It was used to prepare and monitor rubber vulcanization.

3.2.4 A Montech Moving Die Rheometer (MDRH2020) was used to study cure characteristics of rubber compounds. The minimum torque (M_L), maximum torque (M_H), delta torque (M_H-M_L), scorch time (t_{s1}) and cure time (t_{c90}) were obtained.

3.3 Method

3.3.1 Rubber cure monitoring system (RCMS)

The experimental setup of rubber cure monitoring system (RCMS) is displayed in Figure 3.1.
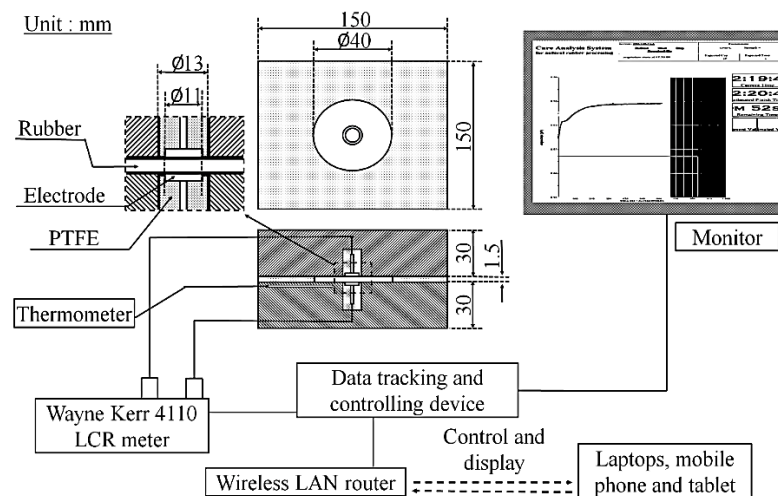
Figure 3.1 Sketch of the experimental set-up for rubber cure monitoring system.

Parallel plates, made from stainless steel and insulated by polytetrafluoroethylene (PTFE), are used as electrodes. The upper and lower electrodes with diameters of 11 mm were embedded in compression mold which has 1.5 mm height and 40 mm diameter as shown in Figure 3.2 to Figure 3.4. Thermocouples (Figure 3.5) were also embedded in the mold nearly the electrodes which connected to the LCR meter (Figure 3.6), Wayne Kerr 4110. The 2 V of alternating voltage is applied between the parallel plate electrodes at a constant frequency. LCR meter was connecting with sensors to monitor electrical changes of rubber compounds during vulcanization. Then, information was sent to the data tracking and controlling device (Figure 3.7).
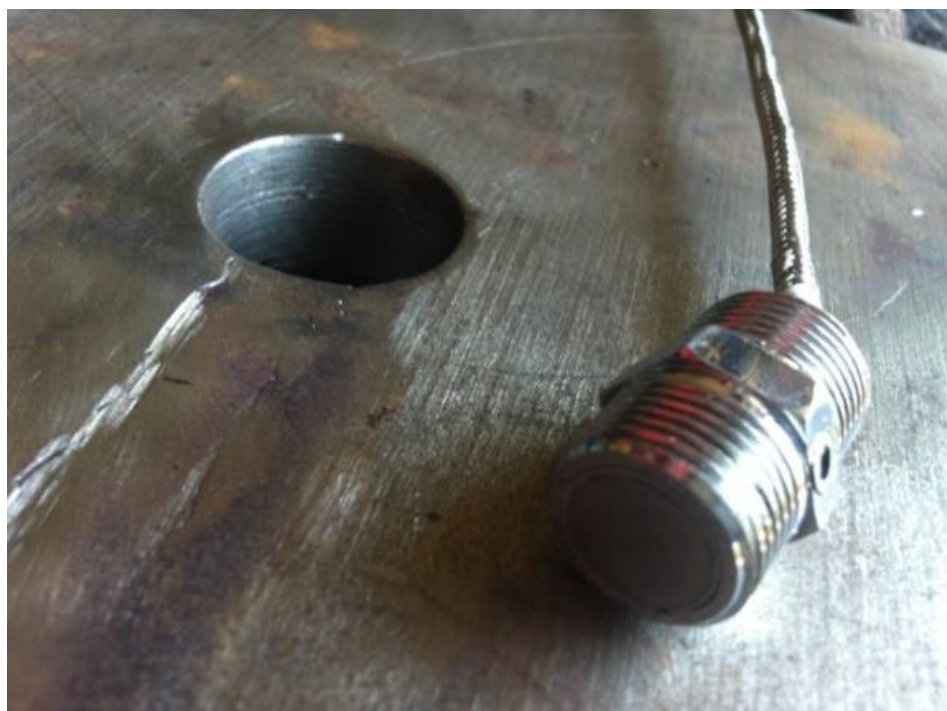
Figure 3.2 The obtained parallel plates electrodes.
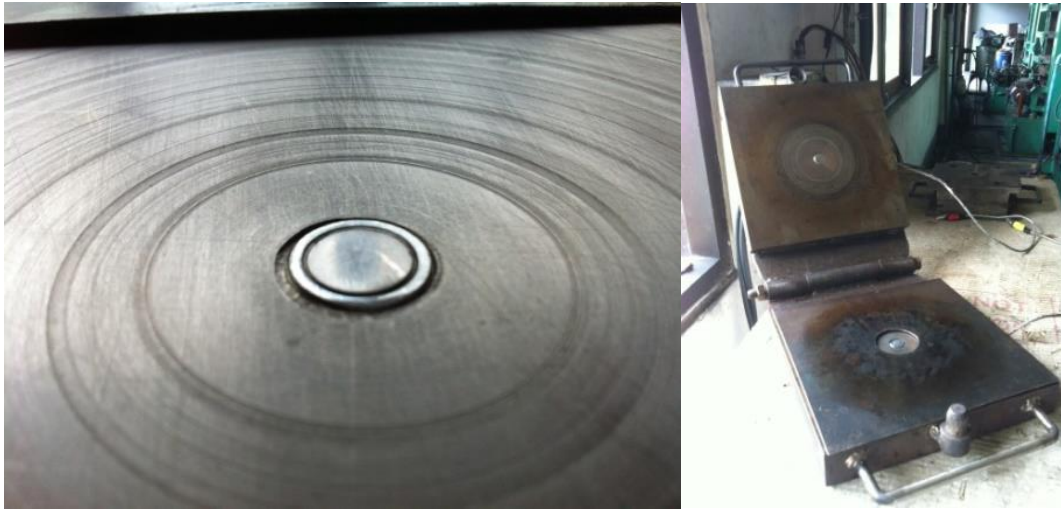
Figure 3.3 The upper and lower electrodes were embedded in a compression mold.

Figure 3.4 The embedded electrodes in compression mold and equipment settings.

Figure 3.5 Thermocouples with a heat resistant strap and display unit.

Figure 3.6 LCR meter.

Figure 3.7 Data tracking and controlling device.

This data tracking and controlling device can control and operate via wireless LAN and display the result via an attached monitor or devices that can connect to other wireless networks (Figure 3.8). During the vulcanization, the system can display the trend of the changed electrical values in real time via a wireless network. And after the test, data can be easily downloaded, saved and displayed on the computer via the wireless network. However, it is necessary to reduce the noise in the system and calibrate the measured electrical values before testing for the accuracy of test results as following:

1. Intercept the noise when the probe on both sides does not touch each other by opening the mold and then transact on the LCR meter. Select Calibrate> Open Circuit Trim > 20 Hz-100 kHz.

2. Intercept the noise when the probes on both sides touch each other by closing the mold and the upper and lower sensors touch each other. And then transact on the LCR meter. Select Calibrate> Short Circuit Trim > 20 Hz-100 kHz.

3. Calibrate the measured value by placing 1mm thick polytetrafluoroethylene (TEFLON) sheet on the sensor position. Close the mold and press <start> in

order to the electrical value𝑛 for 30 seconds. The obtained electrical values should be consistent during the test and should be close to electrical values of TEFLON. Its permittivity and dielectric loss are 2.1 and ~0, respectively. The TEFLON sheet and the calibration values on the display screen are shown in Figure 3.9 and Table 3.1

Table 3.1 Relative permittivity (ε'), dielectric loss (ε'') and tan δ of polytetrafluoroethylene at 5 kHz and 75 kHz

Frequency (kHz)	C_p (F)	G_p (S)	ε'	ε''	tan δ
5	1.58×10^{-12}	3.27×10^{-11}	2.1573	0.0014	0.0007
75	1.58×10^{-12}	5.54×10^{-10}	2.1571	0.0016	0.0007
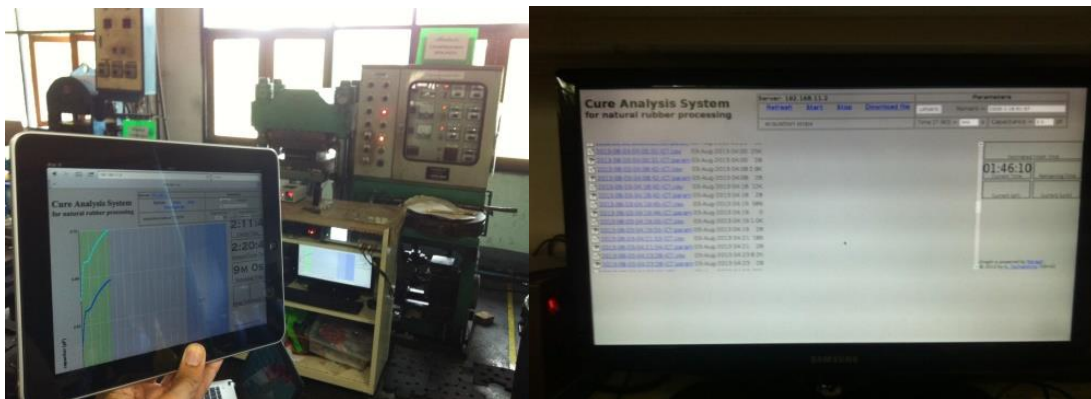
Figure 3.8 Operation screen and wirelessly download data via the prototype system software.
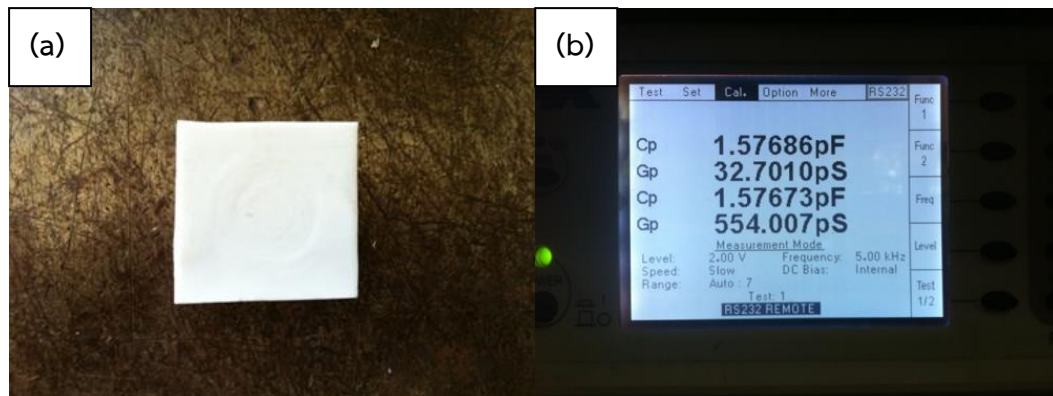
Figure 3.9 (a) The TEFLON sheet and (b) the calibration values on the display screen including capacitance (C_p) and conductance (G_p) at the frequency of 5 kHz and 75 kHz.

The obtained C_p and G_p were used to calculate permittivity (ε'), dielectric loss (ε'') and tan δ as listed in Table 3.1 . It was indicated that the prototype system can accurately measure the electrical values.

3.3.2 Preparation of Natural Rubber Compound

The materials used in this research were commercial-grade, with their quantities listed in Table 3.2. The formulation in per hundred of rubber: natural rubber (NR) 100, zinc oxide (ZnO) 5, stearic acid 2, N-tert-Butyl-2-benzothiazole sulfonamide (TBBS) 1, and sulfur 2 was used to prepare NR compound in 2 steps. The first step involved compounding NR, ZnO, and stearic acid in an internal mixer with a filled factor of 0.75, a rotor speed of 60 rpm, and an initial chamber temperature of 35 ºC according to the mixing schedule shown in Table 3.3 . Then the compound was dumped and kept at room temperature in a desiccator for 24 h before further processing. In the second step, other ingredients such as the accelerator (TBBS) and sulfur were added and were mixed for about 4 min. Finally, the compound was sheeted off to a 2 mm thickness by using a two-roll mixing mill.

Table 3.2 Formulation of NR compound

Ingredients	Part per hundred rubber (phr)
Natural rubber (STR 5L)	100
Zinc oxide (ZnO)	5
Stearic acid	2
N-tert-Butyl-2-benzothiazole sulfonamide (TBBS)	1
Sulfur	2

Table 3.3 The mixing schedule of NR compound

Mixing procedure	Cumulative time (min)
Step 1: Internal mixer	
- NR mastication	0
- Addition of stearic acid	2
- Addition of zinc oxide (ZnO)	3
- Dumping	9
Step 2: Two roll mill	
- Addition of the mixer from step 1	0
- Addition of TBBS and sulfur	2
- Addition of sulfur	3
- Dumping	4
Total	13

3.3.3 Material characterization

Rubber compounds were characterized by using moving die rheometer (MDR) and rubber cure monitoring system (RCMS) under isothermal condition. MDR and RCMS methods are used to monitor the cure reaction by following an increase of torque and a change of electrical properties, respectively, which is indicative of crosslinking as a function of time at a constant temperature.

3.3.3.1 Moving die rheometer (MDR) test

The isothermal cure of a natural rubber compound was investigated by using a Montech Moving Die Rheometer (MDRH2020) at die oscillation angle of 0.5° and a frequency of 1.7 Hz. The sealed torsion shear cure meter was selected according to ASTM D5289. In order to make rheological measurements in condition close to NR compression molding processes, the designed 4 cm^3 NR compound was filled in a closed and sealed die cavity. The torque increment was measured at constant amplitude of oscillation and a designed temperature. The torque required to shear the compound due to the formation of the crosslinked structure of rubber chains is consistently plotted as a function of time to provide the cure curve. The main cure characteristic values obtained from cure curve including:

- The lowest point in the cure curve is defined as the minimum torque (M_L).
- The highest point at curve plateau is termed as the maximum torque (M_H).
- The time to reach a given degree of cure (t_{cx}) can be gotten from the following equation:

$$t_{cx} \quad = \text{minutes to torque being } (M_L \ + \ \frac{x \ \text{ x } \ \Delta M}{100} \ ) \qquad\qquad (3.1)$$

where x is the percentage of cure required and ΔM or delta torque is the difference between the maximum and the minimum torque (M_H - M_L). The optimum cure time (t_{c90}) is used for optimal crosslinking in rubber vulcanizate.

3.3.3.2 Rubber cure monitoring system (RCMS) test

The experimental setup of the rubber cure monitoring system (RCMS) is shown in Figure 3.1. Parallel plates are used as electrodes. The upper and lower electrodes with diameters of 11 mm were embedded in compression mold which has 1.5 mm height and 40 mm diameter. Thermocouples were also embedded in the mold nearly the electrodes which connected to the LCR meter, Wayne Kerr 4110. The 2 V of alternating voltage is applied between the parallel plate electrodes at a constant frequency of 5 kHz. The capacitance (C) and conductance (G) are continuously detected every 4 s as a function of vulcanization time for 15 min. Before testing, 1

mm thickness of PTFE was used as a standard sample to calibrate the RCMS. The volume 4 cm^3 rubber compound was placed into the preheated mold at the designed temperature in the compression machine and then compressed under 10 MPa. Data tracking and controlling device were used to record the electrical properties during NR vulcanization. The curve of capacitance or conductance versus cure time was exhibited on the monitor connected to the local area network of RCMS.

3.4 Study parameters

3.4.1 Effect of frequency

The frequencies i.e., 0.75, 1, 2.5, 5, 7.5, 10, 25, 50, 75, and 100 kHz were examined at 160°C for 15 min, to find an appropriate informative frequency in the initial experiment. The studied material was a natural rubber compound with a conventional sulfur curing system. The formulation of the NR compound is listed in Table 3.2.

3.4.2 Effect of vulcanization temperature

Three different test temperatures of 150, 160, and 170°C were examined and tested for 15 min at a suitable informative frequency of 5 kHz. The investigated material was a natural rubber compound with a CV system. The formulation of the NR compound is given in Table 3.2.

3.4.3 Effect of vulcanization system including sulfur vulcanization system (EV, Semi-EV, CV) and peroxide vulcanization system

In the sulfur vulcanization system, the ratio between accelerator and sulfur is used to determine the quantity and linkage types. In the case of a conventional vulcanization system (CV), the ratio between accelerator and sulfur is low resulting in occurrence in most polysulphides linkages (-S_x-). The sulfur content is in the range of 2.0-3.5 phr and the accelerator is in the range of 0.4-1.0 phr. In a semi- efficient vulcanization system, the sulfur content and the accelerator are in the range of 0.5-1.2 phr and 0.4-1.0 phr, respectively. The efficient vulcanizing (EV) has the sulfur content and the accelerator in the range of 0-0.2 phr and 2.5-3.0 phr, respectively. For the peroxide vulcanization system, dicumyl peroxide has widely been used as a

vulcanizing agent. When heating, peroxide agent will break down, then provide free radicles and finally form C-C crosslinking on polymer chains. Formulation of NR compound by studying the effect of vulcanization system and different type vulcanizing agent on electrical values is shown in Table 3.4.

Table 3.4 Formulation of NR compound by studying the effect of vulcanization system and different vulcanizing agent types on electrical values

Components	Part per hundred rubber (phr)			
	Sulfur system			Peroxide system
	CV	Semi-EV	EV	
Accelerator/Sulfur ratio	0.5:3	1.5:1	3:0	-
Natural rubber (STR 5L)	100	100	100	100
Zinc oxide	5	5	5	-
Stearic acid	2	2	2	-
TBBS	0.5	1.5	3	-
Sulfur	3	1	-	-
Dicumyl peroxide	-	-	-	2

3.4.4 Effect of carbon black

Carbon black is the most fillers used in the rubber industry to improve the product properties such as tensile strength, abrasion resistance, and tear strength and reduce cost. The distributed filler in rubber matrix affects the electrical values due to the different electrical conductivity between the surface of the filler and the rubber. The influence of filler content on electrical values which change during vulcanization has been interesting. The formulation of NR compound by studying the effect of carbon black content on electrical values is listed in Table 3.5.

Table 3.5 Formulation of NR compound by studying the effect of carbon black on electrical values

Components	Part per hundred rubber (phr)		
	Control	C_{30}	C_{60}
Natural rubber	100	100	100
Zinc oxide	5.0	5.0	5.0
Stearic acid	2.0	2.0	2.0
TMTD	1.0	1.0	1.0
Sulfur	2.0	2.0	2.0
Carbon black (N330)	-	30.0	60.0

CHAPTER 4

RESULTS AND DISCUSSION

This research work aims to develop the online pilot system for utilizing electrical properties to monitoring rubber vulcanization. Testing dielectric cure monitoring for its suitability to online monitoring of natural rubber compound vulcanization by compression molding was investigated and compared to conventional curemeter results. This chapter is divided into 3 parts as follow:

Part 4.1 displays the experimental set-up with RCMS and describes the influence of electric field frequency on the dielectric properties during the vulcanization process.

Part 4.2 shows the effect of vulcanization temperature on the change of conductance and capacitance curves during the vulcanization process.

Part 4.3 studies the effect of vulcanization system including sulfur vulcanization system (EV, Semi-EV, CV) and peroxide vulcanization system on the change of conductance and capacitance curves during the vulcanization process.

4.1 The effects of electric field frequency

Figure 4.1 displays a sketch of the experimental set-up with RCMS. Parallel plate electrodes are used in this work because of high accuracy measurements of the average or bulk properties of the sample (McIlhagger *et al.*, 2000). The stainless steel electrodes were covered by polytetrafluoroethylene (PTFE) and were built-in in the upper and lower press molds. PTFE was applied to insulate the electrodes because of its high temperature resistance, low and fairly constant dielectric response over the temperature and frequency ranges of interest (Ehrlich, 1953; Koizumi *et al.*, 1968; Li, 2011). The upper and lower electrodes with 11 mm diameters were embedded in the steel mold for compression molding of the NR compound. The mold cavity is cylindrical with 40 mm diameter and 1.5 mm height. The mold temperature was measured with thermocouples embedded near the electrodes. The mold was pre-heated to the 160 ºC curing temperatures in the compression molding machine, and then the

rubber compound (4 cm^3) was placed into the mold. Finally, the rubber was compressed with 10 MPa pressure. The LCR meter, Wayne Kerr 4110, was used to monitor capacitance and conductance of rubber during vulcanization. A 2 volts alternating voltage was applied between the parallel plate electrodes in the frequency range from 0.75 to 100 kHz, and the response current was measured. The capacitance and conductance were logged every 4 seconds for 15 minutes. The electrical properties were recorded by a data tracking and controlling device, and the time profiles of electrical properties were shown on a monitor connected to the local area network of the rubber cure monitoring system. The RCMS was calibrated and then re-tested with a 1 mm thickness PTFE sheet before each run.
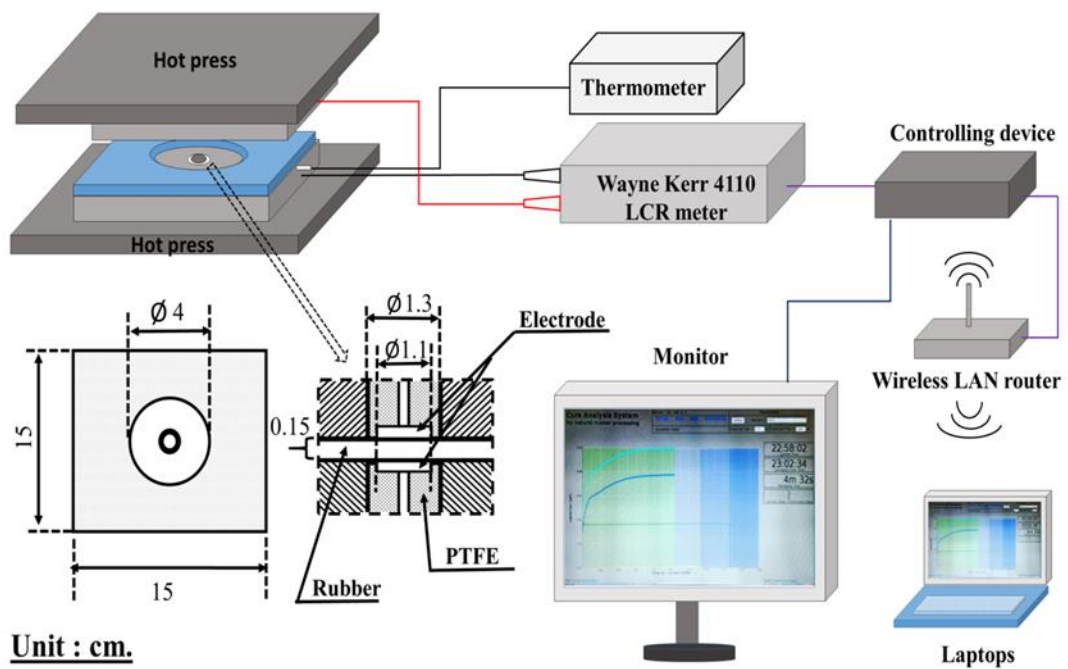
Figure 4.1 Sketch of of the experimental set-up for rubber cure monitoring system (RCMS)

In the initial experiment, ten frequencies including 0.75, 1, 2.5, 5, 7.5, 10, 25, 50, 75 and 100 kHz, were tested at 160°C cure temperature over 15 min, in order to find a suitable informative frequency. The two fundamental electrical characteristics, capacitance and conductance, as functions of cure time are reported in Figures 4.2 and

4.3, respectively. It can be noted that the *C* and *G* curves at frequencies below 5 kHz were inconsistent and scattered over a wide range, because of the polarization and blocking effects at low frequencies (McIihagger *et al.*, 2000). The electrode polarization reduces mobility of ions close to the electrodes. The 100 kHz frequency gave noisy results with the RCMS.
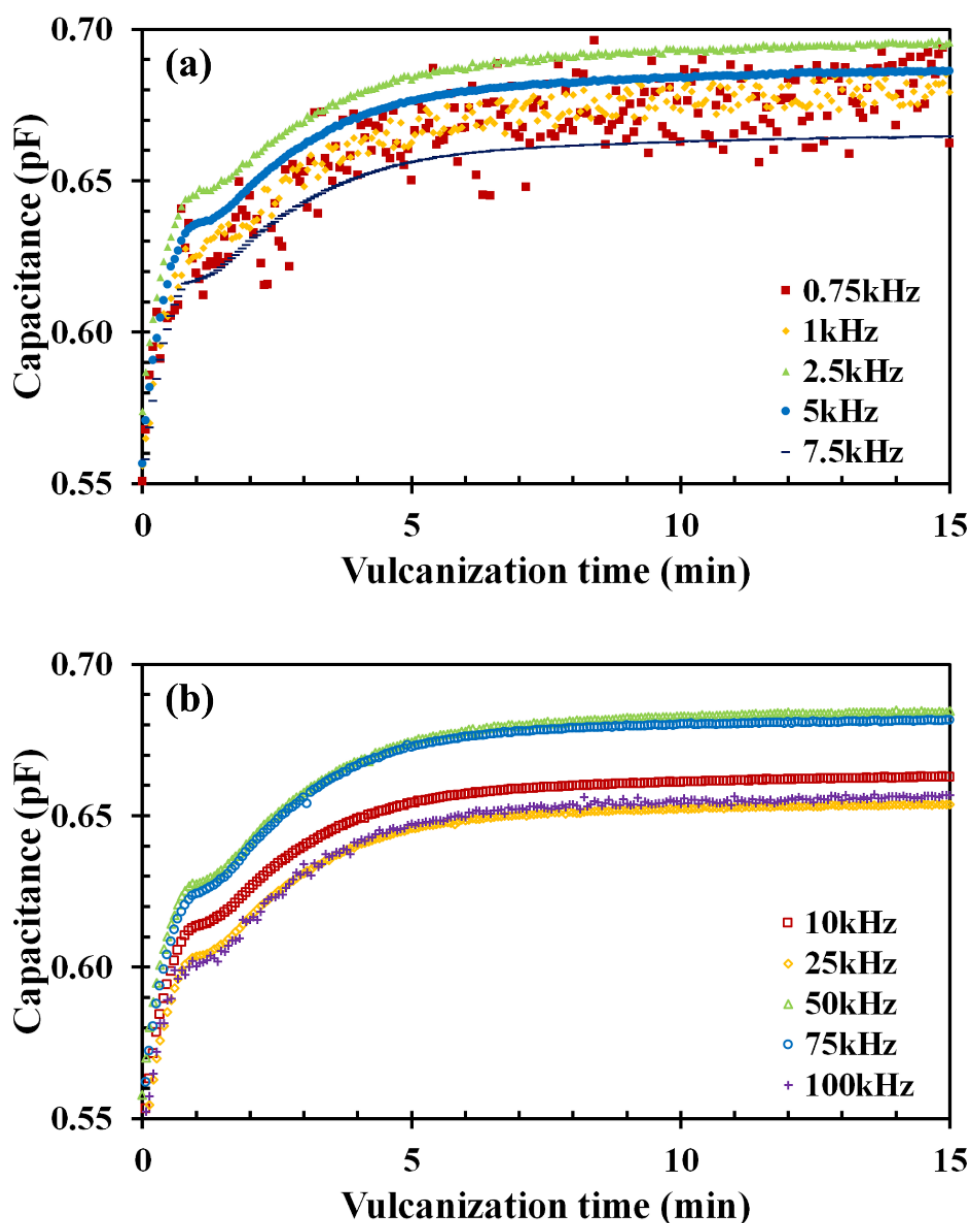
Figure 4.2 Capacitance evolution during the isothermal cure of natural rubber at 160°C observed at various frequencies: (a) 0.75 kHz to 7.5 kHz, and (b) 10 kHz to 100 kHz.
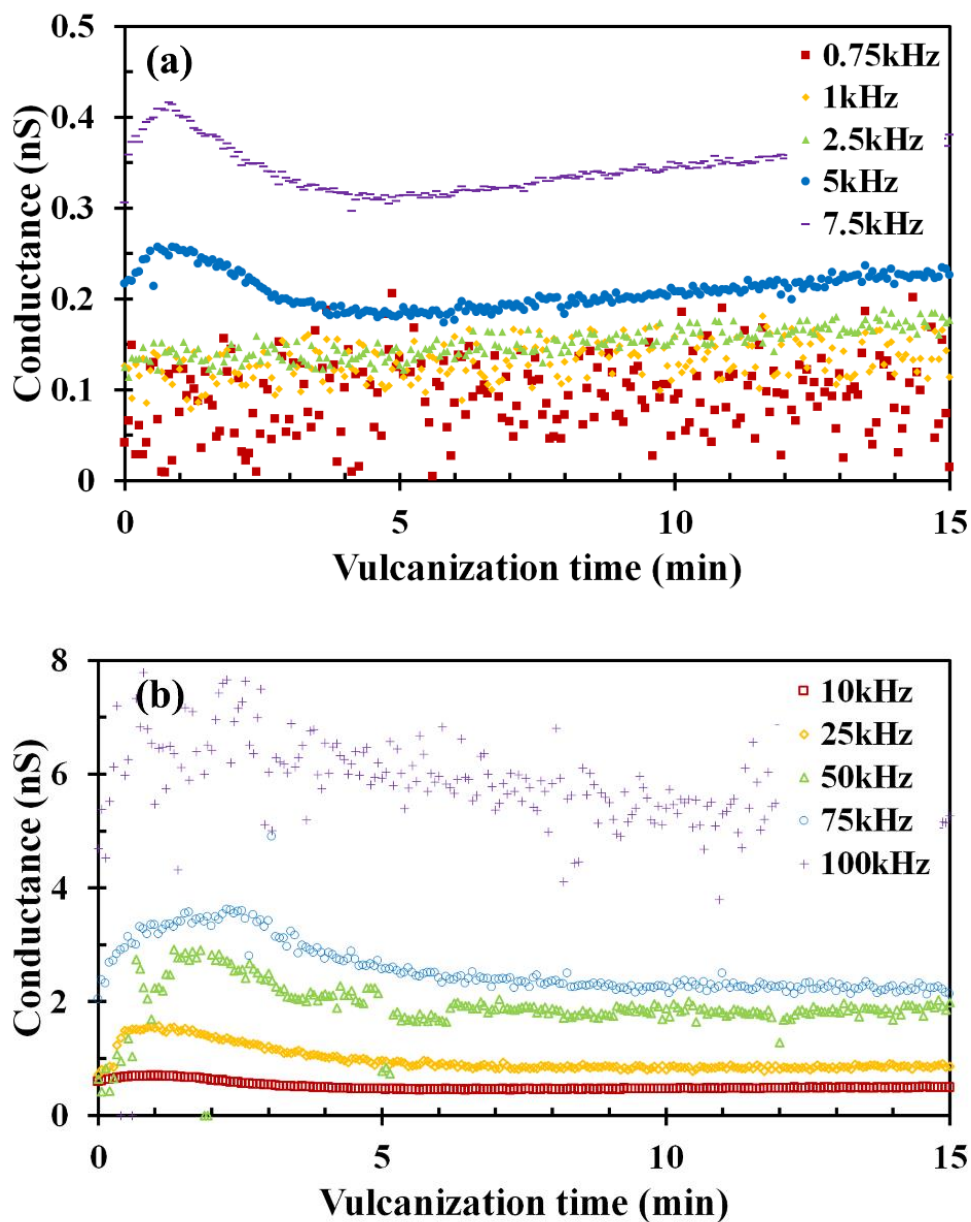
Figure 4.3 Conductance evolution during the isothermal cure of natural rubber at 160°C observed at various frequencies: (a) 0.75 kHz to 7.5 kHz, and (b) 10 kHz to 100 kHz.

To identify the change of slope in the capacitance curves, the first time derivative of signal (dC/dt versus t) is shown in Figure 4.4. Thus, the most useful frequencies with this experimental equipment were in the range from 5 kHz to 75 kHz.

For most accurate results, the frequency for the dielectric cure monitoring was set at 5 kHz in the rest of this work.
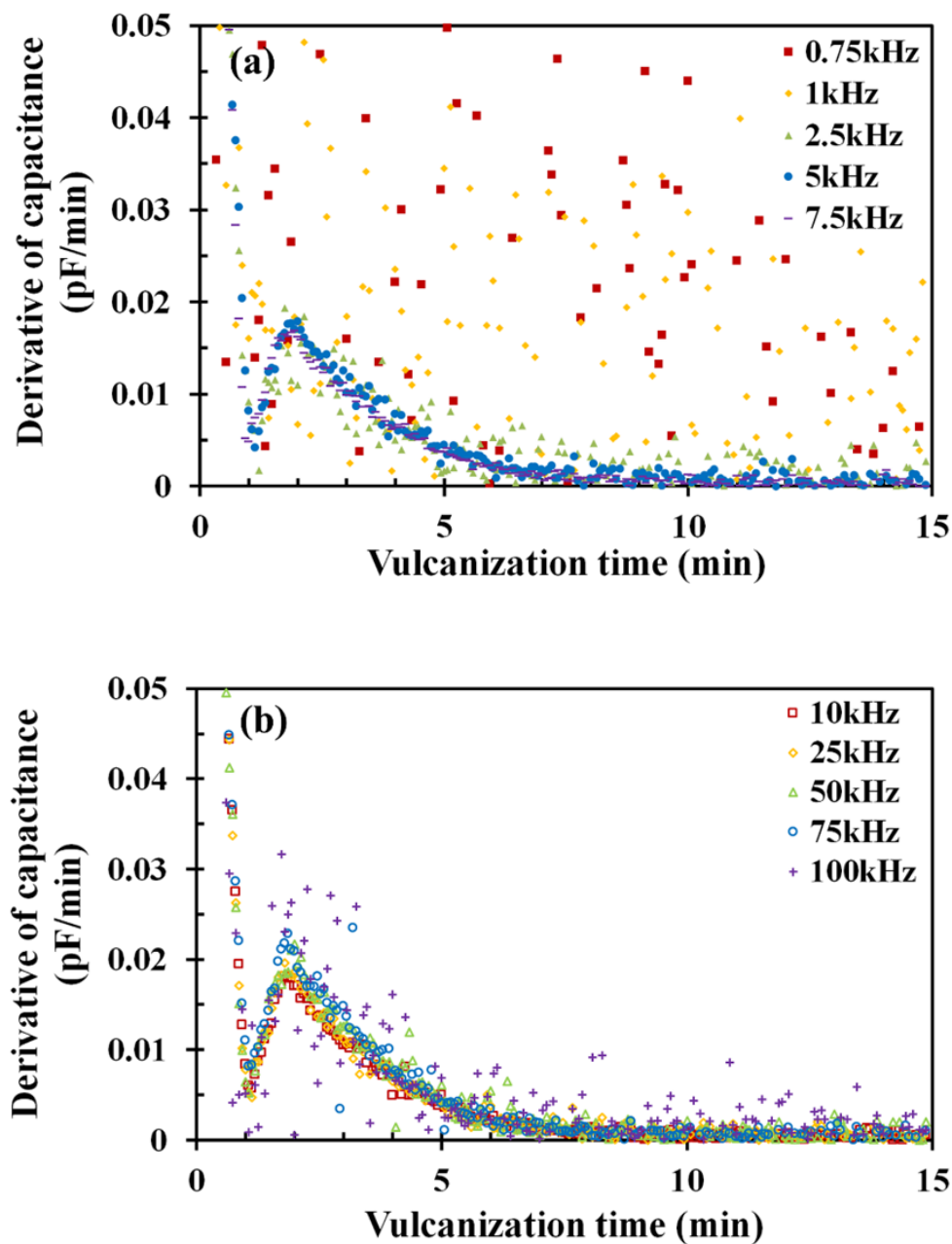
Figure 4.4 Time derivative of capacitance during the isothermal cure of natural rubber at 160°C observed at various frequencies: (a) 0.75 kHz to 7.5 kHz, and (b) 10 kHz to 100 kHz.

In addition, in order to assess the capability of RCMS to determine the characteristic curing parameters of an NR compound, the relationships between torque, capacitance, derivative of capacitance and conductance are shown in Figure 4.5. It was found that the three stages of curing can be observed in torque, capacitance and derivative capacitance curves. These parameters changed clearly with time and indicated the progression of crosslinking the NR. In the induction period (region I), the natural rubber compound is softening. Torque and derivative capacitance curves rapidly decreased to a minimum point, while capacitance and conductance promptly increased to peak at approximately 1 min due to ionic polarization and dipolar polarization were increased by increasing mobilities of ions and rubber molecules in softening state.

The minimum torque and maximum capacitance at onset of first slope change were defined as M_L and C_0, from the torque curve and capacitance curve, respectively. In this stage, an active accelerator complex was produced by chemical reactions between accelerator, activator (ZnO) and sulfur. Then, the sulfurating agent obtained from the reaction of the active accelerator complex and sulfur molecules can react with NR chains to form crosslinking precursors resulting in increasing of ionic polarization and capacitance. These intermediates reach a maximum concentration before crosslinking and decrease with a significant crosslinking extent (Sadequl *et al.*, 1998; Hummel and Rodriguez, 2000; Hummel and Rodriguez, 2001). Furthermore, the times of M_L, C_0 and maximum G, were indicative of the start of vulcanization (t_{c0}).

In the curing stage (region II), the rapid increases were observed in torque and derivative of capacitance, while a gradual increase was seen in capacitance due to the increasing of dipolar polarization of sulfur crosslink during vulcanization. Clearly, the dipole moment per unit volume of rubber was increased by the rubber-sulfur dipoles increasing polarization in an electric field (Desanges *et al.*, 1958; Vassilikou-Dova and Kalogeras, 2009). The steepest parts related to the maximum point of the derivative of capacitance at around 2 min. The end of curing reaction, which reached the plateau, indicates an equilibrium state of vulcanization.
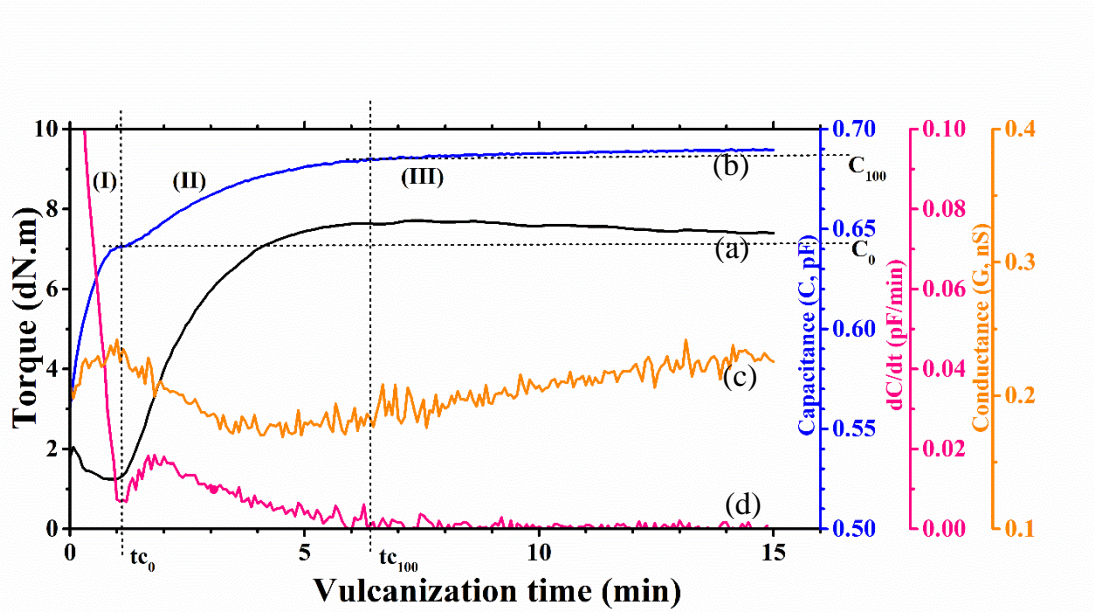
Figure 4.5 Relationship between (a) torque, (b) capacitance, (c) conductance, and (d) derivative of capacitance during vulcanization.

The end of curing reaction point can be detected at around 6.5 min, and is indicated by M_H and C_{100} in torque and capacitance, respectively. Times of M_H and C_{100} represented the state of full cure (t_{c100}). After this region, the overcure stage (region III) followed. The conductance decreased rapidly and did not reach a constant value due to decreased ionic conductivity with increasing rubber viscosity, caused by vulcanization (Skordos and Partridge, 2004; Vassilikou-Dova and Kalogeras, 2009). In addition, it was found that the peak of conductivity shifted to the right (i.e., to higher frequency) as seen in Figure 4.3. Thus, conductance was not informative of the NR vulcanization extent. In the cure stage, the crosslinking precursor reacts with another rubber chain, resulting in crosslink formation between NR chains (Ding and Leonov, 1996). As previously discussed, Tc_{90} is generally used to determine the optimum vulcanization time from an MDR torque-time curve. For RCMS, the equivalent plateau was observed in the capacitance-time curve, and the extent of vulcanization can be represented as:

$$t_{cx} = \text{minutes to } C_0 + \frac{x \ (C_{100} - C_0)}{100} \tag{4.1}$$

where C_0 is the maximum capacitance at onset of first slope change and C_{100} is the maximum capacitance at onset of second slope change

The characteristic cure parameters from MDR and RCMS are listed in Table 4.1. The scorch time was determined as the time to reach a 10% state of cure (t_{c10}), and as the time required for the torque to rise by one unit (dN.m) above the minimum torque (t_{s1}) for MDR (Dick and Pawlowski, 1995). In addition, the time at inflection point (maximum slope of C) or at the peak of derivative of capacitance (t_{dc}) for RCMS were equated. It was found that there was little difference in scorch time and optimum cure time (t_{c90}) obtained from MDR and RCMS. The results from RCMS provided longer scorch and cure times than the MDR because the special die geometry and the large die surface area of MDR give faster heating of the sample. The measured capacitance was related to the progress of vulcanization of natural rubber. The correlation between capacitance and torque is illustrated in Figure 4.6. Polynomial regression fit gave the coefficient of determination (R^2) equal to 0.9979, indicating a tight relationship between capacitance and torque for rubber during vulcanization.

Table 4.1 Characteristic curing parameters of the NR compound as evaluated by MDR and by RCMS at 160°C

Curing parameters	MDR	Curing parameters	RCMS
M_L (dN.m)	1.22 ± 0.04	C_0 (pF)	0.64 ± 0.01
M_H (dN.m)	7.71 ± 0.13	C_{100} (pF)	0.69 ± 0.01
M_H - M_L (dN.m)	6.48 ± 0.10	C_{100} - C_0 (pF)	0.04 ± 0.01
Scorch time (min)		Scorch time (min)	
- t_{c10}	1.38 ± 0.06	- t_{c10}	1.46 ± 0.07
- t_{s1}	1.48 ± 0.05	- t_{dc}	1.80 ± 0.12
Cure time, t_{c90} (min)	4.12 ± 0.11	Cure time, T_{90} (min)	4.85 ± 0.04
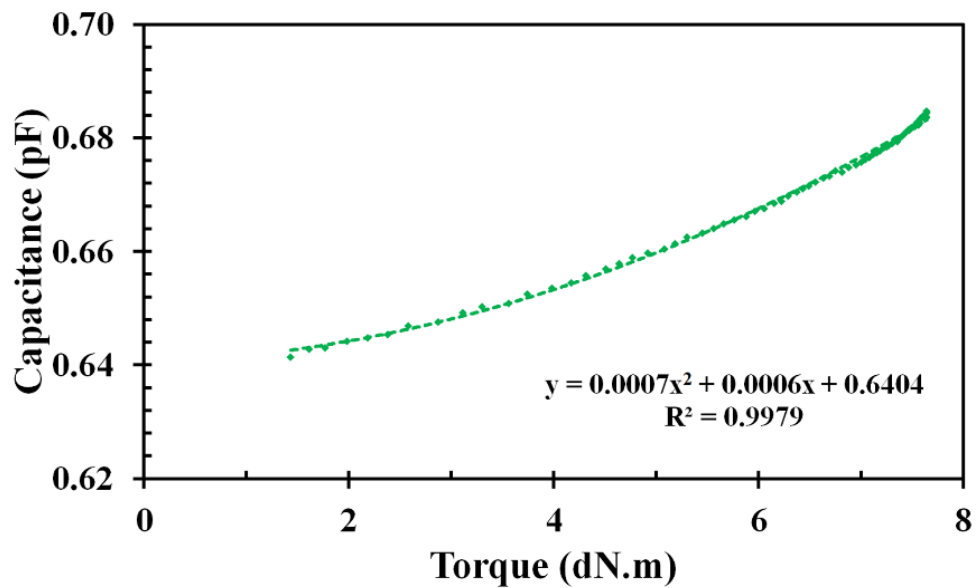
Figure 4.6 The correlation between capacitance and torque during the isothermal cure of natural rubber at 160°C.

The degree of cure (α) as a function of curing time (t) is generally indirectly determined from the torque-time curve obtained with MDR as follows (Ahmadi and Shojaei, 2013; Erfanian *et al.,* 2016), and with RCMS measured capacitance this is analogous to equation 4.2 and 4.3 respectively:

$$\alpha_{(MDR)} = \frac{M_t - M_L}{M_H - M_L} \tag{4.2}$$

$$\alpha_{(RCMS)} = \frac{C_t - C_0}{C_{100} - C_0} \tag{4.3}$$

where M_t and C_t are the torque and the capacitance at a given time during vulcanization. In addition, the cure rate or the vulcanization rate ($d\alpha/dt$) is the time derivative of cure degree. For *in situ* cure monitoring, the results from RCMS should be similar to those from MDR. Thus, the degree of cure and rate of cure from both methods are compared in Figure 4.7. As can be seen, the degrees of cure are very similar, but the degree of cure and rate of cure obtained from RCMS are slightly lower than from MDR because of the slower bulk heating that gave slower reaction rates. In

other words, the heat transport into the sample was faster in the MDR than in the compression mold with RCMS, due to the special die geometry and high surface area of MDR (Jaunich and Stark, 2009).
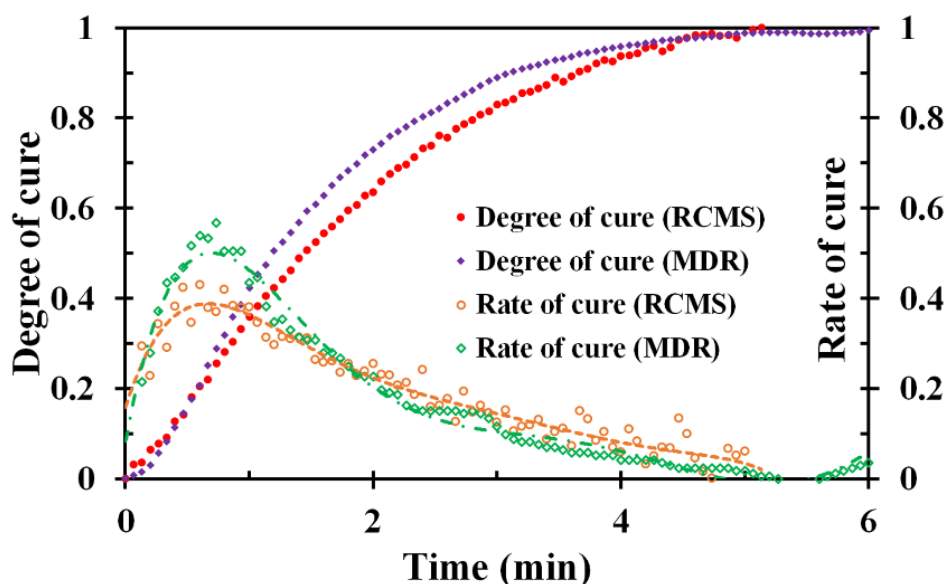
Figure 4.7 Degree of cure and rate of cure comparison between RCMS and MDR during isothermal vulcanization at 160°C.

4.2 Effect of vulcanization temperature

The typical torque versus time curves of rubber compound at three different cure temperatures obtained by MDR were displayed in Figure 4.8 (a). The S-shaped cure curves were observed in curing curve of a usual accelerated sulfur vulcanization process which consisted of three regions i.e. induction period, curing period and overcure period. Firstly, after the rubber compound is placed into the heated cavity of MDR, torque falls because of softening of the compound; yet the crosslink structures have not occurred in the induction period. Then, the three-dimensional crosslinked networks are formed leading to rise of the torque curve. Finally, torque reaches the constant value or torque decreases based on the specific cure system. The capacitance and conductance were plotted as function of the vulcanization time with three different vulcanization temperatures as shown in Figure 4.8(b) and 4.8(c), respectively.

The capacitance curves also consist of three regions. In an induction period, the capacitance and conductance were rapidly elevated until they reached the maximum of first slope change which defined as C_0. It can be explained that after being heated, the occurrence of softening NR compound enhanced the molecular segment mobility and simplified dipole arrangements, which in turn results in a capacitance increase (Švorčík *et al*., 2001). In curing period, the capacitance continuously increased until reached the plateau which is indicated as C_{100}. It can be explained that while the crosslinked networks were occurred, the rubber-sulfur dipoles oscillate in an electric field leading to alter the dipole moment and increasing dipolar polarization (Desanges *et al*., 1958). Time to obtain a degree of cure can be calculated from equation 4.1. After this region, it becomes the overcure stage. Capacitance curves reached the constant value because the rotations of dipoles were restricted by crosslinks between NR molecular chains (Tuckett, 1942). Nevertheless, the conductance-time curve was not useful for evaluating the optimum cure time because it rapidly dropped after induction period, and did not reach the constant value.
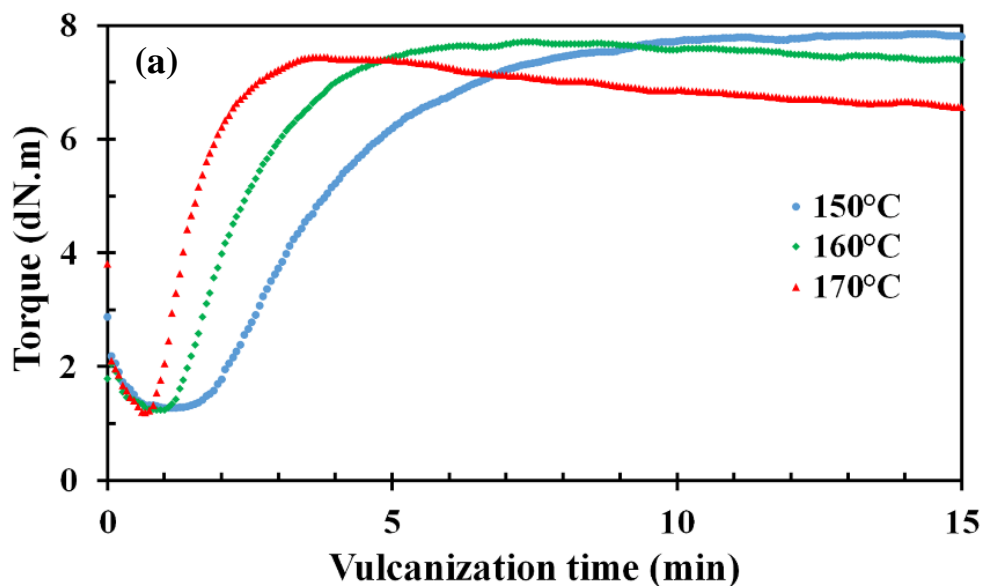
Figure 4.8 Relationship between (a) torque, (b) capacitance and (c) conductance as a function of vulcanization time for the different isothermal cure temperatures.
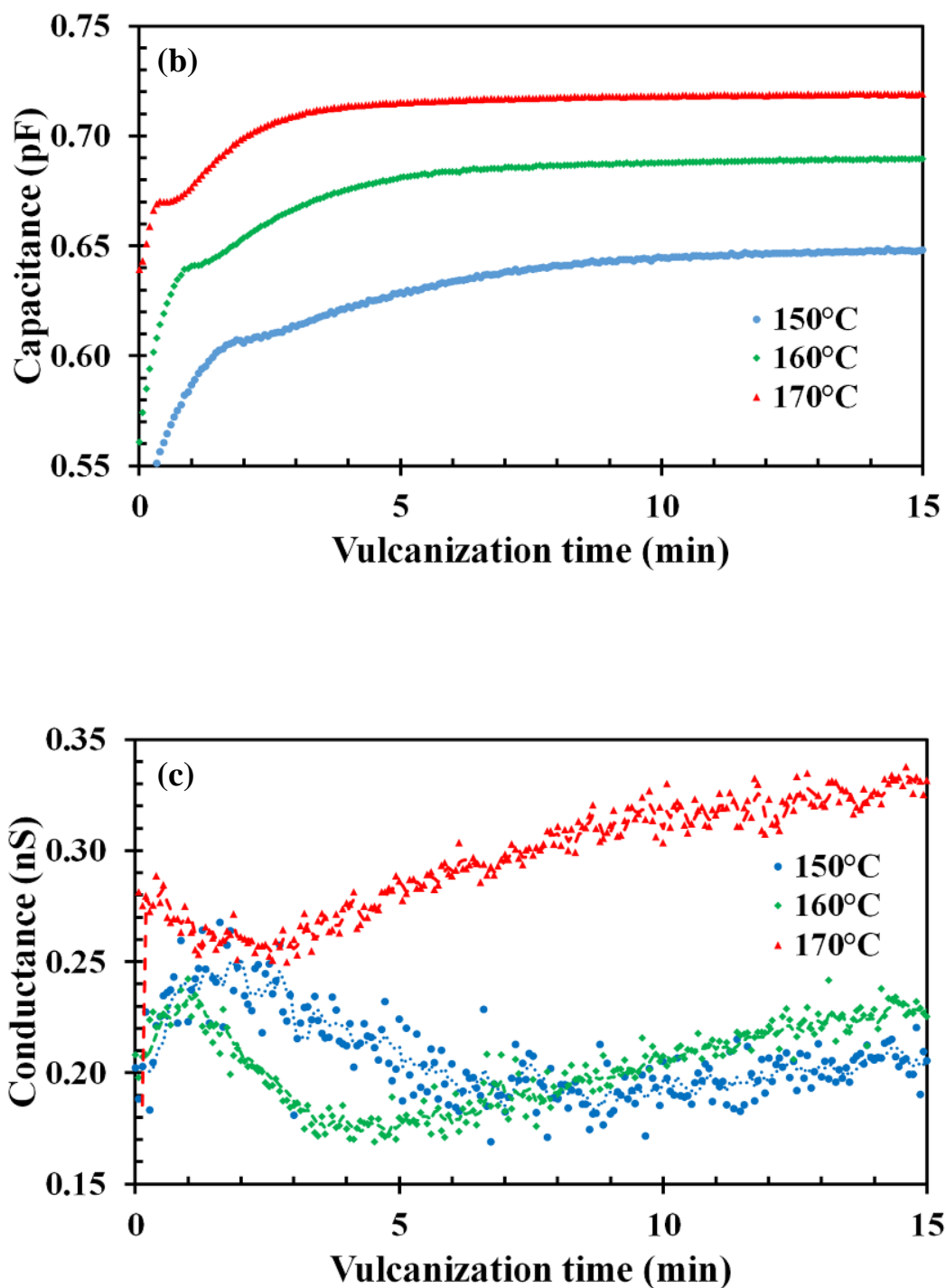
Figure 4.8 (Cont.) Relationship between (a) torque, (b) capacitance and (c) conductance as a function of vulcanization time for the different isothermal cure temperatures.

For MDR curves, it was found that at 150°C the torque increased and then reached to a horizontal plateau in overcure period indicating that the occurred crosslink structures are thermally stable at this temperature, while the decrease of torque in overcure period due to the reversion phenomenon was clearly observed at 160°C and 170°C. However, the capacitance-time curve at 170°C was slightly increased in the overcure period because during the reversion the polysulfidic chains were cleavage and changed to disulfidic, monosulfidic and cyclic sulfides through both radical and polar decomposition mechanism leading to an increment of polarization (Krejsa and Koenig, 1993). The capacitance-time curve at 150°C has the lowest capacitance value, while at 170°C has the highest one. The higher capacitance was observed at elevated temperature because of an enhancement of molecular chain segments mobility and facilitation of dipole orientation polymerization (Švorčík *et al*., 2001). The cure characteristics extracted from both of the MDR and RCMS methods were listed in Table 4.2.

It was observed that the minimum torque (M_L) diminished when vulcanization temperature rose because NR molecular chains has more absorbed the energy to enhance the chains mobility resulting in the lower the rubber viscosity (Lee, 2017). In addition, at 150°C the highest maximum torque (M_H) was observed which is assumed to be the highest crosslink density. M_H tended to decrease with an increment of temperature. It can be explained that the polysulphidic structures were cleaved due to their low thermal stability at the temperature increase (Posadas *et al.*, 2010). This result agreed with the difference between the maximum and minimum torque (M_H-M_L) of rubber compound which exhibited a reduction tendency with increasing vulcanization temperature.

However, the capacitance showed the opposite trend in Table 4.2 and Figure 4.9. Increases in C_0, C_{100} and C_{100}-C_0 were observed with increasing temperature. As the temperature increases, the dipoles comparatively become free and they respond to the applied electric field. Thus, polarization increased and dielectric constant or capacitance is also increased with the increase of temperature (Sheha *et al.,* 2015). In addition, a competitive side reaction i.e., reversion occurs at higher vulcanization temperature. This might be related to an increase in the total number of polar groups

because the decomposition mechanism of polysufidic crosslinks may be either radical, polar or a combination of both (Ghosh P *et al.,* 2003) and decomposition provides insights into the formation of cyclic sulfides (Hernández *et al.,* 2010). Induction time for MDR is assigned as the time between test start point and minimum torque point. Induction time for RCMS is the region which the capacitance (*C*) curves reached to maximum of first slope change and the conductance (*G*) increased to the maximum peak as shown in Figure 4.9.
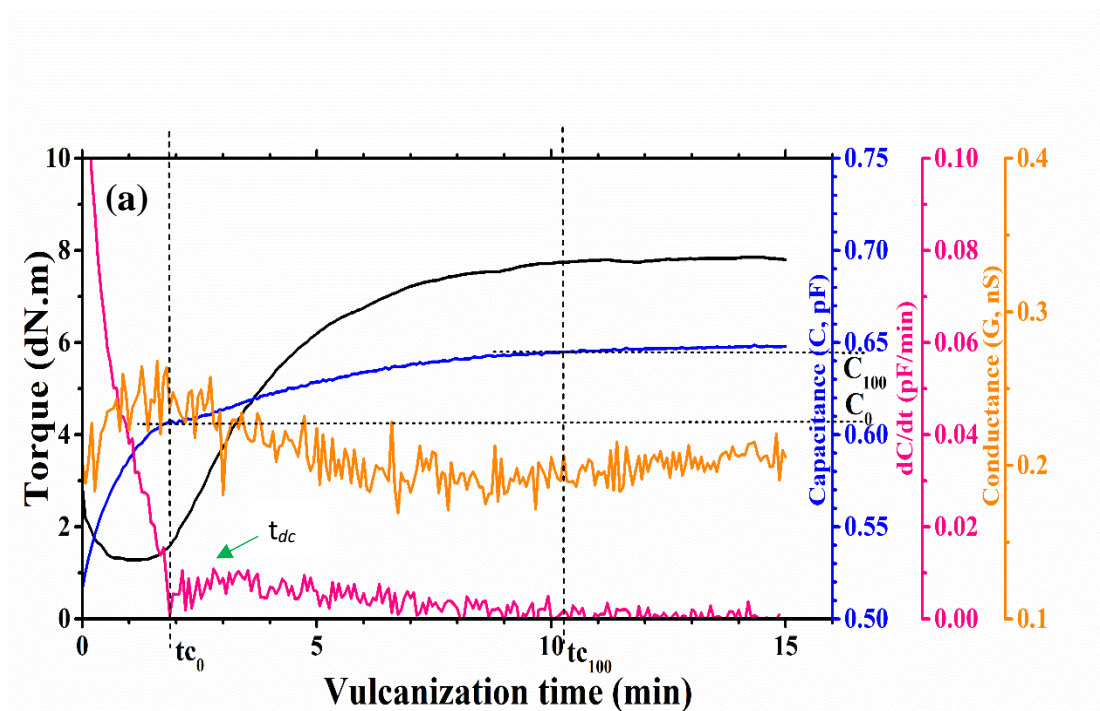
Figure 4.9 Relationship between torque, capacitance and conductance as a function of vulcanization time at (a) 150°C, (b) 160°C and (c) 170°C.
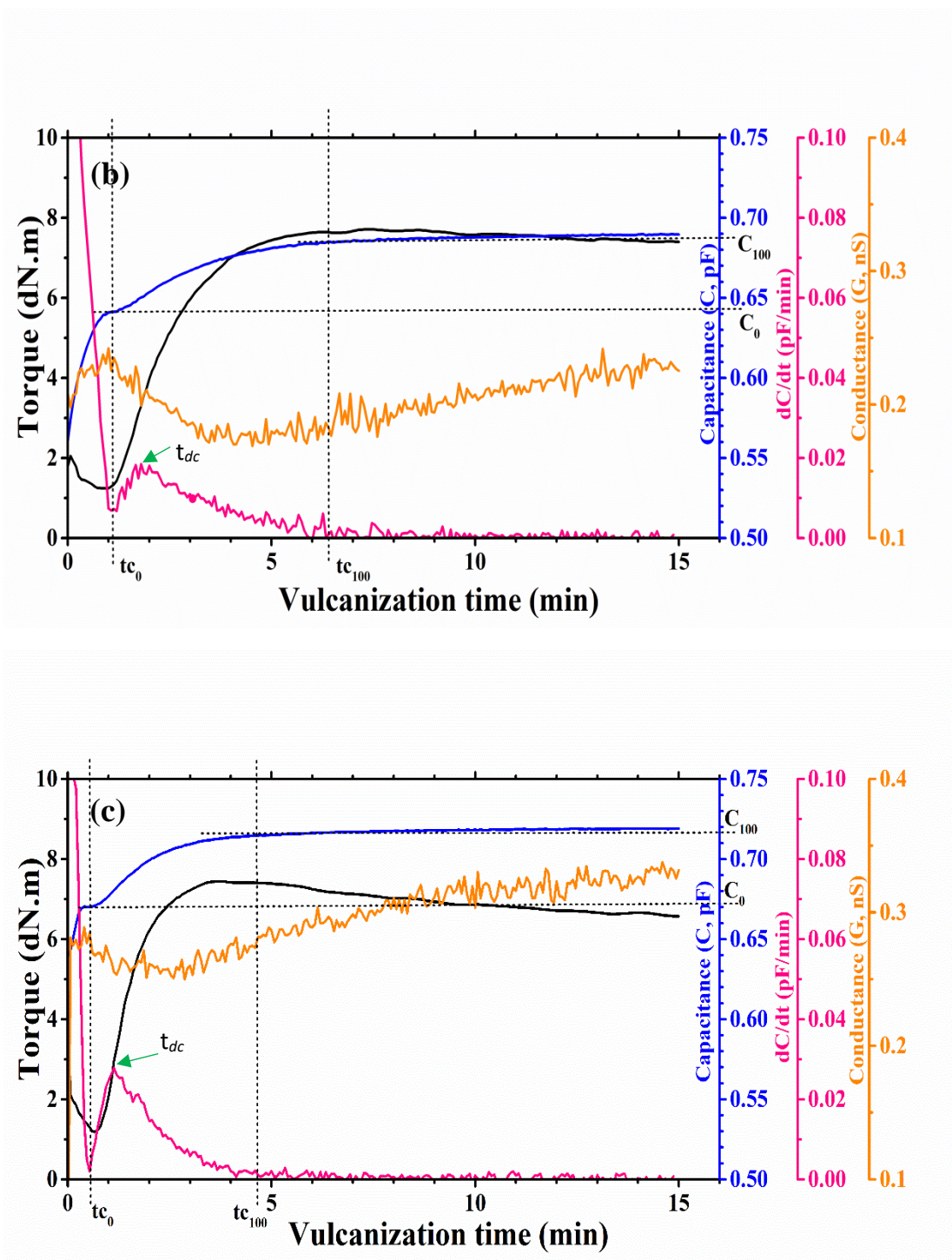
Figure 4.9 (Cont.) Relationship between torque, capacitance and conductance as a function of vulcanization time at (a) 150°C, (b) 160°C and (c) 170°C.

The required time for the torque increases one torque unit (dN.m) above M_L or t_{s1} is normally defined as the scorch time in MDR technique. Nevertheless, a compound

with a low M_H represents a much more percentage of the ultimate state of vulcanization than a relatively high M_H one (Dick and Pawlowski, 1995). In order to avoid the weakness of t_{s1}, t_{c10} is sometimes used to determine scorch time. In the case of RCMS, the time at inflection point (maximum slope of C) or at the peak of derivative of capacitance (t_{dc}) was used to measure the scorch time. The t_{c90} was used to determine the optimum cure time. From results in Table 4.2 and Figure 4.9, it was found that an increasing vulcanization temperature effect on a shorter scorch time and optimum cure time because rubber chains mobility and accelerator activity are advanced at higher temperature (Rabiei and Shojaei, 2016). It was clearly observed that the variation of induction time and cure time as a function of vulcanization temperature from RCMS gave similar data to MDR method.

Table 4.2 Characteristic curing parameters of the NR compound as evaluated by MDR and RCMS at different temperature 150°C, 160°C and 170°C

Cure parameter	150 °C		160 °C		170 °C	
	MDR	RCMS	MDR	RCMS	MDR	RCMS
M_L (dN.m) or C_0 (fF)	1.28±0.07	607.37±7.21	1.22±0.04	641.43±6.74	1.19±0.01	670.14±30.44
M_H (dN.m) or C_{100} (fF)	7.85±0.26	644.45±6.84	7.71±0.13	684.50±8.65	7.37±0.09	714.94±31.32
M_H-M_L (dN.m) or C_{100}- C_0 (fF)	6.57±0.20	37.08±2.10	6.48±0.10	43.07±2.08	6.17±0.09	44.80±1.04
Scorch time (min)						
$-t_{10}$	2.07±0.18	2.34±0.15	1.38±0.06	1.46±0.07	0.93±0.01	0.80±0.16
$-t_{s1}$ or t_{dc}	2.27±0.18	2.80±0.21	1.48±0.05	1.80±0.12	1.02±0.03	1.13±0.24
Cure time (min), t_{c90}	6.98±0.07	8.09±0.10	4.12±0.11	4.91±0.04	2.43±0.01	3.37±0.18
CRI	20.58±0.61	18.89±0.31	36.76±0.65	32.17±0.63	67.11±0.45	44.70±0.44

A tight correlation between capacitance and torque for the different isothermal cure temperatures was exhibited in Figure 4.10. It gave the coefficient of determination (R^2) for polynomial regression equal to 0.9971, 0.9979, and 0.9901 at 150°C, 160°C and 170°C, respectively.
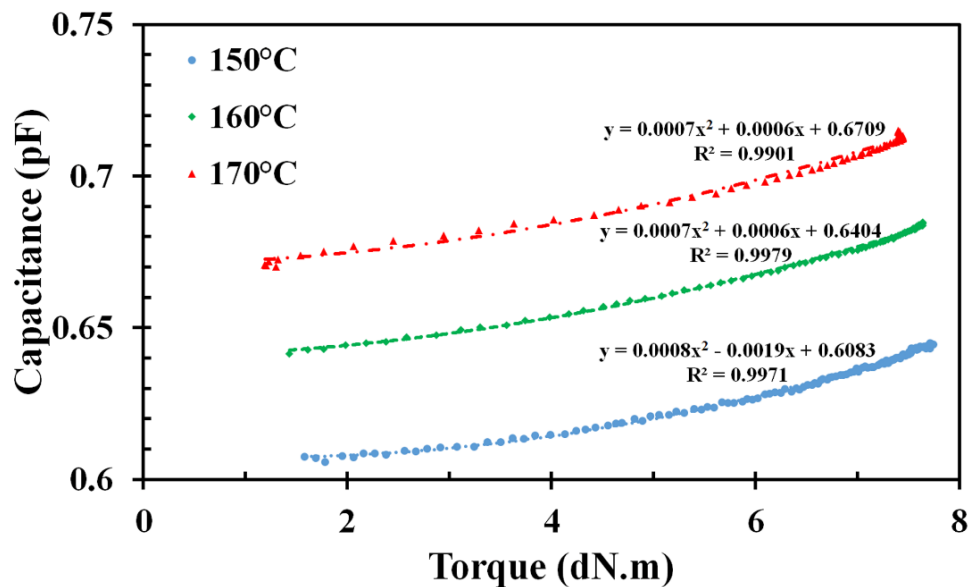
Figure 4.10 The correlation between capacitance and torque during the different isothermal cure of natural rubber.

To understanding on the NR vulcanization process with three different vulcanization temperatures, the torque-time curves and capacitance-time curves from MDR and RCMS were used to determine the degree of cure (α) as a function of curing time (t) as follow equation 4.2 and 4.3.

Consequently, cure rate or vulcanization rate ($d\alpha/dt$) can be defined by derivative of degree of cure with respect to time. With the purpose of investigation in the possibility of RCMS to real-time monitor the NR vulcanization, the similar or the same results from MDR and RCMS is essential. The degree of cure curves (α versus t) and cure rate curves ($d\alpha/dt$ versus t) from both MDR and RCMS are shown in Figure 4.11 and 4.12, respectively.
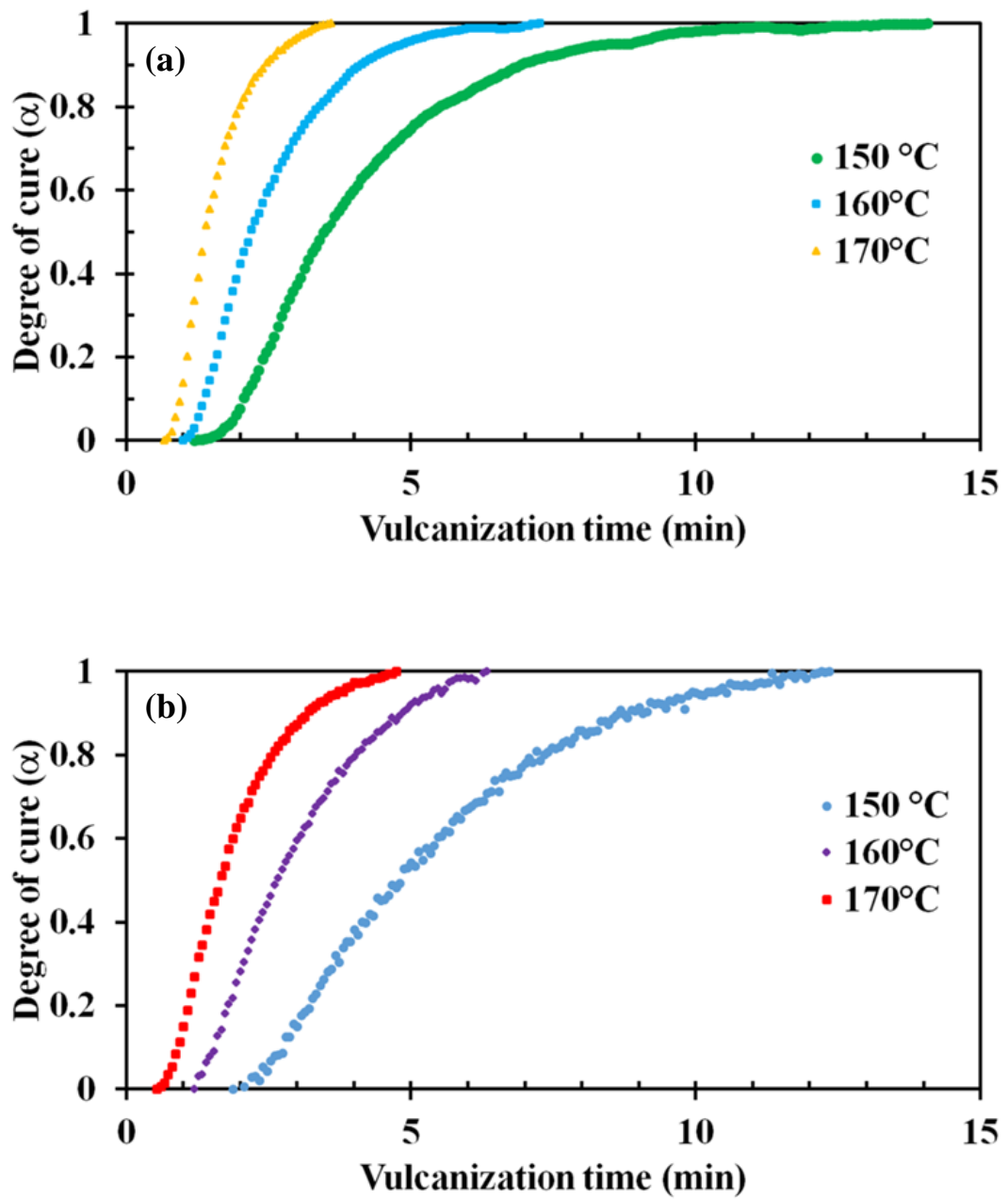
Figure 4.11 Degree of cure as a function of time comparison between (a) MDR and (b) RCMS at 150°C, 160°C and 170°C.
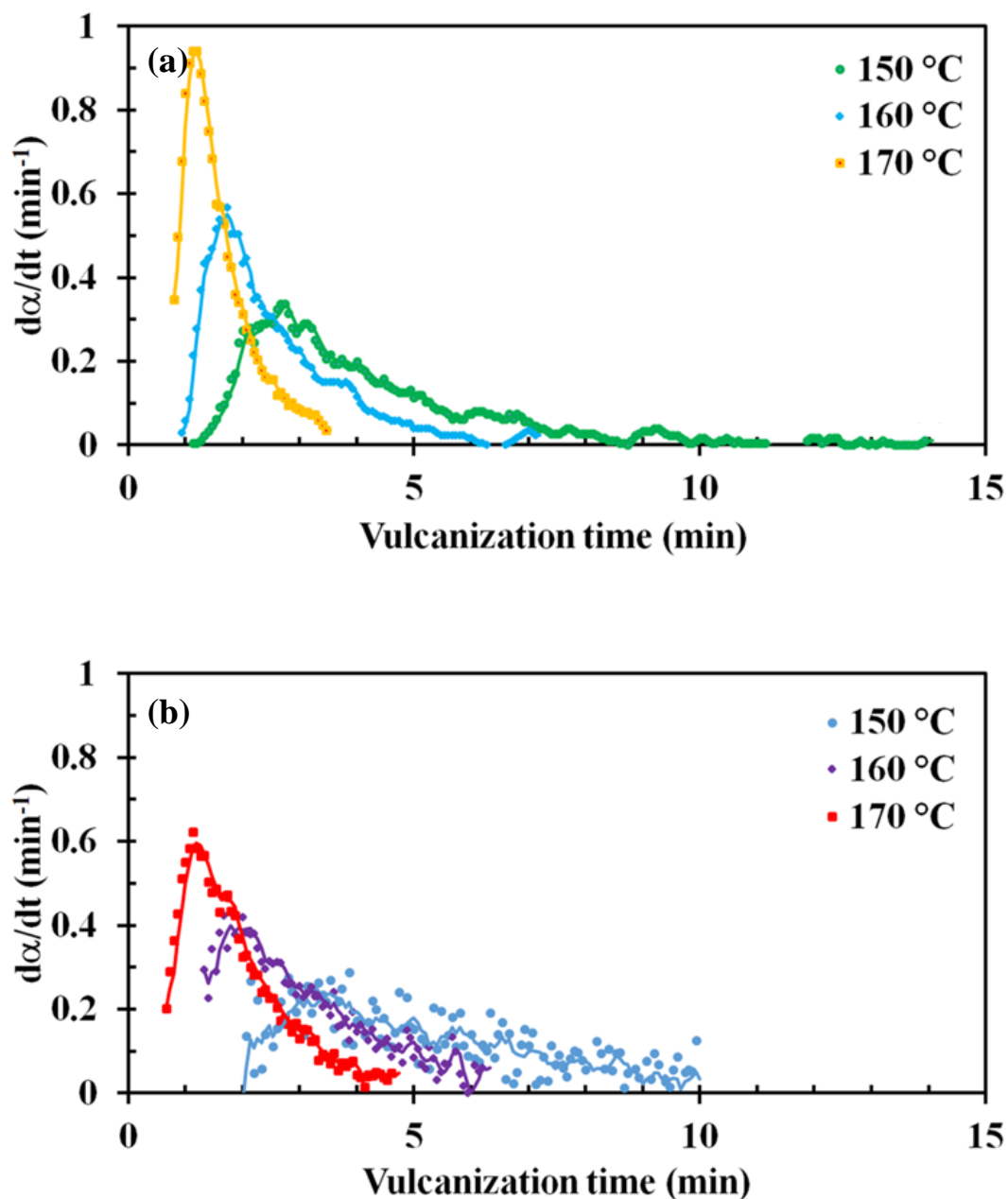
Figure 4.12 Cure rate as a function of time at three isothermal vulcanization temperatures from (a) MDR and (b) RCMS.

It was presented that the highest degree of cure was observed at 170°C in a good agreement between the two methods. MDR exhibited a higher degree of cure at given vulcanization time and temperature. It was calculated from torque which is highly influenced by the viscosity of materials. Thus it has more sensitivity for detecting the vulcanization whereas the degree of cure from RCMS method was calculated from the

capacitance which was affected by the change of dipole moment during vulcanization. Figure 4.12 showed the cure rate curves. It was found that the cure rate curves composed of two regions. In the first region, the increment of cure rate with time was observed and then reached to a maximum point within a short time indicating that an infinite network structure is being initiated. In the second region, the reduction of the cure rate was occurred and subject to zero due to the growing cross-linked formation resulting in the viscosity became high (Casalini *et al.*, 1997). The time at the maximum point of cure rate curves decreased with an increase of the vulcanization temperature because the reactivity of the rubber vulcanization depended on the temperature (Mansilla *et al.,* 2015)

Figure 4.13 exhibits the maximum cure rate at different temperature. It was found that the maximum point of cure rate curves increased with the increment of the vulcanization temperature. 170°C cured samples provided the highest maximum cure rate, while 150°C cured samples provided the lowest value. In addition, MDR provided the maximum cure rate higher than RCMS at all isothermal temperature. However, both techniques exhibited a good correlation of optimum cure time (t_{c90}) in the linear line with R^2 equal to 0.9914 as shown in Figure 4.14.
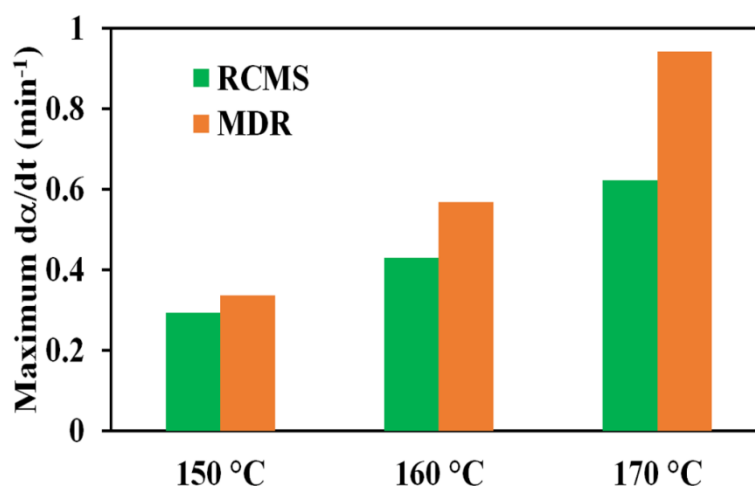
Figure 4.13 Maximum vulcanization rates from both RCMS and MDR at different temperatures.
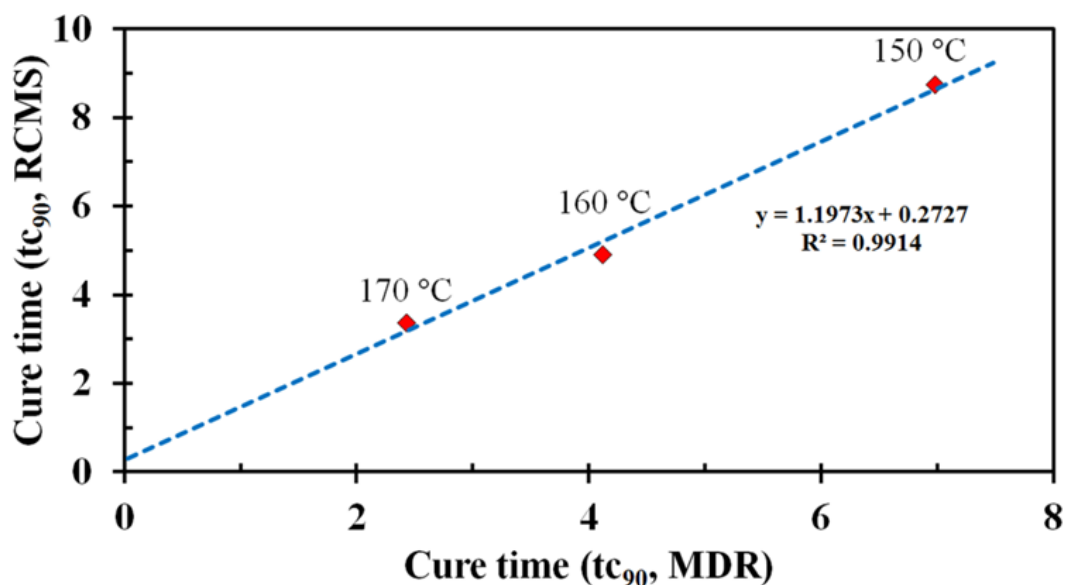
Figure 4.14 Linear correlation of optimum cure time (t_{c90}) obtained from RCMS and MDR with three different vulcanization temperatures.

4.3 Effect of vulcanization system including sulfur vulcanization system (EV, Semi-EV, CV) and peroxide vulcanization system

Vulcanization system is one of the most essential factors which affects the physical property and thermal stability of rubber vulcanized. In the sulfur vulcanization system, the sulfidic linkages between the rubber chain were formed with various sulfur atoms (mono, di, and poly sulfidic) resulting in the different cure characteristics of the rubber compound. These sulfidic linkages were controlled by the ratio between the contents of sulfur and accelerator in the effective vulcanization (EV), semi-EV, and conventional vulcanization (EV) systems of natural rubber.

The effect of the vulcanization system (EV, Semi-EV, CV, and peroxide) on the torque and the electrical properties during vulcanization was shown in Figure 4.15. In the peroxide vulcanization system, the capacitance was slightly reduced in the initial stage, and then it was increased during vulcanization but lower than the sulfur vulcanization system as shown in Figure 4.15(b). It was probably due to the peroxide vulcanization system occurred through free radical mechanism (Kruželák *et al*., 2017). In contrast, numerous types of ions and dipole were generated in the sulfur

vulcanization system since the beginning of the curing process (Hann *et al*., 1994; Hummel and Rodriguez, 2000; Hummel and Rodriguez, 2001). The zinc oxide was reacted with stearic acid which generated zinc stearate. Then, accelerator and sulfur were adsorbed on the Zinc oxide and reacted with zinc stearate to form sulfur cross-linking around Zinc oxide particles in the rubber matrix (Ikeda *et al*., 2009; Sakaki *et al*., 2018). Thus, the polarization of these dipoles and ions in the alternating electric field was increased resulting in higher capacitance in the sulfur vulcanization system, which correlates to the torque from MDR.

The conductance of sulfur and peroxide vulcanization systems was found to be related to the torque from MDR as shown in Figure 4.15(a) and (c) agreed with the torque cure curve. In the case of the sulfur vulcanization system, time at the maximum conductivity in the induction period was close to the time that torque started to increase due to the formation of ionic intermediates which accelerated the vulcanization reaction. After that, the conductivity was decreased from obstructing the flow of electricity because the cross-linkage between rubber chains was reached the equilibrium point. For the peroxide vulcanization system, the conductivity and the difference of changes in conductivity between before and after vulcanization were lower than the sulfur vulcanization system because there was no activator and accelerator which created ions during vulcanization. Moreover, the obstruction of the current flow due to the formation of crosslinks during vulcanization leads to a decrease in conductance of rubber vulcanized.
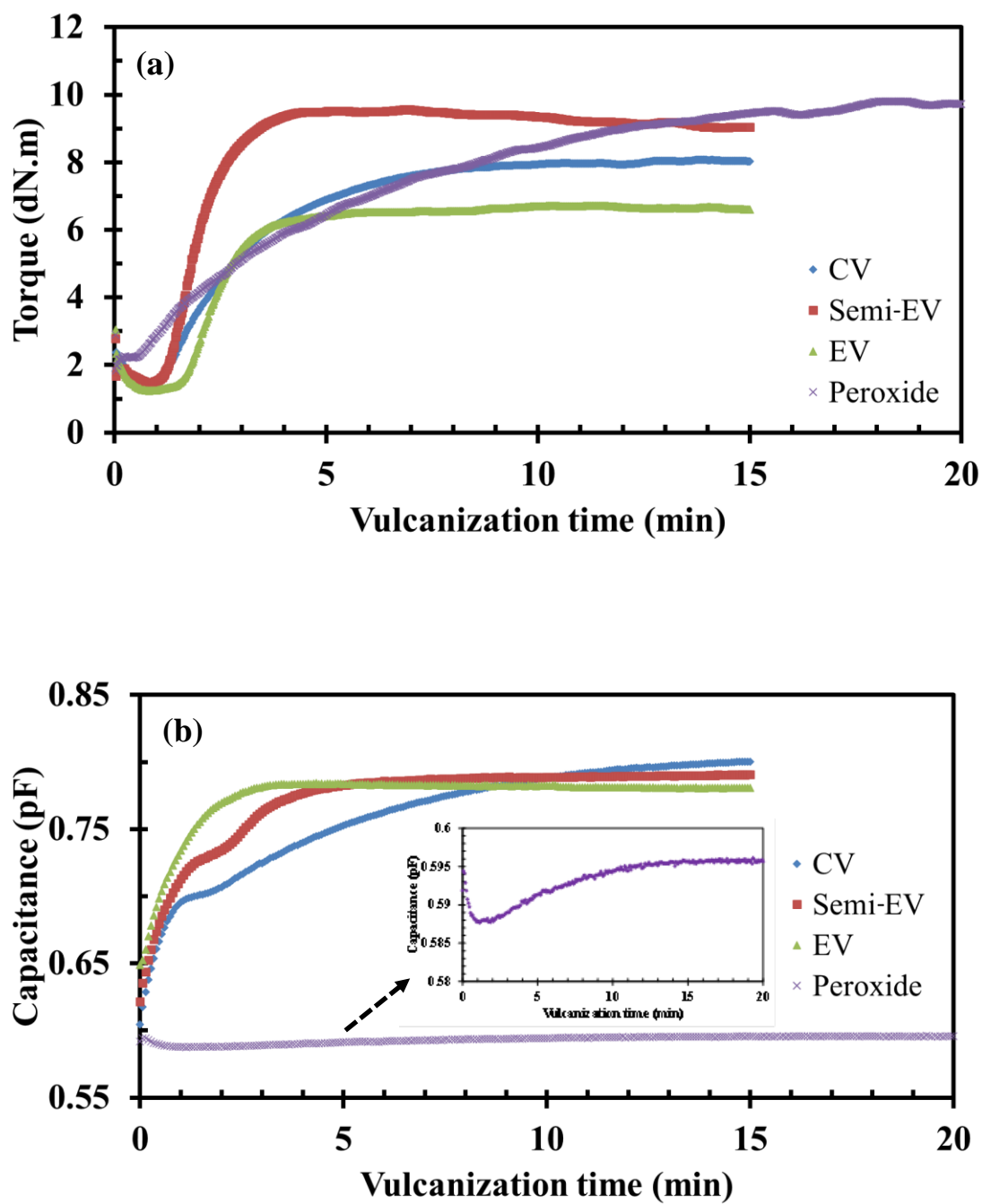
Figure 4.15 Effect of vulcanization system on (a) torque, (b) capacitance and (c) conductance during vulcanization at 160 ºC.
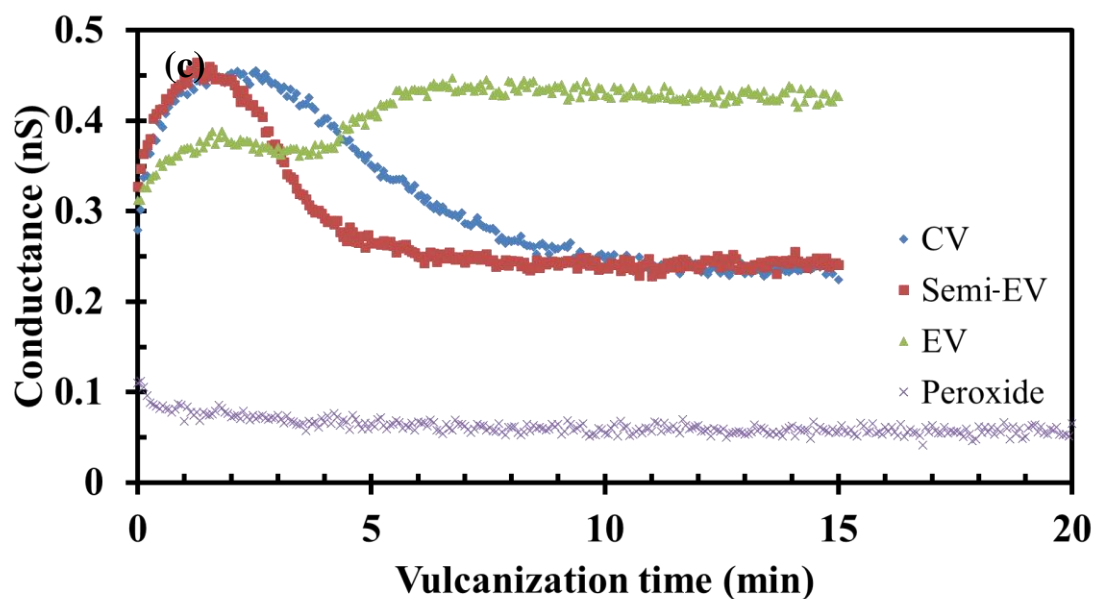
Figure 4.15 (Cont.) Effect of vulcanization system on (a) torque, (b) capacitance and (c) conductance during vulcanization at 160 °C.

.

An interesting result was found in the EV system (Figure 4.15 (c)), the conductance increased again after complete vulcanization. This phenomenon was exposed in Figure 4.16. The vulcanization with sulfur was not to occur uniformly in the rubbery matrix but to occur around Zinc oxide particles as shown in Figure 4.16(a), where the polyisoprene network covers Zinc oxide clusters dispersed in the network domains. The vulcanization process begins with the amounts of adsorbed sulfur and accelerator (TBBS) on each Zinc oxide cluster. The inhomogeneous domains are containing the dispersed area of Zinc sulfide (ZnS) particles which are increased by increasing accelerator content resulting in the increase of network domain size (Ikeda *et al*., 2009; Sakaki *et al*., 2018). Hence, the network domain size which vulcanized by the EV system must larger than Semi EV and CV, respectively.

When the rubber compound was continuously heated after complete vulcanization, the size of the network domain increased due to ZnS was formed during the thermal degradation and oxidation reaction (Larpkasemsuk *et al*., 2019; Kinasih and Fathurrohman, 2018). Therefore, the interconnection between these domains was occurred and create a path that electrons can pass through as shown in Figure 4.16(b) increasing conductance. Moreover, this is corresponding to the results in figure 4.9 which the conductance was increased in the over cure region.

(a) **(b)**
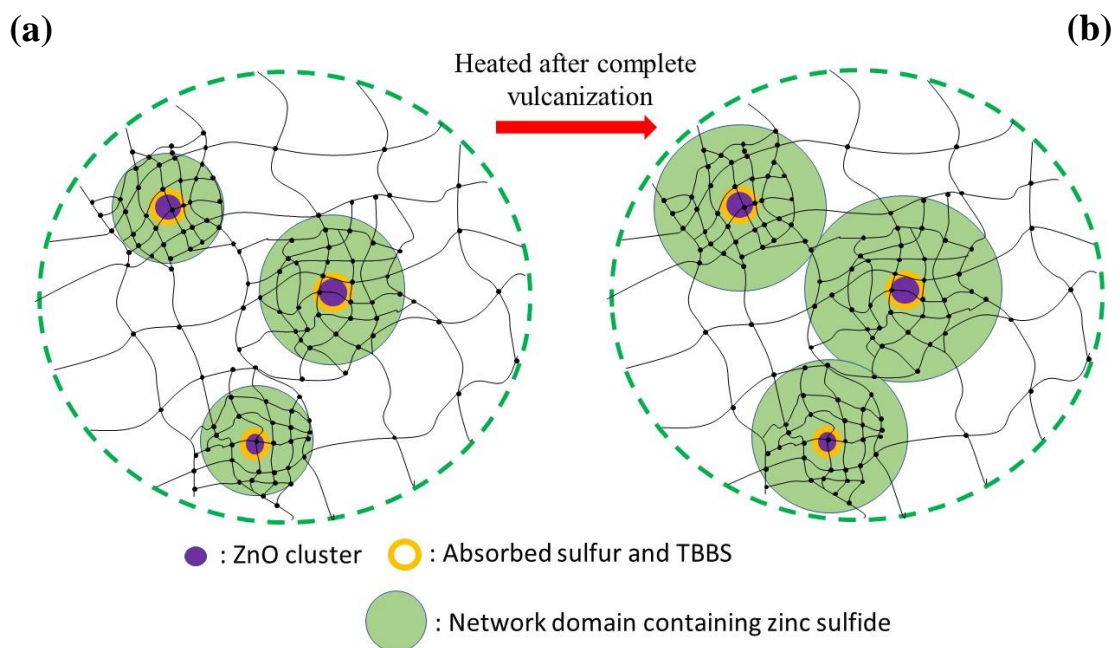
Figure 4.16 Proposed models to explain the interconnection between network domains in natural rubber vulcanizate. (a) The network domain at completely vulcanized. (b) Interconnection between network domains.

As shown in Figure 4.17, the cure characteristics of CV, Semi-EV, EV, and Peroxide vulcanization systems from RCMS and MDR methods were analyzed and compared that show in Table 4.3. A data table expressed in terms of M_L, M_H, C_0, C_{100} scorch time, t_{c90} and CRI, for vulcanized natural rubber in four vulcanization systems. Among the three sulfur vulcanization systems, the EV system contained the highest accelerator concentration. Hence, the cure characteristics from RCMS show the EV system has the lowest scorch time and an increase in the crosslinking in a short time which causes the highest vulcanization rate (CRI). However, the cure characteristics

from MDR showed the highest scorch time but lowest M_H-M_L that corresponding to the research of Sadequl *et. al* (1998) and Sadequl (2000), respectively.

The peroxide vulcanization system showed a longer optimum cure time than the sulfur vulcanization system while CRI was the lowest both characterizing by using MDR and RCMS method. In addition, the C_0, C_{100}, and C_{100}-C_0 of the peroxide vulcanization system were lower than sulfur vulcanization systems. It can be explained that the dipole generated in the curing process of the peroxide vulcanization system was lower than the sulfur vulcanization system (Craig, 2005). Hence, the polarization of these dipoles in the alternating electric field was decreased resulting in lower capacitance in the peroxide vulcanization system. Therefore, it was observed that the RCMS method can provide the cure characteristics of all vulcanization systems of rubber compounds as well as the MDR method.
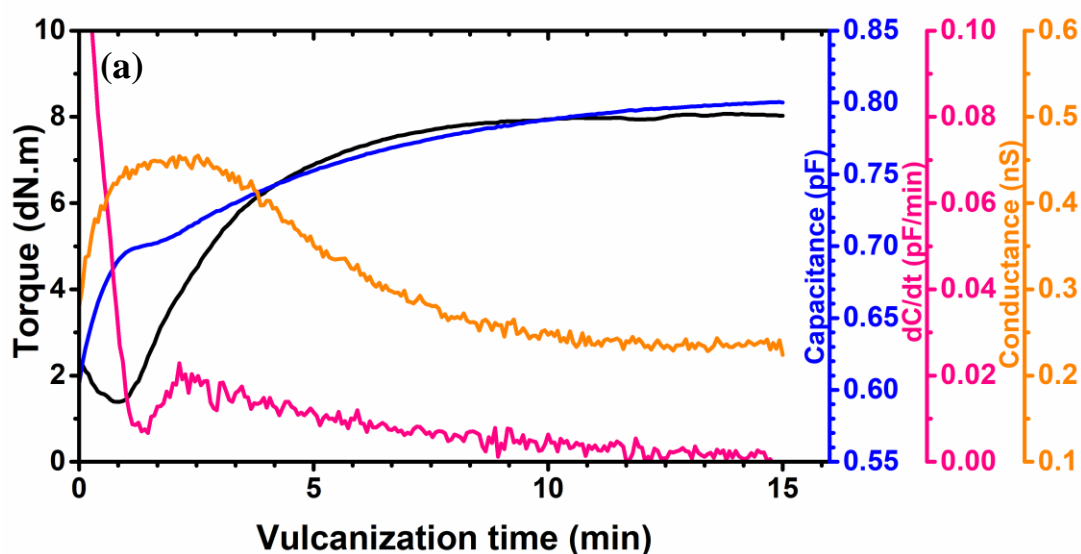
Figure 4.17 Relationship between torque, capacitance and conductance as a function of vulcanization systems (a) CV, (b) Semi-EV, (c) EV and (d) Peroxide.
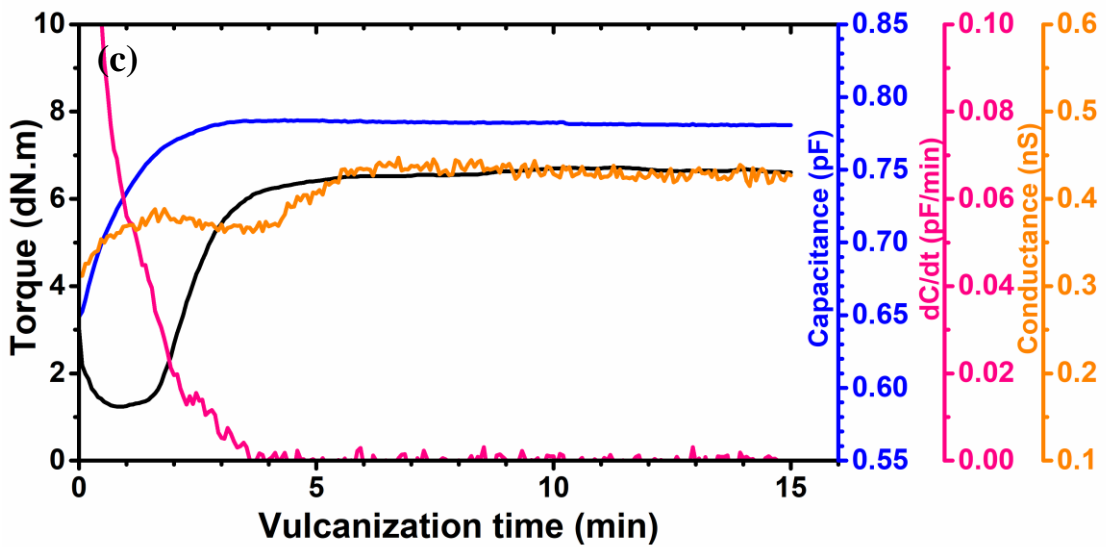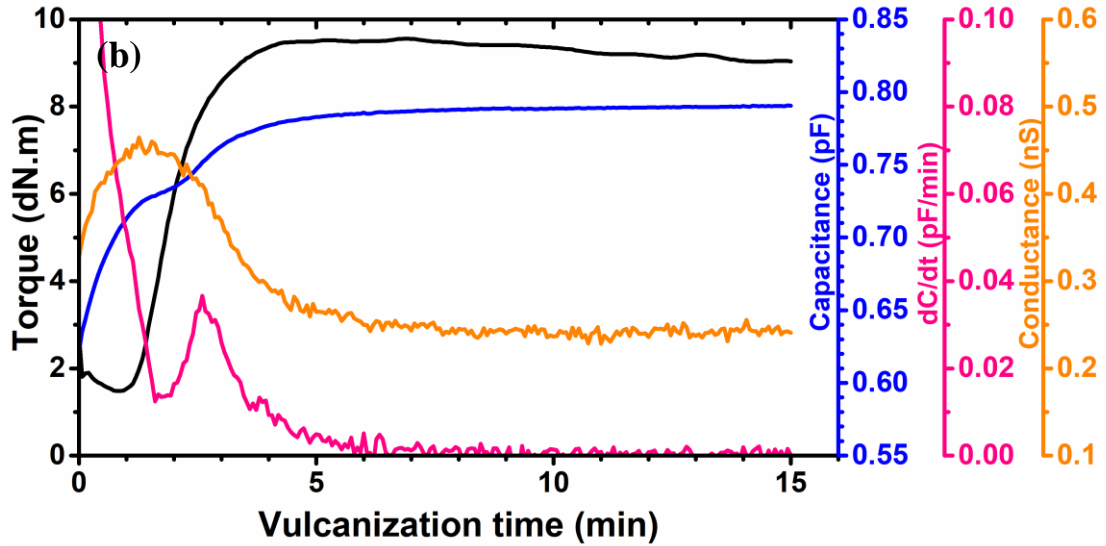
Figure 4.17 (Cont.) Relationship between torque, capacitance and conductance as a function of vulcanization systems (a) CV, (b) Semi-EV, (c) EV and (d) Peroxide.
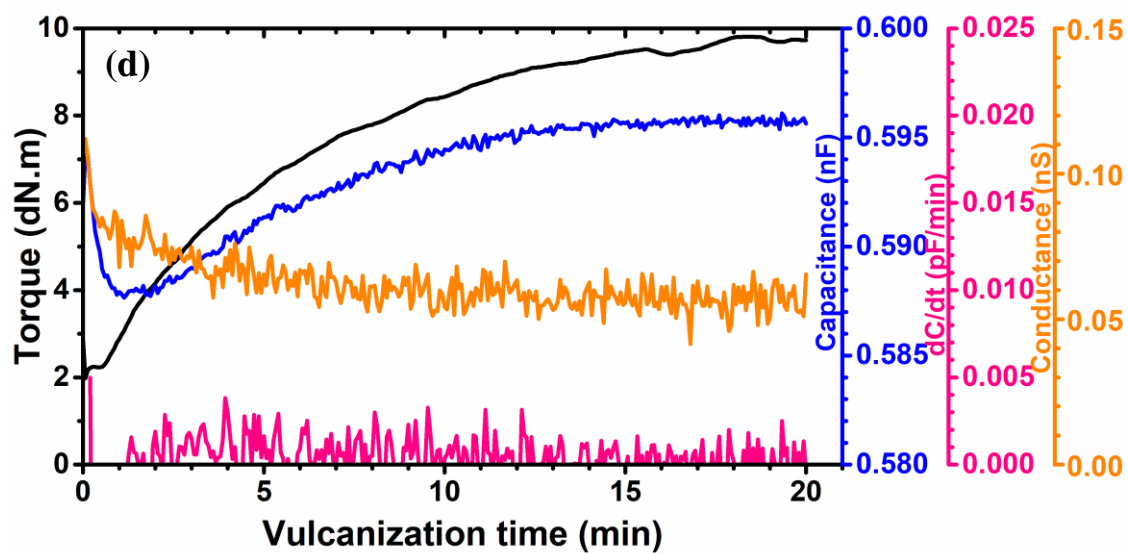
Figure 4.17 (Cont.) Relationship between torque, capacitance and conductance as a function of vulcanization systems (a) CV, (b) Semi-EV, (c) EV and (d) Peroxide.

Table 4.3 Characteristic curing parameters of the NR compounds as evaluated by MDR and RCMS

Cure parameter	CV		Semi-EV		EV		Peroxide	
	MDR	RCMS	MDR	RCMS	MDR	RCMS	MDR	RCMS
M_L (dN.m) or C_0 (fF)	1.53±0.07	702.37±4.31	1.46±0.01	728.57±4.52	1.23±0.02	760.21±9.84	2.16±0.04	587.66±2.29
M_H (dN.m) or C_{100} (fF)	8.57±0.30	794.66±6.55	9.67±0.08	784.83±3.17	6.66±0.03	783.08±4.32	10.34±0.04	595.64±1.48
M_H-M_L (dN.m) or C_{100}- C_0 (fF)	7.04±0.23	92.29±2.28	8.21±0.09	56.26±3.29	5.43±0.46	22.86±5.90	8.18±0.02	7.98±0.87
Scorch time (min)								
-t_{c10}	1.48±0.09	1.96±0.07	1.37±0.01	2.13±0. 26	1.68±0.02	1.60±0.11	1.06±0.04	2.39±0.43
-t_{s1} or t_{dc}	1.60±0.07	2.40±0.04	1.40±0.01	2.60±0.07	1.83±0.03	2.06±0.04	1.18±0.04	-
Cure time (min), t_{c90}	6.275±0.19	6.25±0.19	3.20±0.08	5.44±0.63	3.83±0.02	2.85±0.06	17.93±1.63	13.37±0.34
CRI	20.97±0.69	13.79±1.00	54.55±2.24	30.24±8.92	46.51±0.21	80.20±7.01	5.92±0.69	9.71±0.45

4.5 Effect of carbon black

In this study, carbon black N330 was used as fillers because it provided high abrasion resistance, tear strength and tensile strength. In addition, it is commonly used in the manufacture of tires and products that emphasize good mechanical properties. Figure 4.18 shows that the increment of torque was a result of the reinforcement effect of carbon black. In comparison between Figure 4.18(a) and Figure 4.18(b), it was shown that the capacitance increased with an increase in carbon black loading due to the accumulation of electric charges between the surface of the carbon black particles and rubber matrix (interfacial polarization) and the increased dipoles as functional groups on carbon black surface (Nanda *et al*., 2010). The increment of capacitance was related to the torque in rubber compounds with carbon black loading of 30 phr. However, the capacitance rapidly increased in the early stages of heating due to the occurrence of ionic intermediates in rubber compounds and an increment of dipole content with carbon black 60 phr (Figure 4.18(b)). These ionic intermediates which responded to an arrangement under the electric field can accelerate the vulcanization reaction. After that, the capacitance decreased because carbon black particles moving in melt rubber were contact with each other resulting in the mobility of electric charges which were on the carbon black surface (interfacial polarization). Finally, the capacitance increased again due to the effect of an increase in dipole moment per volume unit from the formation of cross-linkage (Desanges et al., 1958). The capacitance trended to slightly decreased before reaching equilibrium due to the effect of space charge polarization which was the occurrence of an electric discharge due to the movement of electric charges between sensor and rubber surface.
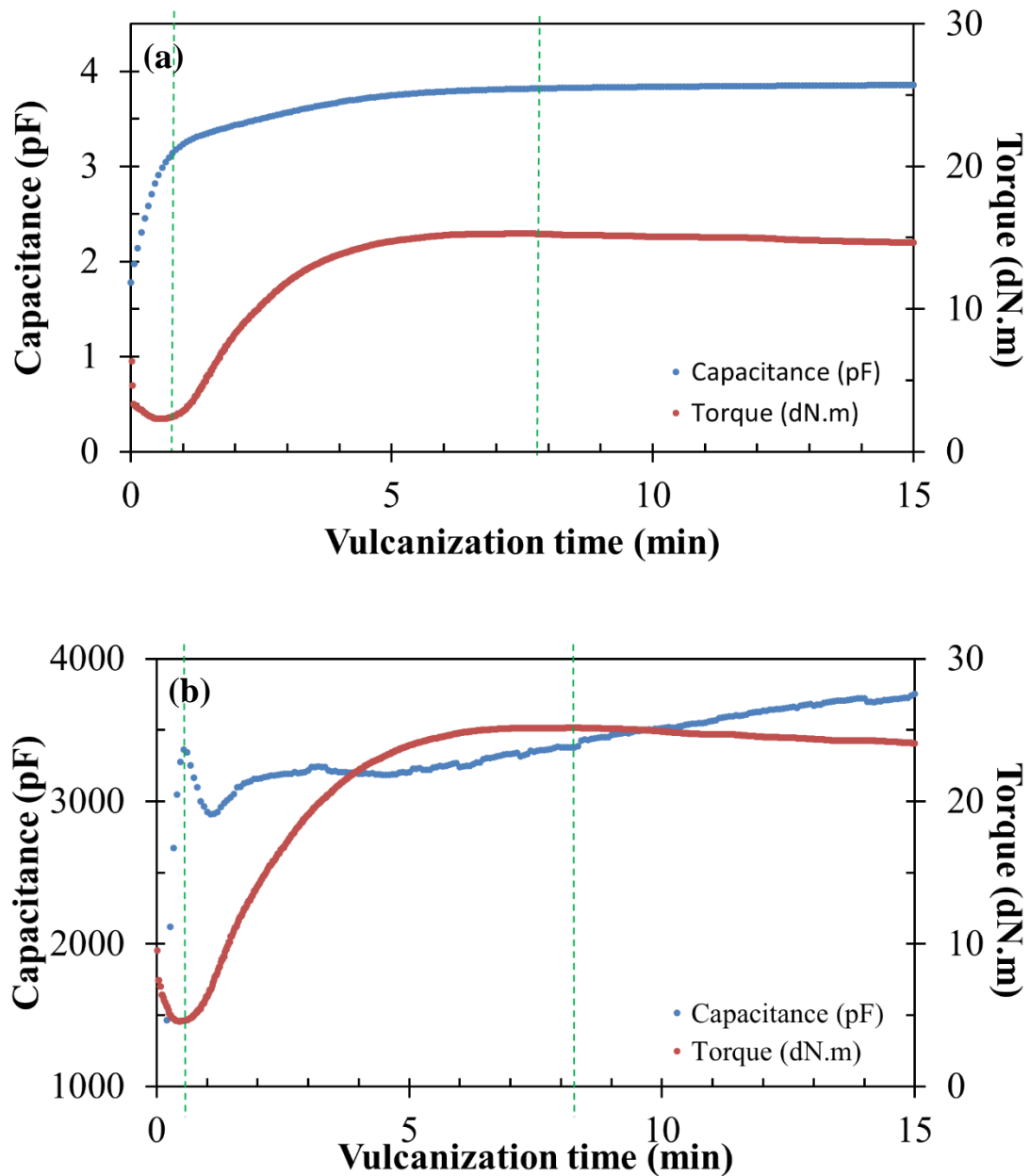
Figure 4.18 Effect of carbon black (N330) on capacitance and torque during vulcanization at 160 ℃ (a) 30 phr and (b) 60 phr

At 60 phr of carbon black content, the electric charges move through the structure of carbon black that was in contact with each other. This phenomenon occurs due to the carbon black content over percolation threshold concentration (Shokr, 2011). Moreover, electric charges moving between sensor and rubber surface occur an electric discharge resulting in the capacitance was not related to the torque. Therefore, we

cannot track the vulcanization process of this rubber compound from capacitance data. Due to this limitation, the researcher modified the contact between sensors and rubber compounds to eliminate the effect of space charge polarization by placing the electrical insulation between the rubber compound and the electrodes. The result was shown in Figure 4.19. The correlation between capacitance and torque in the vulcanization stage was observed which indicates the measured capacitance related to the progress of vulcanization of natural rubber as same as rubber compound with carbon black content below 30 phr.
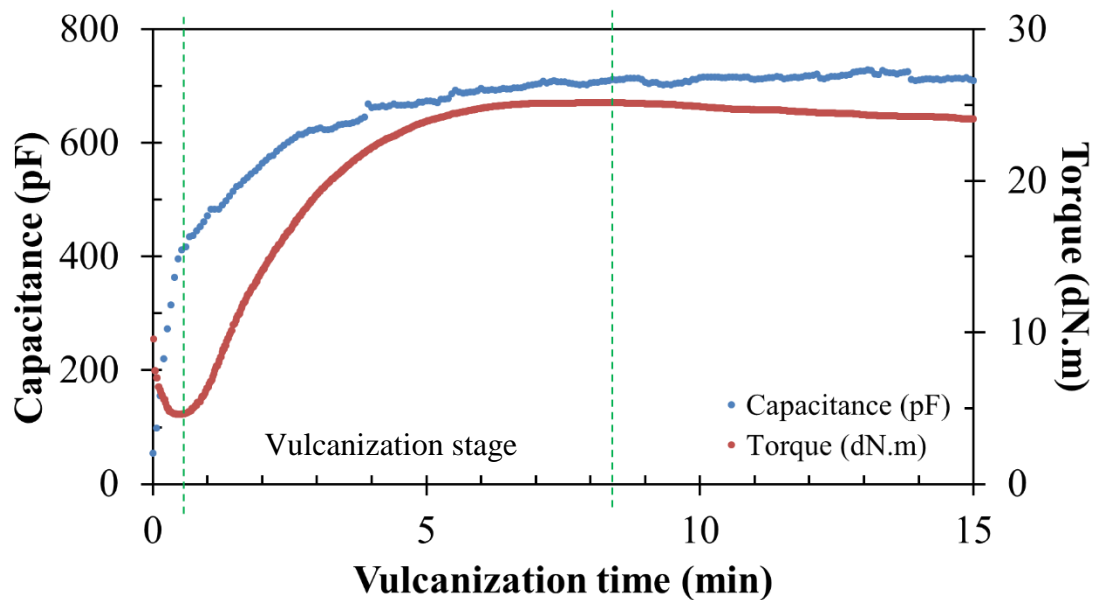
Figure 4.19 Torque and capacitance cure curve of NR with 60 phr of carbon black which placed the electrical insulation between rubber compound and the electrodes

The cure characteristics of rubber compound with 30 phr and 60 phr which placed the electrical insulation between rubber compound and the electrodes from RCMS and MDR methods were analyzed and compared that show in Table 4.4. A data table expressed in terms of M_L, M_H, C_0, C_{100} scorch time, t_{c90} and CRI. The rubber compound with 60 phr carbon black showed a longer optimum cure time than the rubber compound with 30 phr while CRI was the lower both characterizing by using MDR and RCMS method. It was due to the functional groups on the carbon black surface, especially the carboxylic groups and the phenolic groups which reacted with the

accelerator resulting in a slower cure rate (Park *et al*., 2005). In addition, the C_0, C_{100}, and C_{100}-C_0 of rubber compound with 60 phr carbon black were higher than 30 phr due to the high amount of carbon black tends to increase electric charges which were on the carbon black surface or interfacial polarization.

Table 4.4 Characteristic curing parameters of the NR compound as evaluated by MDR and RCMS at different carbon black content 30 and 60 phr.

Cure parameter	30 phr		60 phr (with electrical insulation)	
	MDR	RCMS	MDR	RCMS
M_L (dN.m) or C_0 (fF)	2.31±0.06	323.35±7.32	4.56±0.14	809.51±14.52
M_H (dN.m) or C_{100} (fF)	15.29±0.44	381.74±8.55	25.16±0.63	1232.67±13.23
M_H-M_L (dN.m) or C_{100}- C_0 (fF)	12.98±0.36	58.39±3.24	20.57±0.55	423.16±11.29
Scorch time (min)				
-t_{c10}	1.20±0.11	1.25±0.07	1.03±0.26	1.12±0.10
-t_{s1} or t_{dc}	1.13±0.08	1.36±0.06	0.88±0.22	1.23±0.07
Cure time (min), t_{c90}	4.15±0.21	5.05±0.23	4.48±0.19	5.45±0.63
CRI	33.90±0.80	26.10±1.13	28.99±1.24	23.09±3.93

CHAPTER 5

CONCLUSION

5.1 Effect of electric field frequency

A type of *in situ* cure monitoring for rubber compounds was successfully used to monitor the curing of natural rubber in a compression molding machine. Parallel plate electrodes were embedded in the compression mold, and measurement frequencies from 0.75 to 100 kHz were tested for determining capacitance and conductance during rubber vulcanization. The 5 kHz frequency was chosen for measuring electrical properties during NR vulcanization that were compared to the torque-time curve from MDR. The results obtained with RCMS showed that capacitance was related to NR cure degree, effectively revealing both scorch time and optimum cure time. In addition, the degrees of cure and cure rates from RCMS and MDR were compared and good correlations between the alternative measurements were observed. This RCMS exhibited the good potential to monitor and control the NR production process with real-time monitoring of curing degree.

5.2 Effect of vulcanization temperature

The objective of this part was to find a correlation of the vulcanization temperature with the cure characteristics of natural rubber compound which was examined by both the conventional curemeter (MDR) and the rubber cure monitoring system under isothermal vulcanization temperature. The natural rubber compound was characterized at 150°C, 160°C, and 170°C. In the rheometer curves, a decrease in the minimum torque, maximum torque, delta torque, scorch time, and optimum cure time was observed with the increasing vulcanization temperature. However, in the case of capacitance curves, the capacitance (C_0, C_{100}, and C_{100}-C_0) increases as the cure temperature was increased. The variation of scorch time and cure time as a function of vulcanization temperature from RCMS gave similar data to the MDR method. The maximum point of cure rate curves increased with the increment of the vulcanization temperature, MDR provided the maximum cure rate higher than RCMS at all isothermal temperatures. However, both methods exhibited a good correlation of optimum cure

time (t_{c90}) in the linear line, and a tight correlation between capacitance and torque for the different isothermal cure temperatures was observed.

5.3 Effect of vulcanization system including sulfur vulcanization system (EV, Semi-EV, CV) and peroxide vulcanization system

The vulcanization system and type of curing agent have affected the changes of the torque and the electrical capacity during the vulcanization process. RCMS can monitor the vulcanizing process via the changing electrical properties which correlated with the changes in torque obtained from MDR. Semi EV system provided the optimum cure time (t_{c90}) and cure rate shorter than the EV system and CV system, respectively. In the case of the EV system, the connections between network domains create a conductive path resulting in increasing of conductivity again after completed vulcanization. The peroxide vulcanization system showed a shorter scorch time but longer optimum cure time than the sulfur vulcanization system. The capacitance (C_0, C_{100}, and C_{100}-C_0) of the peroxide vulcanization system was lower than the sulfur vulcanization system. It was observed that the capacitance from the RCMS method can provide the cure characteristics of all vulcanization systems of rubber compound as well as the MDR method.

5.4 Suggestion

With the conclusions above, the researcher would like to suggest for further study to improved rubber cure monitoring system (RCMS) to monitor the curing of natural rubber in the rubber product molding process as follows.

5.4.1　Study the effect of parallel plate electrodes geometry and distance between plates to electrical properties during rubber vulcanization.

5.4.2　Improve the temperature resistance and pressure of electrodes by using ceramics material to replace polytetrafluoroethylene for compression molding of rubber compounds at high temperature or high pressure.

5.4.3　Improve the electrode for the rubber compound which occurs electric discharge due to the carbon black content over the percolation threshold concentration (more than 30 phr) by studying the type of insulator and thickness for coating the insulator layer on parallel plate surface.

5.4.4   Study the effect of accelerator type on electrical properties during rubber vulcanization.

5.4.5   Study the effect of fillers which using in rubber industry such as silica calcium carbonate and clays on electrical properties during rubber vulcanization.

5.4.6   Study the effect of rubber types such as styrene-butadiene rubber, acrylonitrile-butadiene rubber and ethylene-propylene-diene rubber on electrical properties during vulcanization.

REFFERENCE

Abd-El-Messieh, S.L. and Abd-El-Nour, K.N. 2003. Effect of curing time and sulfur content on the dielectric relaxation of styrene butadiene rubber. Journal of Applied Polymer Science. 88, 1613–1621.

Ahmadi, M. and Shojaei, A. 2013. Cure kinetic and network structure of NR/SBR composites reinforced by multiwalled carbon nanotube and carbon blacks. Thermochimica Acta. 566, 238-248.

Ahmad, Z. 2012. Polymeric dielectric materials. In Dielectric material, M.A. Silaghi, editor. InTech, Croatia, pp. 3-26.

Agilent company. 2006. Agilent Basic of measuring the dielectric properties of materials. Application Note, U.S.A.

Alemour, B., Badran, O. and Hassan, M.R. 2019. A Review of Using Conductive Composite Materials in Solving Lightening Strike and Ice Accumulation Problems in Aviation. Journal of Aerospace Technology and Management. 11, e1919.

Al-Hartomy, O.A., Al-Ghamdi, A., Dishovsky, N., Shtarkova, R., Iliev, V., Mutlay, I. and El-Tantawy, F. 2012. Dielectric and microwave properties of natural rubber based nanocomposites containing graphene. Material Sciences and Applications. 3, 453-459.

Arrillaga, A., Zaldua, A.M., Atxurra, R.M. and Farid, A.S. 2007. Techniques used for determining cure kinetics of rubber compounds. European Polymer Journal. 43, 4783–4799.

Bakule, R. and Havránek, A. 1975. The dependence of dielectric properties on crosslinking density of rubbers. Journal of Polymer Science: Polymer Symposia. 53(1), 347-356.

Blythe, A.R. and Bloor, D. 2005. Electrical properties of polymers, Second ed. Cambridge University Press, United Kingdom.

Bovtun, V., Stark , W., Kelm, J., Porokhonskyy, V. and Yakimenko, Y., 2 0 0 1 . Microwave dielectric properties of rubber compounds undergoing vulcanisation part 1 . natural rubber with and without carbon black filler. Kautschuk Gummi Kunststoffe. 54, 673-678.

Bovtun, V., Stark , W., Kelm, J., Porokhonskyy, V. and Yakimenko, Y., 2 0 0 2 , Microwave dielectric properties of rubber compounds undergoing vulcanisation part 2. influence of carbon black. Kautschuk Gummi Kunststoffe. 55, 16-22.

Capps, R. N. and Coughiin, C.S. 1992. Influence of cure system on dielectric viscoelastic relaxations in crosslinked chlorobutyl rubber. Synthesis, characterization and theory of polymeric networks and gels. S.M. Aharoni, editor. Plenum Press, New York. pp. 269-283.

Casalini, R., Corezzi, S., Livi, A., Levita, G. and Rolla, P.A. 1997. Dielectric Parameters to Monitor the Crosslink of Epoxy Resins. Journal of Applied Polymer Science. 65, 17–25.

Chen, J. and Hojjati, M. 2007. Microdielectric analysis and curing kinetics of an epoxy resin system. Polymer Engineering and Science. 47, 150-158.

Choi, J.H., Kim, I.Y. and Lee, D. G. 2003. Development of the simple dielectric sensor for the cure monitoring of the high temperature composites. Journal of Materials Processing Technology. 132, 168-176.

Chueangchayaphan, W., Chueangchayaphan, N., Tanrattanakul, V., Muangsap, S. 2018. Influences of the grafting percentage of natural rubber-graft-poly(2-hydroxyethyl acrylate) on properties of its vulcanizates. Polymer International. 67, 739–746.

Chung, K.T., Sabo, A. and Pica, A.P. 1982. Electrical permittivity and conductivity of carbon black-polyvinyl chloride composites. Journal of Applied Physics. 53, 6867-6879.

Codrington, R.S. 1948. The dielectric properties of natural and synthetic rubber-sulphur compounds. M.Sc. Thesis. The University of British Columbia, Vancouver.

Craig, D.Q.M. 2005. Dielectric analysis of pharmaceutical systems. Taylor & Francis e-Library, U.S.A., pp. 154-187.

Desanges, H., Chasset, R. and Thirion, P. 1958. Changes in the electrical properties of natural rubber/carbon black compounds during vulcanization. Rubber Chemistry and Technology. 31, 631–649.

Dick, J.S. and Pawlowski, H. 1995. Alternate instrumental methods of measuring scorch and cure characteristics. Polymer Testing. 14, 45–84.

Ding, R. and Leonov, A.I. 1996. A Kinetic Model for Sulfur Accelerated Vulcanization of a Natural Rubber Compound. Journal of Applied Polymer Science. 61, 455-463.

Dumbrava, V., Svilainis, L. 2007. The Automated Complex Impedance Measurement System. Electronics and Electrical Engineering. 4(76), 59-62.

Ehrlich, F. 1953. Dielectric Properties of Teflon from Room Temperature to 314 $^{\circ}$C and from Frequencies of 10^2 to 10^5 c/s. Journal of Research of the National Bureau of Standards. 51(4), 185-188.

Erfanian, M., Anbarsooz, M. and Moghiman, M. 2016. A three dimensional simulation of a rubber curing process considering variable order of reaction. Applied Mathematical Modelling. 40, 8592-8604.

Ghosh, P., Katare, S., Patkar, P. and Caruthers, J.M. 2003. Sulfur vulcanization of natural rubber for benzothiazole accelerated formulations: from reaction mechanisms to a rational kinetic model. Rubber Chemistry and Technology. 76, 592–693.

Gondoh, T., Eto, S., Matsuoka, Y., Toh, M., Mori, T. and Okai, D. 1997. In-situ electric measurement of vulcanization process of rubber. Kobunshi Ronbunshu. 54 (5). 359-361.

Gondoh, T., Eto, S., Matsuoka, Y., Toh, M., Okai, D. and Mori, T. 1998. In-situ measurement of electric current and dielectric loss tangent during vulcanisation of nitrie Rubber. Nippon Gomu Kyokaishi. 71 (5), 281-285.

Hann, C.J., Sullivan, A.B., Host, B.C. and Kuhls, G.H. 1994. Vulcanization chemistry. comparison of the new accelerator n-t-butyl-2-benzothiazole sulfenimide (TBSI) with n-t-butyl-2-benzothiazole sulfenamide (TBBS). 67(1), 76–87.

Hardis, R., Jessop, J.L.P., Peters, F.E. and Kessler, M.R. 2013. Cure kinetics characterization and monitoring of an epoxy resin using DSC, Raman spectroscopy, and DEA. Composites: Part A. 49, 100-108.

Hernández, M., Carretero-González, J., Verdejo, R., Ezquerra, T.A. and López-Manchado, M.A. 2010. Molecular dynamics of natural rubber/layered silicate nanocomposites as studied by dielectric relaxation spectroscopy. Macromolecules. 43, 643–651.

Hernández, M., Ezquerra, T.A., Verdejo, R. and Lopez-Manchado M.A. 2012. Role of vulcanizing additives on the segmental dynamics of natural rubber. Macromolecules. 45, 1070-1075.

Hewlett-Packard company. 1992. Basic of measuring the dielectric properties of materials, Application Note 1217-1, U.S.A.

Hosseini, S.M. and Razzaghi-Kashani M. 2014. Vulcanization kinetics of nano-silica filled styrene butadiene rubber. Polymer. 55, 6426-6434.

Hummel, K. and Rodriguez, F.J.S. 2000. Evidence of ionic intermediates in rubber vulcanization detected by on-line electric current measurements in natural rubber/sulfur/tetramethylthiuram monosulfide/zinc oxide and comparison mixtures. Polymer. 41, 3167-3172.

Hummel, K. and Rodriguez, F.J.S. 2001. Electrochemical evidence of transitory ionic species in the vulcanization of natural rubber with sulfur. Kautschuk Gummi Kunststoffe. 54, 122-126.

Ikeda, Y., Higashitani, N., Hijikata, K., Kokubo, Y. and Morita, Y. 2009. Vulcanization: New Focus on a Traditional Technology by Small-Angle Neutron Scattering. Macromolecules. 42, 2741-2748.

Jaunich, M. and Stark, W. 2009. Monitoring the vulcanization of rubber with ultrasound: influence of material thickness and temperature. Polymer Testing. 28, 901–906.

KanakaRaju, P. 2016. Design and development of portable digital lcr meter by auto balancing bridge method. International Journal of Innovations in Engineering and Technology. 7(3), 130-137.

Khang, T.H. and Ariff, Z.M. 2012. Vulcanization kinetics study of natural rubber compounds having different formulation variables. Journal of Thermal Analysis and Calorimetry. 109, 1545-1553.

Khimi, S.R. and Pickering, K.L. 2014. A new method to predict optimum cure time of rubber compound using dynamic mechanical analysis. Journal of Applied Polymer Science. 131, 40008.

Kim, H. and Char, K. 1999. Dielectric changes during the curing of epoxy resin based on the diglycidyl ether of bisphenol A (DGEBA) with diamine. Bulletin of the Korean Chemical Society. 20, 1329-1334.

Kim, H.G. and Lee, D.G. 2002. Dielectric cure monitoring for glass/polyester prepreg composites. Composite Structures. 57, 91-99.

Kinasih, N.A. and Fathurrohman, M.I. 2017. Effect of curing systems on mechanical properties and n-pentane resistance of carbon black filled natural rubber vulcanizates. Journal of Engineering and Science Research. 1(2), 245-251.

Koizumi, N., Yano, S. and Tsuji, F. 1968. Dielectric properties of polytetrafluoroethylene and tetrafluoroethylene-hexafluoropropylene copolymer. Journal of Polymer Science: Polymer Symposia. 23, 499-508.

Kortaberria, G., Solar, L., Jimeno, A., Arruti, P., Gómez, C. and Mondragon, I. 2006. Curing of an epoxy resin modified with nanoclay monitored by dielectric spectroscopy and rheological measurements. Journal of Applied Polymer Science. 102, 5927-5933.

Krejsa, M.R. and Koenig, J.L. 1993. The nature of sulfur vulcanization. . In Elastomer Technology Handbook, N.P. Cheeremisinoff, editor. CRC Press, USA, pp. 475-494.

Kruželák, J., Sýkora, R. and Hudec, I. 2017. Vulcanization of rubber compounds with peroxide curing systems. Rubber Chemistry and Technology. 90(1), 60-88.

Larpkasemsuk, A., Raksaksri, L., Chuayjuljit, S., chaiwutthinan, P. and Boonmahitthisud, A. Effects of sulfur vulcanization system on cure characteristics, physical

properties and thermal aging of epoxidized natural rubber. Journal of Metals, Materials and Minerals. 29(1), 49-57.

Lee, H.L. 2017. The Handbook of Dielectric Analysis and Cure Monitoring, Lambient Technologies, Cambridge.

Lee, K.C., Md Yusoff, N.A., Othman, N., Mohamad Aini, N.A. 2017. Effect of vulcanization temperature on curing characteristic, physical and mechanical properties of natural rubber/palygorskite composites. IOP Conference Series: Materials Science and Engineering. 223, 012017.

Li, Z., Zhang, J. and Chen, S. 2009. Effect of carbon blacks with various structures on electrical properties of filled ethylene-propylene-diene rubber. Journal of Electrostatics. 67, 73-75.

Li, L. 2011. Dielectric properties of aged polymers and nanocomposites. Ph.D. Thesis. Iowa State University, Iowa.

Lvovich, V.F. 2012. Impedance Spectroscopy: Applications to Electrochemical and Dielectric Phenomena, John Wiley & Sons, New Jersey.

Magill, R. and Demin, S. 1999. Using real-time impedance measurement to monitor and control rubber vulcanization. Rubber World. 221, 24–28.

Magill, R. and Demin, S. 2000. Using real-time impedance measurement to monitor and control rubber vulcanization. Rubber World. 221,16–19.

Maiti, M., Patel, J., Naskar, K. and Bhowmick, A.K. 2006. Influence of various crosslinking systems on the mechanical properties of gas phase EPDM/PP thermoplastic vulcanizates. Journal of Applied Polymer Science. 102, 5463–5471.

Mansilla, M.A., Marzocca, A.J., Macchi, C. and Somoza, A. 2015. Influence of vulcanization temperature on the cure kinetics and on the microstructural properties in natural rubber/styrene-butadiene rubber blends prepared by solution mixing. European Polymer Journal. 69, 50–61.

McIihagger, A., Brown. D. and Hill, B. 2000. The development of a dielectric system for the on-line cure monitoring of the resin transfer moulding process. Composites: Part A. 31, 1373-1381.

Miratsu, R., Hirakawa, Y., Gondoh, T., Watanabe, K. and Mori, T. 2013. Temporal measurement of electric impedance of rubber during vulcanization. Proceedings of the 3rd Thailand-Japan Rubber Symposium, March 10-14, 2013, B10.

Müller, U., Pretschuh, C., Zikulnig-Rusch, E., Dolezel-Horwath, E., Reiner, M. and Knappe, S. 2016. Dielectric analysis as cure monitoring system for melamine-formaldehyde laminates. Progress in Organic Coatings. 90, 277–283.

Nam, J.D., Choi, H.R., Koo, J.C., Lee, Y.K. and Kim, K.J. 2007. Dielectric elastomers for artificial muscles. In Electroactive polymers for robotic applications, K.J. Kim and S. Tadokoro, editors. Springer, England, pp. 37-48.

Nanda, M., Chaudhary, R.N.P. and Tripathy, D.K. 2010. Dielectric relaxation of conductive carbon black reinforced chlorosulfonated polyethylene vulcanizates. Polymer Composites. 152-162.

Ortiz-Serna, P., Dı́az-Calleja, R., Sanchis, M.J., Floudas, G., Nunes, R.C., Martins, A.F. and Visconte, L.L. 2010. Dynamics of natural rubber as a function of frequency, temperature, and pressure: A dielectric spectroscopy investigation. Macromolecules. 43, 5094-5102.

Park, S.J., Seo, M.K. and Nah, C. 2005. Influence of surface characteristics of carbon blacks on cure and mechanical behaviors of rubber matrix compoundings. Journal of Colloid and Interface Science. 291, 229–235.

Persson, S. 1986. Dielectric vulcametry. Polymer Testing. 6 (1), 47–77.

Posadas, P., Fernández-Torres, A., Valentín, J.L., Rodríguez, A. and González, L. 2010. Effect of the Temperature on the Kinetic of Natural Rubber Vulcanization with the Sulfur Donor Agent Dipentamethylene Thiuram Tetrasulphide Journal of Applied Polymer Science. 115, 692-701.

Rabiei, S., Shojaei, A. 2016. Vulcanization kinetics and reversion behavior of natural rubber/styrene-butadiene rubber blend filled with nanodiamond – the role of sulfur curing system. European Polymer Journal. 81, 98-113.

Rath, M., Döring, J., Stark, W. and Hinrichsen, G. 2000. Process monitoring of moulding compounds by ultrasonic measurements in a compression mould. NDT and E International. 33(2), 123-130.

Renukappa, N.M., Siddaramaiah, Samuel, R.D., Rajan, J.S. and Lee, J.H. 2009. Dielectric properties of carbon black: SBR composites. Journal of Materials Science: Materials in Electronics. 20, 648–656.

Rodriguez, F.J.S. and Hummel, K. 2000. Evidence of ionic components in vulcanization mixtures by means of electric current measurements: investigations with natural rubber/sulfur/zinc bis(dimethyldithiocarbamate) and comparison mixtures. Journal of Applied Polymer Science. 78, 2206-2212.

Rosca, I.D., Granger, R. and Vergnaud, J.M. 2003. Linear temperature programming rheometers for the cure of rubbers: Effect of the various parameters. Polymers & Polymer Composites. 12(1), 87-98.

Sadequl, A.M., Ishiaku, U.S., Ismail, H. and Poh, B.T. 1998. The effect of accelerator/Sulphur ratio on the scorch time of epoxidized natural rubber. European Polymer Journal. 34, 51-57.

Sadequl, A.M. 2000. The Effect of Accelerator/Sulphur Ratio on the Cure Time and Torque Maximum of Epoxidized Natural Rubber. International Journal of Polymeric Materials and Polymeric Biomaterials. 46(3-4), 597-615.

Sakaki, Y., Usami, R., Tohsan, A., Junkong, P. and Ikeda, Y. 2018. Dominant formation of disulfidic linkages in the sulfur cross-linking reaction of isoprene rubber by using zinc stearate as an activator. Royal Society of Chemistry. 8, 10727-10734.

Senturia, S.D. and Sheppard, N.F. 1986. Dielectric analysis of thermoset cure. Advance in Polymer Science. 80, 1-46.

Shakun, A. 2014. Soft elastomeric material with improved dielectric permittivity. M.Sc. Thesis. Tampere University of Technology, Tampere.

Sheha, E.M., Nasr, M.M., El-Mansy, M.K. 2015. The role of MgBr 2 to enhance the ionic conductivity of PVA/PEDOT:PSS polymer composite. Journal of Advanced Research. 6, 563–569.

Shokr, F.S. 2011. Dielectric properties of carbon black loaded EPDM rubber based conductive composites: Effect of curing method. Journal of American Science. 7(9), 387-397.

Skordos, A.A. and Partridge, I.K. 2004. Determination of the Degree of Cure under Dynamic and Isothermal Curing Conditions with Electrical Impedance Spectroscopy. Journal of Polymer Science: Part B: Polymer Physics. 42, 146-154.

Skordos, A.A. and Partridge, I.K. 2007. Effects of tool-embedded dielectric sensors on heat transfer phenomena during composite cure. Polymer Composites. 28(2), 139-152.

Steinhau., J., Hausnerova, B., Haenel, T., Großgarten, M. and Möginger, B. 2014. Curing kinetics of visible light curing dental resin composites investigated by dielectric analysis (DEA). Dental Materials. 30, 372–380.

Švorčík, V., Králová, J., Rybka V., Plešek, J., Červená, J. and Hnatowicz V. 2001. Temperature dependence of the permittivity of polymer composites. Journal of Polymer Science Part B: Polymer Physics. 39(8), 831-834.

Tuckett, R.F. 1942. The kinetics of high elasticity in synthetic polymers. Transactions of the Faraday Society. 38, 310–317.

Van Doren, J.C., Magill, R. Sellers, B., Erickson, T., Schnieder, S., Courington, S. and Bethel, L. 2005. Process and apparatus for improving and controlling the vulcanization of natural and synthetic rubber compounds. U.S.A. Patent No. 6,855,791 B2. February 15.

Van Krevelen, D.W. 2009. Properties of polymers: their correlation with chemical structure: their numerical estimation and prediction from additive group contributions. Fourth ed., K. te Nijenhuis, editor. Elsevier, Oxford, United Kingdom, pp. 319-352.

Vassilikou-Dova A., Kalogeras I.M. 2009. Thermal analysis of polymers: fundamentals and applications, J.D. Menczel and R.B. Prime, editors. John Wiley & Sons Inc., New Jersey, USA, pp. 497-603.

Wang, P., Qian, H., Yu and H., Chen. 2003. Study on kinetic of natural rubber vulcanization by using vulcameter. Journal of Applied Polymer Science. 88, 680-684.

Wang, X., Xia, Z., Yuan, B., Zhou, H., Li, Z. and Chen, N. 2013. Effect of curing temperature on the properties of conductive silicone rubber filled with carbonyl permalloy powder. Materials & Design. 51, 287-292.

Zhang, B., Wang, Y., Wang, P. and Huang, H. 2013. Study on vulcanization kinetics of constant viscosity natural rubber by using a rheometer MDR2000. Journal of Applied Polymer Science. 130, 47–53.

Zhou, B., He, D., Quan, Y. and Chen, Q. 2012. The investigation on the curing process of polysulfide sealant by In situ dielectric analysis. Journal of Applied Polymer Science. 126, 1725–1732.

Zhang, H., Li, Y., Shou, J., Zhang, Z., Zhao, G. and Liu, Y. 2016. Effect of curing temperature on properties of semi-efficient vulcanized natural rubber Journal of Elastomers & Plastics. 48, 331-339.

APPENDICES

APPENDIX A

Published Article in

Advances in Polymer Technology, 37: 3384-3391 (2018)

WILEY

RESEARCH ARTICLE

Evaluation of dielectric cure monitoring for in situ measurement of natural rubber vulcanization

Narong Chueangchayaphan[1] [ID] | Nattapong Nithi-Uthai[1] | Kittiphan Techakittiroj[2] |
Hathaikarn Manuspiya[3]

[1]Department of Rubber Technology and Polymer Science, Faculty of Science and Technology, Prince of Songkla University, Pattani, Thailand

[2]Department of Mechatronics Engineering, Faculty of Engineering, Assumption University, Samut Prakan, Thailand

[3]The Petroleum and Petrochemical College, Chulalongkorn University, Bangkok, Thailand

Correspondence
Narong Chueangchayaphan, Department of Rubber Technology and Polymer Science, Faculty of Science and Technology, Prince of Songkla University, Pattani, Thailand.
Email: narong.c@psu.ac.th

Funding information
the National Research Council of Thailand (NRCT), Grant/Award Number: RDG5550112; graduate school of Prince of Songkla University

Abstract

A novel in situ rubber cure monitoring system (RCMS) has been developed for monitoring the progress of vulcanization based on the measurement of electrical properties. The sensors connected to an LCR meter were embedded in the compression mold and measured changes in the electrical properties of rubber during vulcanization. Frequencies ranging from 0.75 to 100 kHz were probed for capacitance and conductance, and 5 kHz frequency was found suitable for monitoring natural rubber vulcanization. The results show that capacitance during curing correlated with the time profile of torque from a moving die rheometer (MDR). The scorch time and optimum cure time obtained from MDR and RCMS were reported. The degree of cure and the cure rate from two methods were compared. Good correlations between the alternative methods were observed, supporting the potential of in situ RCMS during the vulcanization of natural rubber.

KEYWORDS

dielectric cure monitoring, rubber cure characterization, rubber cure monitoring system, vulcanization

1 | INTRODUCTION

Natural rubber (NR) is an elastomer obtained from *Hevea brasiliensis* trees. It is nearly 100% *cis*-1,4-polyisoprene, which is a linear, unsaturated, long chain aliphatic hydrocarbon. As a result of its highly regular structure, NR has a tendency to crystallize spontaneously at low temperatures or when it is stretched. NR exhibits outstanding tack and strength in unvulcanized state; and high mechanical strength, resilience, damping, tear strength, and fatigue resistance in vulcanized state.[1,2] Due to its remarkable and desirable properties, it is used in many products, such as tires, conveyor belts, dampers, hoses, bearings, seals. For optimal engineering properties, the rubber molecules are cross-linked to form three-dimensional elastic networks. The cross-linking reactions are named vulcanization or curing, and require elevated temperature and pressure,

giving these materials unique properties. Sulfur curing systems are widely used to vulcanize rubber compounds, forming sulphidic cross-links between the rubber chains.[3] The degree of vulcanization of a rubber compound has a great influence on the final product properties. Thus, knowing the optimum cure time at a certain temperature is crucial. In general, the main approach to determine the vulcanization characteristics of a rubber compound is to use the moving die rheometer (MDR), for an indirect measurement of the reaction extent. Rheometry provides approximate data on behavior of the rubber compound, but is not representative of the actual process conditions due to various factors affecting the molding process, such as actual temperature, geometry, and material heat-up rate. Therefore, the cure time obtained by rheometry is not necessarily optimal for rubber manufacturing, resulting in poor product quality, waste of materials, and longer than

needed cycle time.[4,5] In general, ultrasound and dielectric methods are available, and are commonly used at high temperatures and pressures for direct cure monitoring of thermoset materials.[5–7] However, direct cure monitoring is not much practiced with elastomer vulcanization. The observation of sound velocity to monitor rubber during cross-linking has been described,[5,8] and the use of dielectric analysis to monitor the curing of elastomers has also been described.[4,9,10]

Dielectric analysis (DEA) measures changes in the electrical properties of a material, such as permittivity and conductivity that depend on temperature and frequency. The main advantages of DEA include a very broad frequency range and a variety of sample configurations, for high precision study of both very fast molecular motions and very slow motions. A limitation of DEA is that it is only applicable to materials with a suitable concentration of dipole groups or trace ions, while electrically conductive materials cannot be measured at low frequencies.[11] The applicability of DEA to cure monitoring of various resins and adhesives has been investigated in many studies.[6,7,12–22] There are also quite a few reports on the use of DEA to monitor rubber vulcanization.[4,9,23] In polymeric dielectric materials, the polarization correlates to the vector sum of all dipoles in the polymer chains.[11] Basically, NR consists of cis-1,4-polyisoprene chains with asymmetric repeating units. Therefore, natural rubber has nonzero dipole moment both vertically and horizontally relative to the chain contour.[24] The free rotations of single carbon–carbon bonds in its long molecular chains are responsible for dielectric losses in vulcanized rubber, because the rubber-sulfur dipoles oscillate in an electric field.[23] The addition of sulfur not only changes dipole moments but also alters other physical properties. The cross-links between rubber chains restrict rotations of the dipoles proportionally to the cross-link density.[25]

The changes in dipole moment and viscosity of NR during vulcanization can be monitored by DEA, enabling real-time observation of natural rubber vulcanization. However, the fundamentals of relationship between rheology and chemistry of NR curing need to be clarified. Thus, in this study, we describe results from testing dielectric cure monitoring for its suitability to online monitoring of natural rubber compound vulcanization by compression molding. The aim of the study was to develop and extend the use of dielectric cure monitoring in rubber manufacturing, demonstrating application to practical production methods, to support improving product quality and productivity. The stages in NR curing were observed by dielectric measurements, and were related to conventional curemeter results. The effects of signal frequency on capacitance (C) and conductance (G) are discussed.

2 | BACKGROUND

2.1 | Moving die rheometer

Moving die rheometer is commonly used as a curemeter for characterizing rubber vulcanization and for quality control in rubber manufacturing, based on ASTM D5289. It measures the torque required for constant amplitude rotational oscillations at a given temperature in a cavity. The oscillations deform the rubber specimen torsionally and the force is detected. From the measured torque, the shear modulus ($G*$) can be obtained as the ratio of shear stress (τ) and strain (γ) as follows:

$$G^* = \frac{\tau}{\gamma} \tag{1}$$

During isothermal vulcanization, the shear modulus increases due to the formation of a three-dimensional network of rubber molecular chains. The torque required to shear the compound is commonly plotted as a function of time to get a so-called rheograph or cure curve. A typical cure curve of rubber vulcanization is shown in Figure 1. The cure curve for rubber vulcanization typically shows three main steps.

The first region, which limits processing safety, is an induction period or a scorch delay. It involves with the accelerator reaction. The required time for the torque to rise one unit (dN.m) above the minimum torque or t_{s1} is usually defined as the MDR scorch time. However, t_{c10} is the time to reach a 10% cure extent, and is occasionally used as a measure of scorch time. Because t_{c10} is not dependent on a specified increment in torque, it has an advantage over t_{s1}. The t_{s1} of a compound with a high M_H represents a much smaller percent of the ultimate state of cure than for a compound with a relatively low M_H.[26] Therefore, ASTM D 5289 also permits t_{c10} to be used as a measure of scorch, which indicates the
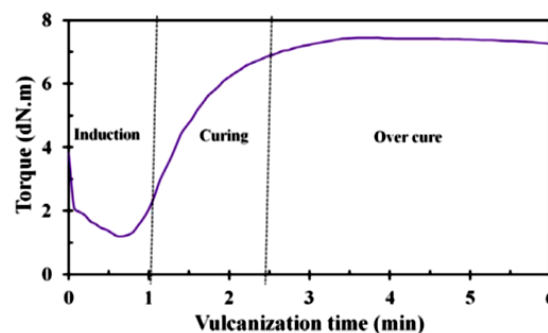

FIGURE 1   A typical cure curve for rubber vulcanization

beginning of cross-linking or vulcanization. The second region is the cure period, in which the networks are formed by cross-linking. The third region is the overcure with network maturation. The main numerical characteristics obtained from the cure curve are as follows:

- The minimum torque (M_L) is the lowest point in the cure curve. It relates to the material viscosity.
- The maximum torque (M_H) is the highest point where the curve plateaus. It relates to the highest cross-linking level.
- x is the percentage of cure required.
- t_{cx} is the time to achieve a given degree of cure. It can be calculated from:

$$t_{cx} = \text{minutes to torque being } M_L + \frac{x(M_H - M_L)}{100} \quad (2)$$

In rubber terminology, t_{c90} is termed "the optimum cure time" at which 90% of the change from minimum torque toward maximum is reached.

2.2 | Dielectric analysis (DEA)

The measurement of electrical properties of a material, that is, permittivity, conductivity and polarization, and their dependence on temperature or signal frequency, is known as DEA. Normally, the ions and dipoles that induce capacitive and conductive characteristics tend to have random orientations. When the material is placed between parallel electrodes and an alternating voltage is applied, the ions shift toward the attracting electrode while the dipoles become aligned with the electric field, changing the amplitude of the excitation voltage input (V_{EXC}) and causing a phase shift (θ) in the current output response (I_{RES}), which gives the admittance (Y) (Figure 2)[22] as:

$$Y = \frac{I_{RES}}{V_{EXC}} = G + i\omega C \quad (3)$$

where ω is the angular frequency of alternating voltage (Hz). The measurements of C and G can provide the electrical properties of a material placed in a parallel-plate capacitor under an alternating voltage of angular frequency as follows:

$$\varepsilon' = \frac{C}{\varepsilon_0 \frac{A}{d}} \quad (4)$$

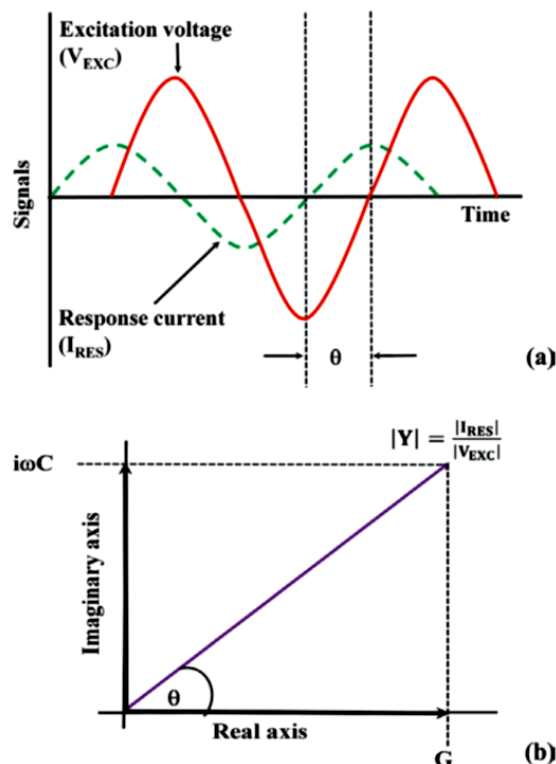$$\varepsilon'' = \frac{G}{\omega \varepsilon_0 \frac{A}{d}} \quad (5)$$

FIGURE 2 (a) Excitation voltage (V_{EXC}) and response current (I_{RES}) between two electrodes, (b) The calculation of conductance (G) and capacitance (C) from admittance (Y) and phase shift (θ) of the current output response from DEA

where ε' is the relative permittivity or real part, ε'' is the relative loss factor or imaginary part, ε_0 is the vacuum permittivity (8.85×10^{-14} F/cm), and A/d is the ratio of electrode area (A) to sample thickness or distance between electrodes (d). The complex permittivity (ε^*) is defined as:

$$\varepsilon^* = \varepsilon' - i\varepsilon'' \quad (6)$$

The ε' is generally related to dipole orientation and describes the ability of a dielectric medium to store energy. On the other hand, ε'' expresses the energy losses effected by ionic flow and dipole motion.[11,22]

3 | METHODS AND EQUIPMENT

3.1 | Preparation of natural rubber compound

The investigated material was a natural rubber compound with conventional sulfur curing system. The formulation of the NR compound is given in Table 1. The NR compound

was prepared in two steps, as presented in Table 2. In the first step, NR, ZnO, and stearic acid were mixed in an internal mixer. The mixing conditions were as follows: fill factor 0.75, initial chamber temperature 35°C, rotor speed 60 rpm, and mixing time 9 min. After the mixing, the sample was kept in desiccator for 24 hr, then accelerator (TBBS) and sulfur were added and continuosly mixed in an internal mixer for 4 min in the second step. At last, the NR compound was sheeted out on a two-roll mill to give samples of about 2 mm thickness.

3.2 | Cure characterization

A Montech Moving Die Rheometer (MDRH2020) was used to measure the selected vulcanization characteristics of rubber compounds, using the sealed torsion shear cure meter according to ASTM D5289. A 4 cm^3 rubber compound volume was filled in the closed and sealed die cavity. The frequency and oscillation amplitude were fixed at 1.7 Hz and 0.5°, respectively. The forces were recorded during torsional deformations of the rubber specimen. The oscillating force or torque was plotted as a function of time. During vulcanization at a given temperature, the

stiffness of rubber sample increases with the formation of cross-links. The cure characteristics determined by MDR are listed in Table 3.

3.3 | Rubber cure monitoring system (RCMS)

Scheme 1 shows a sketch of the experimental set-up with RCMS. Parallel plate electrodes are used in this study because of high accuracy measurements of the average or bulk properties of the sample.[27] The stainless steel electrodes were insulated from surroundings by polytetrafluoroethylene (PTFE) and were built-in in the upper and lower press molds. PTFE was used to insulate the electrodes because of its high-temperature resistance, and low and fairly constant dielectric response over the temperature and frequency ranges of interest.[28,29] The upper and lower electrodes with 11 mm diameters were embedded in the steel mold for compression molding of the NR compound. The mold cavity is cylindrical with 40 mm diameter and 1.5 mm height. The mold temperature was measured with thermocouples embedded in the mold near the electrodes. The mold was preheated to the 160°C curing temperature in the compression molding machine, and then the rubber compound (4 cm^3) was placed into the mold. At last, the rubber was compressed with 10 MPa pressure. The LCR meter, Wayne Kerr 4110, was used to monitor capacitance and conductance. A 2V alternating voltage was applied between the parallel plate electrodes in the frequency range from 0.75 to 100 kHz, and the response current was measured. The capacitance and conductance were logged every 4 s for a period of 15 min. The electrical properties were recorded by a data tracking and controlling device, and the time profiles of electrical properties were shown on a monitor connected to the local area network of the rubber cure monitoring system. The RCMS was calibrated and then re-tested with a 1 mm thickness PTFE sheet before each run.

**TABLE 1** Formulation of NR compound

Ingredients	Part per hundred rubber (phr)
Natural rubber (STR 5L)	100
Zinc oxide (ZnO)	5
Stearic acid	2
N-tert-Butyl-2-benzothiazole sulfonamide (TBBS)	1
Sulfur	2

TABLE 2 The mixing schedule of NR compound

Mixing procedure	Cumulative time (min)
Step 1 : Internal mixer	
NR mastication	0
Addition of stearic acid	2
Addition of zinc oxide (ZnO)	3
Dumping	9
Step 2: Internal mixer	
Addition of the mixer from step 1	0
Addition of TBBS and sulfur	2
Addition of sulfur	3
Dumping	4
Total	13

TABLE 3 Characteristic curing parameters of the NR compound as evaluated by MDR and by RCMS at 160°C

Curing parameters	MDR	Curing parameters	RCMS
M_L (dN.m)	1.22 ± 0.04	C_0 (pF)	0.64 ± 0.01
M_H (dN.m)	7.71 ± 0.13	C_{100} (pF)	0.69 ± 0.01
$M_H{-}M_L$ (dN.m)	6.48 ± 0.10	$C_{100}{-}C_0$ (pF)	0.04 ± 0.01
Scorch time (min)		Scorch time (min)	
t_{c10}	1.38 ± 0.06	t_{c10}	1.46 ± 0.07
t_{s1}	1.48 ± 0.05	t_{dc}	1.80 ± 0.12
Cure time, t_{c90} (min)	4.12 ± 0.11	Cure time, t_{c90} (min)	4.85 ± 0.04

97
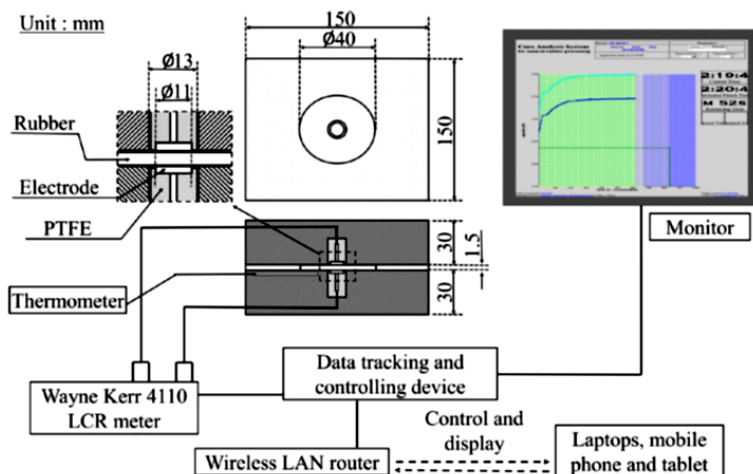
SCHEME 1 Sketch of the experimental set-up for rubber cure monitoring system (RCMS)

4 | RESULTS AND DISCUSSION

In the initial experiment, 10 frequencies (0.75, 1, 2.5, 5, 7.5, 10, 25, 50, 75, and 100 kHz) were tested at 160°C cure temperature over 15 min, to find a suitable informative frequency. The two fundamental electrical characteristics, capacitance, and conductance, as functions of cure time are reported in Figures 3 and 4, respectively. It can be noted that the C and G curves at frequencies below 5 kHz were inconsistent and scattered over a wide range, because of the polarization and blocking effects at low frequencies.[27] The electrode polarization reduces mobility of ions close to the electrodes. The 100 kHz frequency gave noisy results with the RCMS. To identify the change of slope in the capacitance curves, the first time derivative of signal (dC/dt versus t) is shown in Figure 5. Thus, the most useful frequencies with this experimental equipment were in the range from 5 kHz to 75 kHz. For most accurate results, the frequency for the dielectric cure monitoring was set at 5 kHz in the rest of this study.

In order to assess the capability of RCMS to determine the characteristic curing parameters of an NR compound, the relationships between torque, capacitance, derivative of capacitance, and conductance are shown in Figure 6. It was found that the three stages of curing can be observed in torque, capacitance, and derivative of capacitance curves. These parameters changed clearly with time and indicated the progression of cross-linking the NR. In the induction period (region I), the natural rubber compound is softening. Torque and derivative of capacitance rapidly decreased to their minima, while capacitance and conductance promptly increased to peak at approximately 1 min due to increasing mobilities of ions and rubber molecules. The points of minimum torque and maximum capacitance at onset of first slope change were defined as M_L and C_0, from the torque
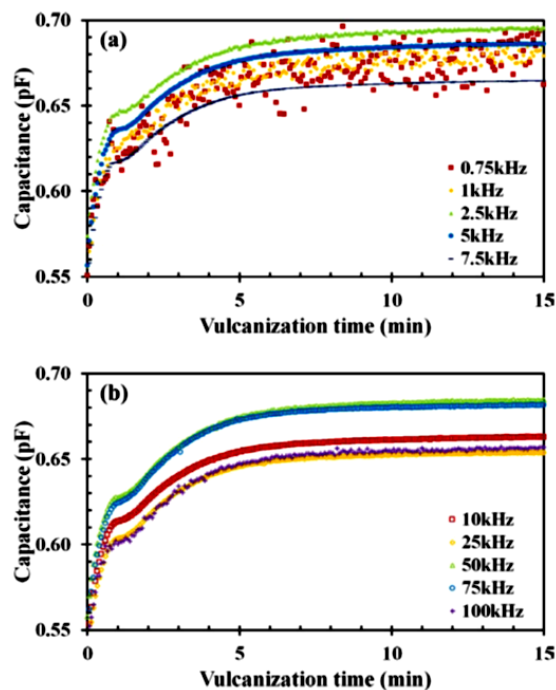

FIGURE 3 Capacitance evolution during the isothermal cure of natural rubber at 160°C observed at various frequencies: (a) 0.75 kHz to 7.5 kHz, and (b) 10 kHz to 100 kHz

curve and the capacitance curve, respectively. In this stage, an active accelerator complex was produced by chemical reactions between accelerator, activator (ZnO) and sulfur. Then, the sulfurating agent obtained from the reaction of the active accelerator complex and sulfur molecules can
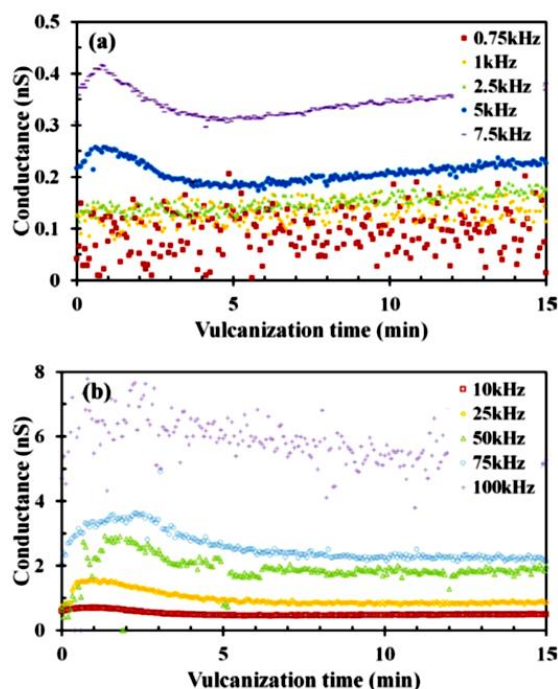
FIGURE 4 Conductance evolution during the isothermal cure of natural rubber at 160°C observed at various frequencies: (a) 0.75 kHz to 7.5 kHz, and (b) 10 kHz to 100 kHz

FIGURE 5 Time derivative of capacitance during the isothermal cure of natural rubber at 160°C observed at various frequencies: (a) 0.75 kHz to 7.5 kHz, and (b) 10 kHz to 100 kHz

react with NR chains to form cross-linking precursors. These intermediates reach their maximum concentrations prior to cross-linking with their decrease caused by significant cross-linking extent.[30–32] Furthermore, the times of M_L, C_0 and maximum G, were indicative of the start of vulcanization (t_{c0}).

In the curing stage (region II), rapid increases were observed in torque and derivative of capacitance, while a gradual increase was seen in capacitance due to sulfur cross-linking. Thus, the dipole moment per unit volume of rubber was increased by the rubber-sulfur dipoles increasing polarization in an electric field.[11,23] The steepest parts related to the maximum point of the derivative of capacitance at around 2 min. The end of curing reaction, which reached the plateau, indicates an equilibrium state of vulcanization. This point can be detected at around 6.5 min, and is indicated by M_H and C_{100} in torque and capacitance, respectively. Times of M_H and C_{100} represent the state of full cure (t_{c100}). After this region, the overcure stage (region III) followed. The conductance decreased rapidly and did not reach a constant value due to decreased ionic conductivity with increasing rubber viscosity, caused by vulcanization.[11,33] In addition, it was found that the peak of conductivity shifted to the right (i.e., to higher frequency) as seen in Figure 4. Thus, conductance was not informative of the NR vulcanization
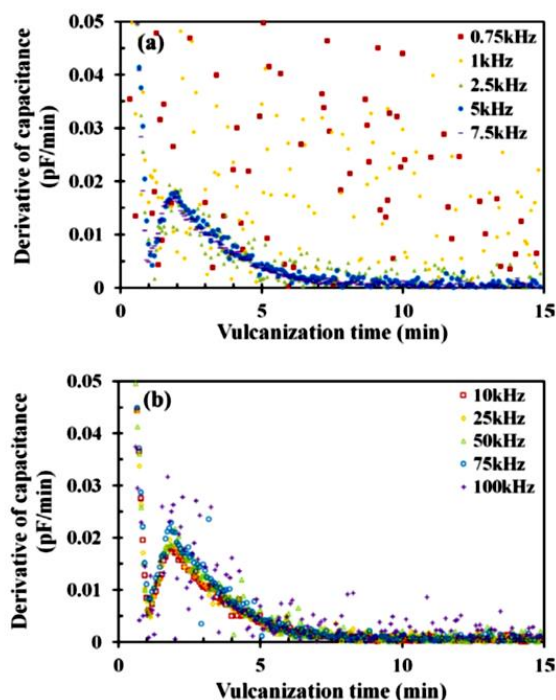
extent. In the cure stage, the cross-linking precursor reacts with another rubber chain, resulting in cross-link formation between NR chains.[34] As previously discussed, T_{90} is generally used as the optimum vulcanization time from an MDR torque-time curve according to equation (2). With the RCMS, an equivalent plateau was observed in the capacitance-time curve, and the extent of vulcanization can be represented as:

$$t_{cx} = \text{minutes to capacitance level } C_0 + \frac{x(C_{100} - C_0)}{100} \quad (7)$$

where C_0 is the maximum capacitance at onset of first slope change and C_{100} is the maximum capacitance at onset of second slope change.

The characteristic cure parameters from MDR and RCMS are listed in Table 3. The scorch time was determined as the time to reach a 10% state of cure (t_{c10}), and as the time required for the torque to rise by one unit (dN.m) above the minimum torque (t_{s1}) for MDR. In addition, the time at inflection point (maximum slope of C) or at the peak of derivative of capacitance (t_{dc}) for RCMS were equated. It was found that there was little difference in scorch time and optimum cure time (t_{c90}) obtained from MDR and
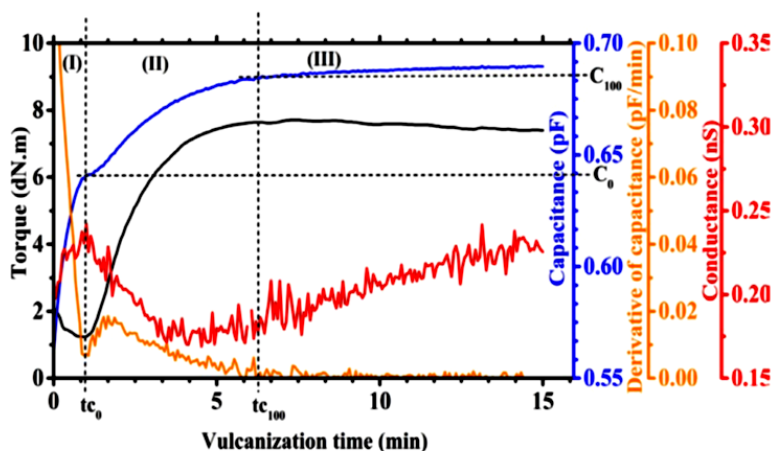
FIGURE 6 Relationship between (a) torque, (b) capacitance, and (c) conductance during vulcanization at 160°C

RCMS. The results from RCMS provided longer scorch and cure times than the MDR, because the special die geometry and the large die surface area of MDR give faster heating of the sample. The measured capacitance was related to the progress of vulcanization of natural rubber. The correlation between capacitance and torque is illustrated in Figure 7. Polynomial regression fit gave the coefficient of determination (R^2) equal to 0.9979, indicating a tight relationship between capacitance and torque for rubber during vulcanization.

The degree of cure (α) as a function of curing time (t) is generally indirectly determined from the torque-time curve obtained with MDR as follows,[35,36] and with RCMS measured capacitance this is analogous to equation (9):
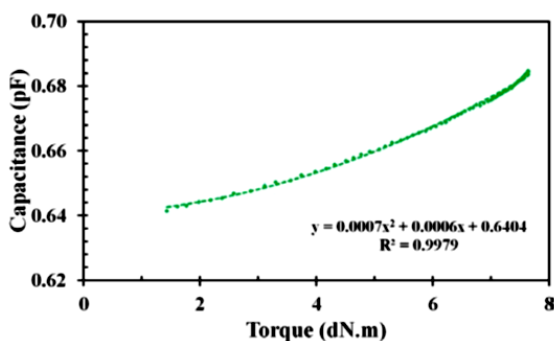
$$\alpha_{(MDR)} = \frac{M_t - M_l}{M_H - M_L} \tag{8}$$

$$\alpha_{(RCMS)} = \frac{C_t - C_0}{C_{100} - C_0} \tag{9}$$

where M_t and C_t are the torque and the capacitance at a given time during vulcanization. In addition, the cure rate or the vulcanization rate ($d\alpha/dt$) is the time derivative of cure degree. For in situ cure monitoring, the results from RCMS should be similar to those from MDR. Thus, the degree of cure and the rate of cure from both methods are compared in Figure 8. As can be seen, the degrees of cure are very similar, but the degree of cure and rate of cure obtained from RCMS are slightly lower than from MDR because of the slower bulk heating that gave slower reaction rates. In other words, the heat transport into the sample was faster in the MDR than in the compression mold with RCMS, due to the special die geometry and high surface area of MDR.[8]

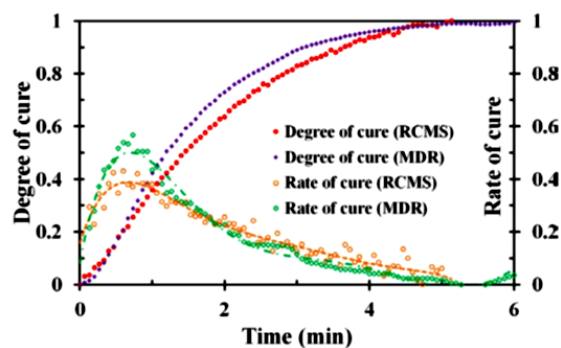

FIGURE 7 The correlation of capacitance and torque during the isothermal cure of natural rubber at 160°C

FIGURE 8 Degree of cure and rate of cure comparison between RCMS and MDR during isothermal vulcanization at 160°C

5 | CONCLUSION

In this study, a new type of in situ cure monitoring for rubber compound was successfully used to monitor the curing of natural rubber in a compression molding machine. Parallel plate electrodes were embedded in the compression mold, and measurement frequencies from 0.75 to 100 kHz were tested for determining capacitance and conductance during vulcanization. The 5 kHz frequency was chosen for measuring electrical properties during NR vulcanization that were compared to the torque-time curve from MDR. The results obtained with RCMS showed that capacitance was related to NR cure degree, effectively revealing both scorch time and optimum cure time. In addition, the degrees of cure and cure rates from RCMS and MDR were compared and good correlations between the alternative measurements were observed. This RCMS clearly exhibited good potential to monitor and control NR production process with real-time monitoring of curing degree.

ORCID

Narong Chueangchayaphan http://orcid.org/0000-0002-8507-5663

REFERENCES

[1] M. Hernandez, T. A. Ezquerra, R. Verdejo, M. A. Lopez-Manchado, *Macromolecules* **2012**, *45*, 1070.

[2] T. Kurian, N. M. Mathew, in Biopolymers: Biomedical and environmental applications (Eds: S. Kalia and L. Avérous), Scrivener Publishing LLC, Massachusetts **2011**, 403.

[3] J. Kruželák, R. Sýkora, I. Hudec, *Chem. Pap.* **2016**, *70*, 1533.

[4] R. Magill, S. Demin, *Rubber World* **1999**, *221*, 24.

[5] M. Jaunich, W. Stark, B. Hoster, *Polym. Test.* **2009**, *28*, 84.

[6] M. Rath, J. Döring, W. Stark, G. Hinrichsen, *NDT&E Int.* **2000**, *33*, 123.

[7] U. Müller, C. Pretschuh, R. Mitter, S. Knappe, *Int. J. Adhes. Adhes.* **2017**, *73*, 45.

[8] M. Jaunich, W. Stark, *Polym. Test.* **2009**, *28*, 901.

[9] R. Magill, S. Demin, *Rubber World* **2000**, *221*, 16.

[10] T. Mori, S. Etoh, Y. Matsuoka, T. Gondoh, M. Toh, D. Okai, *Rubber World* **2000**, *221*, 33.

[11] A. Vassilikou-Dova, I. M. Kalogeras, in Thermal analysis of polymers: Fundamentals and applications (Eds: J. D. Menczel and R. B. Prime), John Wiley & Sons Inc., New Jersey **2009**, 497.

[12] H. G. Kim, D. G. Lee, *Compos. Struct.* **2002**, *57*, 91.

[13] G. Kortaberria, L. Solar, A. Jimeno, P. Arruti, C. GÓmez, I. Mondragon, *J. Appl. Polym. Sci.* **2006**, *102*, 5927.

[14] J. Chen, M. Hojjati, *Polym. Eng. Sci.* **2007**, *47*, 150.

[15] M. Sernek, F. A. Kamke, *Int. J. Adhes. Adhes.* **2007**, *27*, 562.

[16] A. A. Skordos, I. K. Partridge, *Polym. Compos.* **2007**, *28*, 139.

[17] B. Zhou, D. He, Y. Quan, Q. Chen, *J. Appl. Polym. Sci.* **2012**, *126*, 1725.

[18] R. Hardis, J. L. P. Jessop, F. E. Peter, M. R. Kessler, *Compos. Part A* **2013**, *49*, 100.

[19] J. Steinhausa, B. Hausnerovaa, T. Haenela, M. Großgarten, B. Möginger, *Dent. Mater.* **2014**, *30*, 372.

[20] U. Müller, C. Pretschuh, E. Zikulnig-Rusch, E. Dolezel-Horwath, M. Reiner, S. Knappe, *Prog. Org. Coat.* **2016**, *90*, 277.

[21] L. Garden, R. A. Pethrick, *Int. J. Adhes. Adhes.* **2017**, *74*, 6.

[22] H. Park, *J. Appl. Polym. Sci.* **2017**, *134*, 44707.

[23] H. Desanges, R. Chasset, P. Thirion, *Rubber Chem. Technol.* **1958**, *31*, 631.

[24] P. Ortiz-Serna, R. Dı́az-Calleja, M. J. Sanchis, G. Floudas, R. C. Nunes, A. F. Martins, L. L. Visconte, *Macromolecules* **2010**, *43*, 5094.

[25] R. F. Tuckett, *Trans. Faraday Soc.* **1942**, *38*, 310.

[26] J. S. Dick, H. Pawlowski, *Polym. Test.* **1995**, *14*, 45.

[27] A. McIlhagger, D. Brown, B. Hill, *Compos. Part A* **2000**, *31*, 1373.

[28] N. Koizumi, S. Yano, F. Tsuji, *J. Polym. Sci. Polym. Symp.* **1968**, *23*, 499.

[29] L. Li, Ph.D. Iowa State University (Ames, Iowa, USA) **2011**.

[30] K. Hummel, F. J. S. Rodriguez, *Polymer* **2000**, *41*, 3167.

[31] K. Hummel, F. J. S. Rodriguez, *Kautsch. Gummi Kunstst.* **2001**, *54*, 122.

[32] A. M. Sadequl, U. S. Ishiaku, H. Ismail, B. T. Poh, *Eur. Polym. J.* **1998**, *34*, 51.

[33] A. A. Skordos, I. K. Partridge, *J. Polym. Sci., Part B: Polym. Phys.* **2004**, *42*, 146.

[34] R. Ding, A. L. Leonov, *J. Appl. Polym. Sci.* **1996**, *61*, 455.

[35] M. Ahmadi, A. Shojaei, *Thermochim. Acta* **2013**, *566*, 238.

[36] M. R. Erfanian, M. Anbarsooz, M. Moghiman, *Appl. Math. Model.* **2016**, *40*, 8592.

APPENDIX B

Published Article in

Polymer Bulletin, 78: 3169-3182 (2021)

ORIGINAL PAPER

In-situ dielectric cure monitoring as a method of measuring the influence of cure temperature on natural rubber vulcanization

Narong Chueangchayaphan[1] · Nattapong Nithi-Uthai[1] ·
Kittiphan Techakittiroj[2] · Hathaikarn Manuspiya[3]

Abstract

Real-time determination of the optimum curing time for molded rubber parts is a challenge in the rubber industry. This research focused on the development of an in-situ rubber cure monitoring system (RCMS) capable of real-time monitoring of the natural rubber vulcanization process in a compression molding machine. The influence of vulcanization temperature (150 °C, 160 °C and 170 °C) on the cure characteristic properties, degree of cure and cure rate of a natural rubber compound in a conventional vulcanization system were compared when monitored with both a moving die rheometer (MDR) and the RCMS testing system. The degree of correlation between the measurements of the cure characteristics at the various vulcanization temperatures obtained from MDR and RCMS was established. The study found that RCMS can be used to determine the scorch time and the optimum cure time in a compression mold in real time.

Keywords Vulcanization · Capacitance · Dielectric cure monitoring · Rubber cure monitoring system · Vulcanization temperature

✉ Narong Chueangchayaphan
narong.c@psu.ac.th

[1] Department of Rubber Technology and Polymer Science, Faculty of Science and Technology, Prince of Songkla University, Pattani 94000, Thailand

[2] Department of Mechatronics Engineering, Faculty of Engineering, Assumption University, Samut Prakan 10540, Thailand

[3] The Petroleum and Petrochemical College, Chulalongkorn University, Bangkok 10330, Thailand

Introduction

Natural rubber (NR) is an important agricultural product obtained from *Hevea Brasiliensis* trees, of which the *cis*-1,4-polyisoprene molecule, comprising of only carbon and hydrogen atom, is the main constituent, produced from a bio-synthetic process. NR plays a key role in the socio-economic structure of many countries, especially Thailand. It is extensively used in a wide range of products, such as mechanical goods and tires. Unvulcanized NR has low mechanical properties, and thus vulcanization of raw NR is necessary to improve its mechanical properties. Among vulcanization systems, sulfur vulcanization is the most widely employed process which is used to cross-link the rubber [1]. The conditions used in the vulcanization process especially the vulcanization temperature and time has an important impact on the structure, physio-mechanical properties and quality of the final products [2, 3]. In particular, the vulcanization temperature is of great interest, because it has a major influence on the three-dimensional cross-linked network structure, with the optimum properties being obtained when using the lowest possible vulcanization temperature. Nevertheless, in industrial-scale processes, higher vulcanization temperatures are usually employed to increase productivity.

In previous studies, several techniques have been used to characterize the curing of elastomers such as differential scanning calorimetry (DSC), oscillating disc rheometry (ODR), dynamic mechanical analysis (DMA), rubber processing analysis (RPA) and moving die rheometry (MDR) [4–8]. The analysis of rheometer curves is an indirect method of evaluating the vulcanization level in rubbers through the monitoring of an increase in the torque value which is produced in the three stages of the vulcanization process. The cross-link density of the rubber network is related to the delta torque value in the curing curves [9, 10]. However, the limitations of rheometry tests are the different mold geometry, sample thickness and the different processing conditions, which lead to the wasting of materials, defective products and longer cycle times [11, 12]. Therefore, direct or real-time cure monitoring is an important means of solving the drawbacks of rheometry tests. Dielectric analysis (DEA) is one of the methods which is commonly used to monitor the direct curing of thermoset materials such as resins and adhesives [13–21]. The application of DEA in the real-time monitoring of rubber vulcanizate properties during NR vulcanization is advantageous, because *cis*-1,4-polyisoprene, which has a non-zero dipole moment, is the main component of NR and changes in dipole moment occur due to the addition of sulfur and the formation of rubber-sulfur dipoles [22–24]. Therefore, The DEA is a good experimental alternative to obtain a deeper insight into the vulcanization mechanisms. Although DEA can be used to observe the elastomer vulcanization process, there has been little research reported on the use of DEA to measure NR vulcanization in real time [11, 23–25]. The influence of vulcanization parameters on the dielectric properties of natural rubber have been described in literature related to vulcanizing additives [23, 26], vulcanization systems [24, 27] and fillers [23, 28, 29], etc. As noted above, during the vulcanization process, the vulcanization

temperature is one of the main parameters which affect the structure, chemical cross-link density, type of cross-links and mechanical properties of vulcanized rubber [2, 30–32].

Therefore, to assess the ability of DEA to monitor the NR vulcanization process in real time and whether it can be incorporated in the manufacturing process, a rubber cure monitoring system (RCMS) was set up. The effect of three different vulcanization temperatures, 150, 160 and 170 °C on the cure characteristic properties, degree of cure and cure rate of a natural rubber compound in a conventional vulcanization (CV) system are reported and compared using both MDR and RCMS as a method of characterization.

Materials and methods

Preparation of natural rubber compound

The materials used in this research were all of commercial grade and their density, sources, and quantities are listed in Table 1. The formulation (in parts per hundred of rubber) was natural rubber (NR) 100, zinc oxide (ZnO) 5, stearic acid 2, N-tert-Butyl-2-benzothiazole sulfonamide (TBBS) 1, and sulfur 2, which were combined to prepare an NR compound in two steps based on a CV system. The first step involved compounding the NR, ZnO and stearic acid in an internal mixer with a fill factor of 0.75, a rotor speed of 60 rpm, and an initial chamber temperature of 35 °C, according to the mixing schedule shown in Table 2. The compound was then kept at room temperature in a desiccator for 24 h before further processing. In the second step, other ingredients such as the accelerator (TBBS) and sulfur were added and the compound continuously mixed for 9 min. Finally, the compound was sheeted to a 2 mm thickness using a two-roll mixing mill.

Table 1 Density, sources and quantities of the materials used

Ingredients	Density (g/cm^{-3})	Source	Quantities (phr)
Natural rubber (STR 5L)	0.92	Yala latex industry, Yala, Thailand	100
Zinc oxide (ZnO)	5.57	Global chemical Co., Ltd., Samut Prakarn, Thailand	5
Stearic acid	0.85	Imperial Chemical Co., Ltd., Bangkok, Thailand	2
N-tert-Butyl-2-benzo-thiazole sulfonamide (TBBS)	1.28	Flexsys America L.P., West Virginia, USA	1
Sulphur	2.07	Siam Chemical Co., Ltd., Samut Prakarn, Thailand	2

Mixing procedure	Cumulative time (min)
Step 1: Internal mixer	
NR mastication	0
Addition of stearic acid	2
Addition of zinc oxide (ZnO)	3
Dumping	9
Step 2: Internal mixer	
Addition of the mixer from step 1	0
Addition of TBBS and sulfur	2
Addition of sulfur	3
Dumping	4

Table 2 The mixing procedure and cumulative time used for the NR compound

Material characterization

Samples of the rubber compound were characterized using MDR and RCMS under isothermal conditions. As noted above, three different test temperatures of 150, 160 and 170 °C were examined. MDR and RCMS were used to monitor the cure reaction by following the increase in torque and the change in electrical properties, respectively, which are indicative of cross-linking, as a function of time at a constant temperature.

MDR test

The isothermal curing of the natural rubber compound was investigated using a Montech MDR (MDRH2020) at a die oscillation angle of 0.5° and a frequency of 1.7 Hz. The sealed torsion shear cure meter was set according to ASTM D5289. To make the rheological measurements as close as possible to the NR compression molding process, a 4 cm^3 sample of the NR compound was placed in the closed and sealed die cavity. The increment of torque was measured at constant amplitude of oscillation and the designated temperature. The torque required to shear the compound due to the formation of a cross-linked structure of rubber chains was plotted as a function of time to construct the cure curve. The main cure characteristic values obtained from the cure curve were:

- The lowest point in the cure curve, defined as the minimum torque (M_L).
- The highest point at the curve plateau, termed the maximum torque (M_H).
- The time to reach a given degree of cure (t_{cx}) which was obtained from the following equation:

$$t_{cx} = \text{minutes to torque being } M_L + \frac{x \times \Delta M}{100}, \tag{1}$$

where x is the percentage of cure required and ΔM or delta torque is the difference between the maximum and the minimum torque ($M_H - M_L$). The optimum cure time (t_{c90}) is used as the time for optimal cross-linking in rubber technology.

RCMS test

The experimental set-up of the RCMS is displayed in Scheme 1. Parallel stainless steel plates with a diameter of 1.1 cm, insulated with polytetrafluoroethylene, were used as electrodes. The upper and lower electrodes were embedded in a 0.15 cm high compression mold, with a 4.00 cm diameter. Thermocouples were also embedded in the mold near to the electrodes which were connected to an LCR meter (Wayne Kerr 4110). In our previous work, it was found that an alternating electric field at 5 kHz was suitable for monitoring natural rubber vulcanization [33]. Therefore, a 2 V alternating voltage was applied between the parallel-plate electrodes at a constant frequency of 5 kHz. The capacitance and conductance were continuously detected every 4 s as a function of the vulcanization time for 15 min. Before testing, a 1 mm thickness of PTFE was used as a standard sample to calibrate the RCMS. The 4 cm^3 rubber compound sample was placed into the preheated mold at the designated temperature in the compression machine and was then compressed under a pressure of 10 MPa. A controlling device was used to record the electrical properties during the NR vulcanization and the capacitance and conductance curves versus cure time were exhibited on the monitor connected to the RCMS via a local area network.
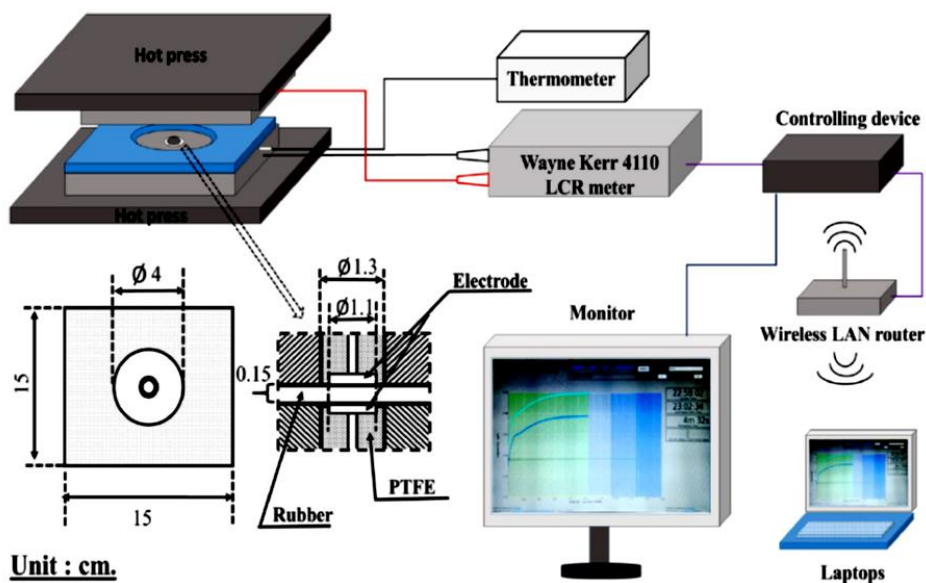
Scheme 1 The experimental set-up for the rubber cure monitoring system (RCMS)

Results and discussion

The typical torque versus time curves of the rubber compounds produced at the three different cure temperatures obtained from MDR are displayed in Fig. 1. S-shaped curing curves typical of an accelerated sulfur vulcanization process were observed, which consisted of three regions, i.e., induction (scorch) period, curing period and overcure period. First, after the rubber compound is placed into the heated cavity of the MDR, the torque falls because of softening of the compound and because the cross-link structures have not occurred during the induction period. When the three-dimensional cross-linked networks are formed, this leads to a rise in the torque curve. Finally, the torque reaches a constant value or it decreases based on the specific cure system.

The capacitance and conductance were plotted as a function of the vulcanization time at the three different vulcanization temperatures as shown in Fig. 2. The capacitance curves also consist of three regions. In the induction period, the capacitance and conductance increase rapidly until they reached the maximum first slope change, which is defined as C_0. This can be explained, because after being heated, the NR compound softens which enhances the molecular segment mobility and simplifies the arrangement of the dipoles, which in turn results in an increase in capacitance [33, 34]. In the curing period, the capacitance continuously increases until it reaches a plateau which is indicated as C_{100}. This occurs because as the cross-linked networks form, the rubber-sulfur dipoles oscillate in the electric field leading to alteration of the dipole moment [23]. The time required to obtain a specific degree of cure (t_{cx}) can be calculated from:

$$t_{cx} = \text{minutes to capacitance being } C_0 + \frac{x(C_{100} - C_0)}{100}, \tag{2}$$

where C_0 is the maximum capacitance at onset of the first slope change and C_{100} is the maximum capacitance at onset of the second slope change.

After the optimum cure time is reached. The capacitance curve reaches a constant value because the rotation of the dipoles is restricted by the cross-links between the NR molecular chains [22]. Moreover, the conductance-time curve is not a useful means of evaluating the optimum cure time, because it drops rapidly after the induction period, and does not reach a constant value.

Based on the MDR and the capacitance–time curves at 150 °C, the curves increased and then reached a horizontal plateau in the overcure period, indicating

Fig. 1 Relationship between torque as a function of vulcanization time for the different isothermal cure temperatures
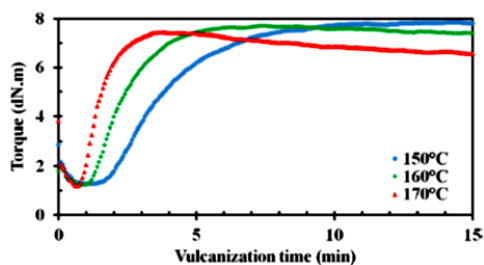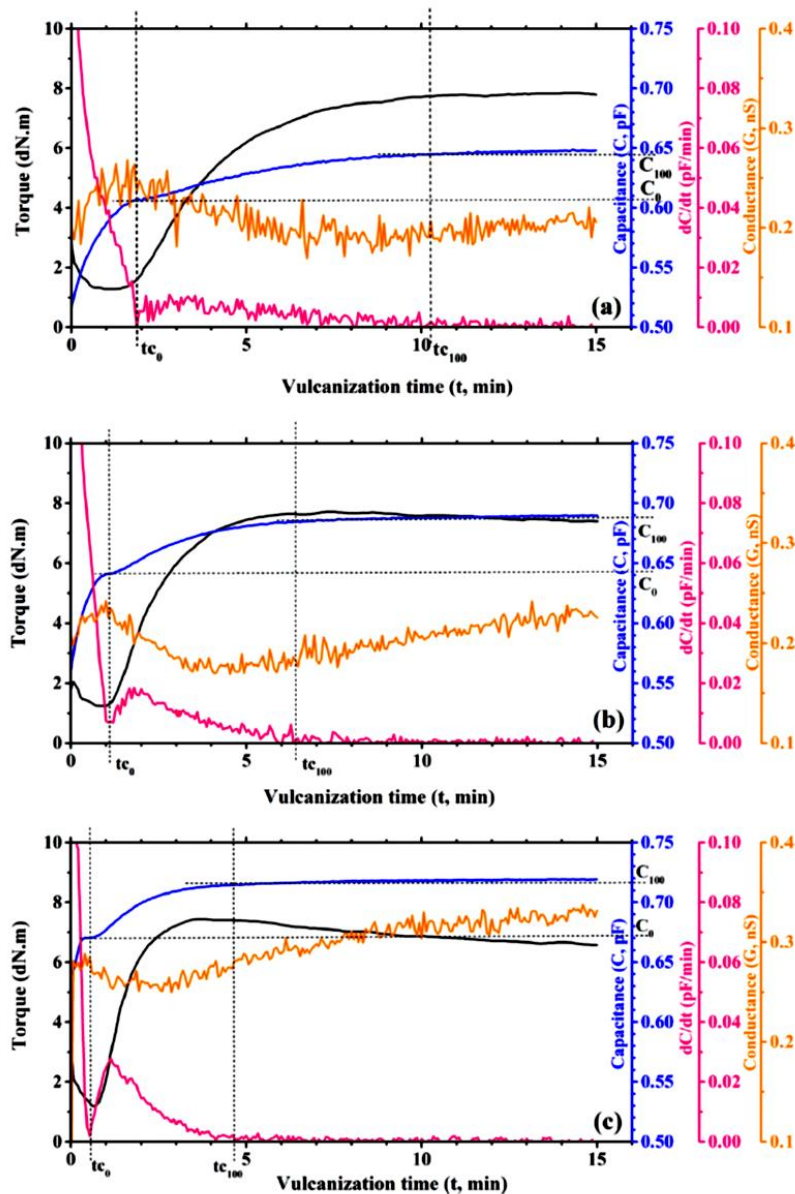
Fig. 2 Relationship between torque, capacitance and conductance as a function of vulcanization time at **a** 150 °C, **b** 160 °C and **c** 170 °C

the formation of cross-link structures, which are thermally stable at this temperature, while a decrease in torque during the overcure period due to the reversion phenomenon was clearly observed by MDR at 170°C. However, the capacitance–time curve at 170°C was slightly increased in the overcure period because during the reversion the polysulfidic chains were cleavage and changed to disulfidic, monosulfidic and cyclic sulfides through both radical and polar decomposition mechanism leading

to an increment of polarization [35]. The capacitance–time curve at 150°C had the lowest capacitance value, while that at 170°C was highest. Higher capacitance was observed at elevated temperatures because of the enhancement of the mobility of the molecular chain segments and the facilitation of dipole orientation polarization [34]. The cure characteristics extracted from both the MDR and RCMS methods are listed in Table 3. It can be observed that the value of M_L diminished when the vulcanization temperature rose, because the NR molecular chains had absorbed more energy, thus enhancing their mobility and resulting in lower rubber viscosity [32]. In addition, at a temperature of 150°C, the highest M_H value was observed which is assumed to coincide with the highest cross-link density. The value of M_H tended to decrease with increases in temperature, which can be explained by the polysulphidic structures being cleaved due to their low thermal stability as the temperature increased [32, 36]. This result agreed with the difference between the maximum and minimum torque (M_H-M_L) of the rubber compound which exhibited a tendency to reduce with increasing vulcanization temperature. However, the capacitance showed the opposite trend as seen in Table 3. Increases in C_0, C_{100} and C_{100}-C_0 were observed with increasing temperature. As the temperature increases, the dipoles comparatively become free and they respond to the applied electric field. Thus, polarization increased and dielectric constant or capacitance is also increased with the increase of temperature [37]. In addition, a competitive side reaction, i.e., reversion occurs at higher vulcanization temperature. This might be related to an increase in total number of polar groups, because the decomposition mechanism of polysufidic cross-links may be either radical, polar or a combination of both [38] and decomposition provides insights in the formation of cyclic sulfides [28].

The induction time for MDR is taken as the time between the test start point and the minimum torque point. Similarly, the induction time for RCMS is the region in which the capacitance curves reach the maximum first slope change and the conductance increases to its maximum as shown in Fig. 2. The time required for the torque to increase by one torque unit (dN.m) above M_L, known as t_{s1} is normally defined as the scorch time when using the MDR technique. Nevertheless, a compound with a low M_H will achieve a much higher ultimate percentage of vulcanization than a compound with a relatively high M_H and in order to avoid the problem of t_{s1}, t_{c10} is sometimes used to determine the scorch time [39].

In the case of RCMS, the time at inflection point or at the peak of the derivative of the capacitance (t_{dc}) was used to measure the scorch time and t_{c90} was used to determine the optimum cure time. It was found that increasing the temperature resulted in a shorter scorch time and the optimum cure time because the rubber chains' mobility and the activity of the accelerator were promoted at higher temperatures [36, 39]. It was clearly observed that the variation of the induction time and cure time as a function of the vulcanization temperature observed by the RCMS gave similar data to that obtained with the MDR method. Furthermore, a close correlation between capacitance and torque for the different isothermal cure temperatures can be observed in Fig. 3. Polynomial regression produced coefficients of determination (R^2) of 0.9971, 0.9979, and 0.9901 at 150°C, 160°C and 170°C, respectively.

To further understand the NR vulcanization process at three different vulcanization temperatures, the torque–time curves and capacitance–time curves from MDR

Table 3 Characteristic curing parameters of the NR compound as evaluated by MDR and RCMS at different temperatures of 150 °C, 160 °C and 170 °C

Cure parameter	150 °C		160 °C		170 °C	
	MDR	RCMS	MDR	RCMS	MDR	RCMS
M_L (dN m) or C_0 (fF)	1.28 ± 0.07	607.37 ± 7.21	1.23 ± 0.04	641.43 ± 6.74	1.19 ± 0.01	670.14 ± 30.44
M_H (dN m) or C_{100} (fF)	7.85 ± 0.26	646.72 ± 6.84	7.71 ± 0.13	684.50 ± 8.65	7.37 ± 0.09	714.94 ± 31.32
M_H–M_L (dN m) or C_{100}–C_0 (fF)	6.57 ± 0.20	39.35 ± 2.10	6.48 ± 0.10	43.07 ± 2.08	6.17 ± 0.09	44.80 ± 1.04
Scorch time (min)						
t_{10}	2.07 ± 0.18	2.59 ± 0.16	1.38 ± 0.06	1.46 ± 0.07	0.93 ± 0.01	0.80 ± 0.16
t_{s1} or t_{dc}	2.27 ± 0.18	2.80 ± 0.21	1.48 ± 0.05	1.80 ± 0.12	1.02 ± 0.03	1.13 ± 0.24
Cure time (min), t_{c90}	6.93 ± 0.07	8.09 ± 0.10	4.12 ± 0.11	4.91 ± 0.04	2.43 ± 0.01	3.37 ± 0.18
CRI	21.43 ± 0.67	16.83 ± 0.91	36.76 ± 0.65	32.17 ± 1.66	67.11 ± 0.45	44.70 ± 1.34

Fig. 3 The correlation between capacitance and torque during the different isothermal cure conditions
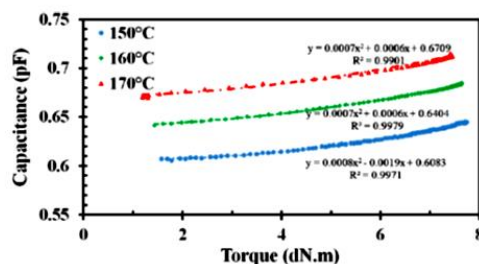
and RCMS were used to determine the degree of cure (α) as a function of curing time (t) as follows:

$$a_{(MDR)} = \frac{M_t - M_L}{M_H - M_L},$$

$$a_{(RCMS)} = \frac{C_t - C_0}{C_{100} - C_0},$$

where M_t and C_t are the torque value and the capacitance value corresponding to a time during vulcanization, respectively. Consequently, cure rate or vulcanization rate ($d\alpha/dt$) can be defined as the derivative of the degree of cure with respect to time [40]. To investigate the possibility of RCMS as a means of monitoring the NR vulcanization in real-time, similar or the same results from MDR and RCMS are essential. The degree-of-cure curves (α versus t) and cure-rate curves ($d\alpha/dt$ versus t) derived from both MDR and RCMS are shown in Figs. 4 and 5, respectively. It can be observed that the highest degree of cure was at 170 °C and that there was close agreement between the two methods. MDR exhibited a higher degree of cure at a given vulcanization time and temperature calculated based on the torque, which

Fig. 4 Degree of cure as a function of time at different isothermal cure conditions from **a** MDR and **b** RCMS
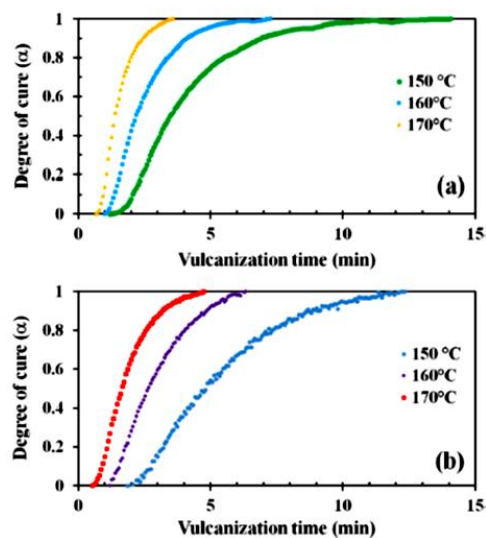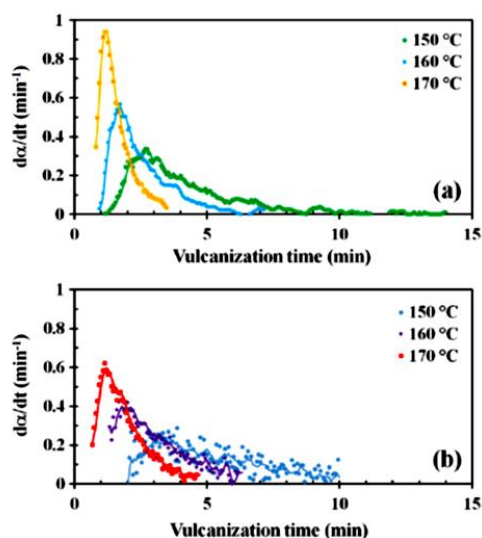
Fig. 5 Cure rate as a function of time at three isothermal vulcanization temperatures from **a** MDR and **b** RCMS

is highly influenced by the viscosity of the material [2, 3], and is thus a more sensitive means of detecting vulcanization. On the other hand, the degree of cure for RCMS was calculated from the capacitance which was affected by the change of dipole moment during vulcanization. Figure 5 shows the cure-rate curves, which it can be observed are composed of two regions. In the first region, an increase of cure rate with time which quickly reached a maximum point was observed because of the low viscosity of rubber compound. This indicated that a complex network structure was being formed. In the second region, the viscosity became high due to the growing cross-linked formation resulting in a reduction in the cure rate [41]. The time at which the maximum point in the cure rate curve was reached decreased with increasing in the vulcanization temperature, because the reactivity of the rubber vulcanization depended on the temperature [2].

Figure 6 exhibits the maximum cure rate at different temperatures. It was found that the maximum cure rate increased with increases in the vulcanization temperature. The samples cured at 170 °C provided the highest maximum cure rate, while the 150 °C cured samples produced the lowest value. In addition, MDR recorded a maximum cure rate higher than that found by RCMS at all isothermal

Fig. 6 Maximum vulcanization rate from RCMS and MDR at different temperatures
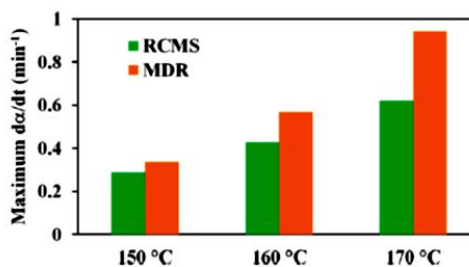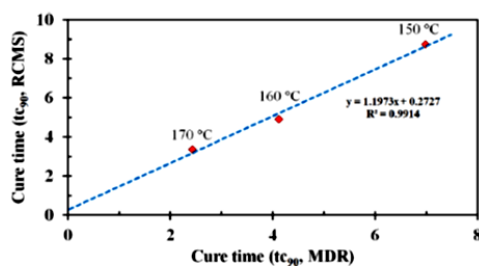
Fig. 7 Linear correlation of optimum cure time (t_{c90}) obtained from RCMS and MDR with three different vulcanization temperatures

temperatures. However, the two techniques exhibited good correlation for the optimum cure time (t_{c90}) with an R^2 equal to 0.9914, as shown in Fig. 7.

Conclusion

The objective of this study was to investigate the vulcanization temperature in relation to the cure characteristics of a natural rubber compound with a conventional vulcanization (CV) system using both the conventional curemeter (MDR) and a novel RCMS, under isothermal conditions. The NR compound was characterized at vulcanization temperatures of 150 °C, 160 °C and 170 °C. Decreases in the minimum torque, maximum torque, delta torque, scorch time and optimum cure time were observed with increasing vulcanization temperature. Torque and capacitance showed a close correlation at all cure temperatures. Linear correlation of optimum cure time (t_{c90}) obtained from RCMS and MDR with different vulcanization temperatures was achieved. It can be concluded that RCMS is a convenient and rapid real-time method for monitoring the whole vulcanization process and determining the optimum cure time in a compression mold.

References

1. Khang TH, Ariff ZM (2012) Vulcanization kinetics study of natural rubber compounds having different formulation variables. J Therm Anal Calorim 109:1545–1553
2. Mansilla MA, Marzocca AJ, Macchi C, Somoza A (2015) Influence of vulcanization temperature on the cure kinetics and on the microstructural properties in natural rubber/styrene-butadiene rubber blends prepared by solution mixing. Eur Polym J 69:50–61
3. Erfanian M, Anbarsooz M, Moghiman M (2016) A three dimensional simulation of a rubber curing process considering variable order of reaction. Appl Math Model 40:8592–8604
4. Wang P, Qian H, Yu H, Chen J (2003) Study on kinetic of natural rubber vulcanization by using vulcameter. J Appl Polym Sci 88:680–684
5. Arrillaga A, Zaldua AM, Atxurra RM, Farid AS (2007) Techniques used for determining cure kinetics of rubber compounds. Eur Polym J 43:4783–4799

115

6. Zhang B, Wang Y, Wang P, Huang H (2013) Study on vulcanization kinetics of constant viscosity natural rubber by using a rheometer MDR2000. J Appl Polym Sci 130:47–53

7. Raa Khimi S, Pickering KL (2014) A new method to predict optimum cure time of rubber compound using dynamic mechanical analysis. J Appl Polym Sci 131:40008

8. Hosseini SM, Razzaghi-Kashani M (2014) Vulcanization kinetics of nano-silica filled styrene butadiene rubber. Polymer 55:6426–6434

9. Maiti M, Patel J, Naskar K, Bhowmick AK (2006) Influence of various crosslinking systems on the mechanical properties of gas phase EPDM/PP thermoplastic vulcanizates. J Appl Polym Sci 102:5463–5471

10. Chueangchayaphan W, Chueangchayaphan N, Tanrattanakul V, Muangsap S (2018) Influences of the grafting percentage of natural rubber-graft-poly(2-hydroxyethyl acrylate) on properties of its vulcanizates. Polym Int 67:739–746

11. Magill R, Demin S (1999) Using real-time impedance measurement to monitor and control rubber vulcanization. Rubber World 221:24–28

12. Jaunich M, Stark W (2009) Monitoring the vulcanization of rubber with ultrasound: influence of material thickness and temperature. Polym Test 28:901–906

13. Kim HG, Lee DG (2002) Dielectric cure monitoring for glass/polyester prepreg composites. Compos Struct 57:91–99

14. Kortaberria G, Solar L, Jimeno A, Arruti P, Gómez C, Mondragon I (2006) Curing of an epoxy resin modified with nanoclay monitored by dielectric spectroscopy and rheological measurements. J Appl Polym Sci 102:5927–5933

15. Chen J, Hojjati M (2007) Microdielectric analysis and curing kinetics of an epoxy resin system. Polym Eng Sci 47:150–158

16. Skordos AA, Partridge IK (2007) Effects of tool-embedded dielectric sensors on heat transfer phenomena during composite cure. Polym Compos 28:139–152

17. Steinhaus J, Moeginger B, Großgarten M, Hausnerova B (2011) Evaluation of dielectric curing monitoring investigating light-curing dental filling composites. Mater Eng 18:30–35

18. Zhou B, He D, Quan Y, Chen Q (2012) The investigation on the curing process of polysulfide sealant by In situ dielectric analysis. J Appl Polym Sci 126:1725–1732

19. Hardis R, Jessop JLP, Peters FE, Kessler MR (2013) Cure kinetics characterization and monitoring of an epoxy resin using DSC, Raman spectroscopy, and DEA. Compos A 49:100–108

20. Steinhaus J, Hausnerova B, Haenel T, Großgarten M, Möginger B (2014) Curing kinetics of visible light curing dental resin composites investigated by dielectric analysis (DEA). Dent Mater 30:372–380

21. Müller U, Pretschuh C, Zikulnig-Rusch E, Dolezel-Horwath E, Reiner M, Knappe S (2016) Dielectric analysis as cure monitoring system for melamine-formaldehyde laminates. Prog Org Coat 90:277–283

22. Tuckett RF (1942) The kinetics of high elasticity in synthetic polymers. Trans Faraday Soc 38:310–317

23. Desanges H, Chasset R, Thirion P (1958) Changes in the electrical properties of natural rubber/carbon black compounds during vulcanization. Rubber Chem Technol 31:631–649

24. Persson S (1986) Dielectric vulcametry. Polym Test 6:47–78

25. Magill R, Demin S (2000) Using real-time impedance measurement to monitor and control rubber vulcanization. Rubber World 221:16–19

26. Hernández M, Ezquerra TA, Verdejo R, López-Manchado MA (2012) Role of vulcanizing additives on the segmental dynamics of natural rubber. Macromolecules 45:1070–1075

27. Hernández M, Valentín JL, López-Manchado MA, Ezquerra TA (2015) Influence of the vulcanization system on the dynamics and structure of natural rubber: comparative study by means of broadband dielectric spectroscopy and solid-state NMR spectroscopy. Eur Polym J 68:90–103

28. Hernández M, Carretero-González J, Verdejo R, Ezquerra TA, López-Manchado MA (2010) Molecular dynamics of natural rubber/layered silicate nanocomposites as studied by dielectric relaxation spectroscopy. Macromolecules 43:643–651

29. Ravikumar K, Palanivelu K, Ravichandran K (2015) Vulcanization, mechanical and dielectric properties of carbon black/nanoclay reinforced natural rubber hybrid composites. Appl Mech Mater 766–767:377–382

30. Wang X, Xia Z, Yuan B, Zhou H, Li Z, Chen N (2013) Effect of curing temperature on the properties of conductive silicone rubber filled with carbonyl permalloy powder. Mater Des 51:287–292

31. Zhang H, Li Y, Shou J, Zhang Z, Zhao G, Liu Y (2016) Effect of curing temperature on properties of semi-efficient vulcanized natural rubber. J Elastom Plast 48:331–339
32. Lee KC, Md Yusoff NA, Othman N, Mohamad Aini NA (2017) Effect of vulcanization temperature on curing characteristic, physical and mechanical properties of natural rubber/palygorskite composites. IOP Conf Ser Mater Sci Eng 223:012017
33. Chueangchayaphan N, Nithi-Uthai N, Techakittiroj K, Manuspiya H (2018) Evaluation of dielectric cure monitoring for in situ measurement of natural rubber vulcanization. Adv Polym Technol 37:3384–3391
34. Švorčík V, Králová J, Rybka V, Plešek J, Červená J, Hnatowicz V (2001) Temperature dependence of the permittivity of polymer composites. J Polym Sci B Polym Phys 39:831–834
35. Cheremisinoff NP (2001) Condensed encyclopedia of polymer engineering terms. Butterworth-Heinemann, Boston
36. Posadas P, Fernandez-Torres A, Valentın JL, Rodrıguez A, Gonzalez L (2010) Effect of the temperature on the kinetic of natural rubber vulcanization with the sulfur donor agent dipentamethylene thiuram tetrasulphide. J Appl Polym Sci 115:692–701
37. Sheha EM, Nasr MM, El-Mansy MK (2015) The role of MgBr 2 to enhance the ionic conductivity of PVA/PEDOT:PSS polymer composite. J Adv Res 6:563–569
38. Ghosh P, Katare S, Patkar P, Caruthers JM (2003) Sulfur vulcanization of natural rubber for benzothiazole accelerated formulations: from reaction mechanisms to a rational kinetic model. Rubber Chem Technol 76:592–693
39. Dick JS, Pawlowski H (1995) Alternate instrumental methods of measuring scorch and cure characteristics. Polym Test 14:45–84
40. Rabiei S, Shojaei A (2016) Vulcanization kinetics and reversion behavior of natural rubber/styrene-butadiene rubber blend filled with nanodiamond—the role of sulfur curing system. Eur Polym J 81:98–113
41. Casalini R, Corezzi S, Livi A, Levita G, Rolla PA (1997) Dielectric parameters to monitor the cross-link of epoxy resins. J Appl Polym Sci 65:17–25

VITAE

Name   Mr. Narong Chueangchayaphan

Student ID   6120330103

Educational Attainment

Degree	Name of Institution	Year of Graduation
B.Sc. (Physics)	Prince of Songkla University, Songkhla, Thailand	2003
M.Sc. (Polymer Technology)	Prince of Songkla University, Pattani, Thailand	2006

Scholarship Awards during Enrolment

1. Research grants from The National Research Council of Thailand (NRCT), (Grant No. RDG5550112)
2. Thesis Research Grant, The graduate school of Prince of Songkla University
3. Prince of Songkla University Teacher Development Scholarship to study at the doctoral level or a diploma in the country (Ph.D. 50%), Prince of Songkla University, Surat Thani Campus

Work – Position and Address

I work as a lecturer in the Material Technology and Industrial Management, Faculty of Science and Industrial Technology, Prince of Songkla University, Surat Thani Campus, Surat Thani 84000, Thailand.

List of Publication and Proceeding

1. Chueangchayaphan, N., Nithi-Uthai, N., Techakittiroj, K. and Manuspiya, H. 2015. Prototype system for monitoring natural rubber vulcanization. In: the 2nd Asia Pacific Rubber Conference (APRC 2015), Phuket, Thailand. pp. 41.

2. Chueangchayaphan, N., Nithi-Uthai, N., Techakittiroj, K. and Manuspiya, H. 2018. Evaluation of dielectric cure monitoring for in situ measurement of natural rubber vulcanization. Advances in Polymer Technology, 37: 3384-3391.

3. Chueangchayaphan, N., Nithi-Uthai, N., Techakittiroj, K. and Manuspiya, H. 2021. In-situ dielectric cure monitoring as a method of measuring the influence of cure temperature on natural rubber vulcanization. Polymer Bulletin. 78, 3169–3182.